SYNTHESIS OF HETEROATOM CONTAINING AROMATIC CONJUGATED POLYMERS USING ACYCLIC DIENE METATHESIS (ADMET)

by

ARIJIT SENGUPTA

A dissertation submitted to the Graduate Faculty in Chemistry in partial fulfillment of the requirements for the degree of Doctor of Philosophy, The City University of New York

2012

This manuscript has been read and accepted for the Graduate Faculty in Chemistry in satisfaction of the dissertation requirement for the degree of Doctor of Philosophy.

	Prof. Ralf M Peetz
Date	Chair of Examining Committee
	Prof. Maria C. Tamargo
Date	Executive Officer

Prof. Krishnaswami Raja

Prof. Frieder Jäkle

Supervision Committee

THE CITY UNIVERSITY OF NEW YORK

Abstract

Synthesis of heteroatom containing aromatic conjugated polymers using Acyclic Diene Metathesis (ADMET)

by

Arijit Sengupta

Adviser: Prof. Ralf M. Peetz

This doctoral thesis describes the synthesis of heteroatom (B/Si/Ge/Sn) containing conjugated macromolecules via Acyclic Diene Metathesis (ADMET) polycondensation. The main objective was to obtain a library of macromolecules with unique optical properties based on different aromatic segments and heteroatoms.

In chapter 2, the selective synthesis and characterization of a germanium containing macrocycle with two stilbene fluorophores is reported. The structure and size of the macrocycle were determined by ^{1}H NMR, ^{13}C NMR, GPC (polystyrene standards) and MALDI – TOF. The macrocycle features "*all – trans*" configuration at the vinylene bonds. The optical properties were studied by UV/Vis and fluorescence spectroscopy. The material emits in the blue region around 363 nm with a quantum efficiency of 0.4 relative to trans – stilbene. Theoretical calculations using B3LYP/6-31G** and Lanl2dz basis sets offered a better understanding of structural and electrooptical properties. They showed the presence of two important transitions in the absorption and the involvement of germanium orbital in the electronic conjugation with the stilbene segments.

Chapter 3 outlines the extension of this aforementioned synthetic strategy to the group 14 element boron, in order to generate a new class of conjugated macromolecules – homopolymers based on boron (**p2a**, **p2b)** and co-polymers based on silicon and boron (**p12a**, **p12b)**. The

structures and these new systems were determined by ^{1}H NMR, ^{13}C NMR and correlation NMR spectroscopy. The molecular weights were determined by GPC using polystyrene standards. Both the homopolymers and copolymers have "*all – trans*" configuration around the internal vinylene bonds. The copolymers were found to be random. The optical properties showed that all the macromolecules absorbed in the range of 327 – 406 nm and emitted at 416 nm (**p2a**, **p12a**) and 494 nm (**p12b**). The quantum efficiencies of these macromolecules were in the range of 0.28 – 0.30. **p12a** was found to be a potential fluoride ion sensor with very high sensitivity due to a polymer co-operative effect. Two distinct emissions dominated the emission spectrum of **p12b**, investigation of which indicated possible intermolecular energy transfer. The thermal properties indicated higher stability of the copolymers compared to the homopolymers. Degradation of **p12a** followed a two-step process and **p12b** was found to be more stable than **p12a**.

Chapter 4 of this thesis reports the synthesis of a library of homologous polymers based on Si, Ge, or Sn alternating with dithienylthiophene segments. The microstructures were analyzed by ^{1}H NMR, ^{13}C NMR and Correlation spectroscopy (HSQC, COSY). All the polymers **p3a – c** showed "*all – trans*" configuration at the vinylene bonds. The molecular weights were determined by GPC using polystyrene standards. No significant side products were observed under the ADMET conditions employed. Optical property analysis showed that the monomers were non-emissive whereas they absorb in the range of 263 – 264 nm. The polymers were highly fluorescent emitting in the range of 419 – 423nm. The quantum efficiencies were found to decrease from 0.18 to 0.11 from Si over Ge to Sn along with a small gradual blue shift of the emission maximum with the increase in size of the heteroatom. Thermogravimetric analysis indicated that Si based **p3a** showed the highest stability among the three homologous polymers.

Chapter 5 is strongly related and involves alkyloxy homologous side – chain substituted systems. The microstructures of the macromolecular products were analyzed by ^{1}H NMR, ^{13}C NMR showing that these polymers also have an "*all – trans*" configuration around the vinylene bond. The molecular weights were determined by GPC using polystyrene standards. Alkyloxy substituted silicon containing stilbene polymers showed a strong red shift compared to their stilbene homologous without side chains, with an absorption maximum at 371 nm. The emission maximum was observed at 412 nm. The quantum yield was 0.50 – 0.52 indicating that, there is no photo – induced cis – trans isomerization.

Acknowledgements

I, the author of this thesis greatly appreciate my Ph.D. supervisor, Professor Ralf M. Peetz, for his constructive criticism, recommendations, suggestions, discussions, encouragement, and problem solving which have resulted in this thesis. I am also grateful to Professor Krishnaswami Raja and Professor Frieder Jäkle for serving as thesis committee members and their suggestions and criticism during this work.

I would also like to thank Dr. Ami Doshi (Rutgers University) for her help with the synthesis and characterization of boron containing monomers.

Financial support from the City University of New York (PSC – CUNY and Graduate Center Student Grants) is gratefully acknowledged.

I also wish to thank Dr. Juanqin Zhang and Dr. Boris Arshava for their help and advice with NMR experiments, Mr. Tai Park for his help with thermal characterization, and GPC. During the last 5years, I was able to train and work with several undergraduate students, including especially Ms. Jacqueline Gurrieri, Mr. Yuri Viknevich, Mr. Louis Gude. I would like to thank them for their contributions. Moreover, I would like to thank all my colleagues, especially Mr. Gagandeep Singh, friends, and other people whose names are not mentioned above for their help and providing facilities during the academic years. Finally, acknowledgement is gratefully extended to my wife and parents for their love, understanding, encouragement, which has been a constant source of inspiration.

This thesis is dedicated to my late grandmother

Mrs. Anima Sengupta

Table of Contents

List of Schemes

List of Figures

List of Tables

1. Introduction

1.1 Conjugated polymers – Toward novel electronic materials

The discovery of a drastic increase in the conductivity of polyacetylene after doping led to an increase in the development of numerous generations of organic materials,[1] with goals that included reaching conductivity values in the metallic regime[2]. Over the last 20 years, researchers have reported various conducting or conjugated polymers based on different aromatic units with unique electronic properties. In 1990, Friend, et al reported the synthesis of well-defined poly(*p*-phenylene vinylene) (PPV) systems and studied the photophysical properties.[3] In particular, polymers based on heterocyclic systems such as polypyrrole, polythiophene etc. have been studied much before PPV based materials were reported.[4] The interest in such polymers is rooted in the ease of structural variations on these materials.[5] The conducting or semiconducting properties of such polymers depend on the delocalization of π electrons over the polymer backbone. In general, as the length of delocalization increases the HOMO – LUMO band gap decreases, enabling electron excitation at lower energies. This is often accompanied by a relaxation of the excited electron to the ground state with the emission of light (photo/electroluminescence). The photophysical properties associated with these polymers have been exploited extensively in organic light emitting systems, photovoltaics and sensory materials. Typical examples of conjugated or conducting polymers are shown in Scheme 1.1.

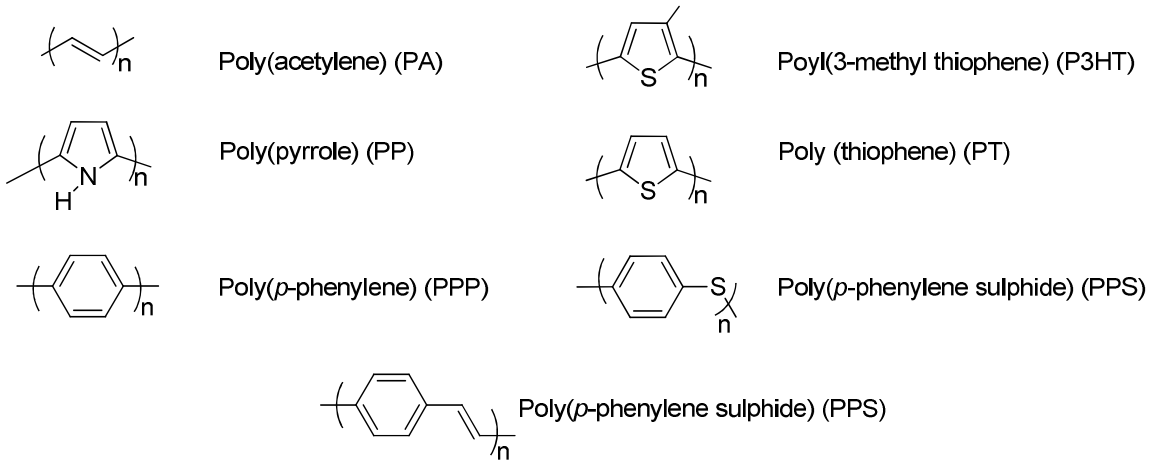

Scheme 1.1 Examples of conjugated polymers[2]

1.2 Heteroatoms in conjugated polymers

Our interest focuses on boron, silicon, germanium and tin containing conjugated polymeric systems. In particular, silicon containing conjugated systems have been an active area of research over the last decade as potential materials for conductors, semiconductors, light emitters (especially blue light), and photovoltaic systems.[6-15] In such polymers made of alternating conjugated segments and silylene linkages, the conjugated segment, often an oligomeric mimic of a homologous conjugated polymer, features a discrete size and structure and hence defined electro-optical properties, in comparison to average distributions of conjugated segments in their polymeric analogues. The polymers feature σ-π-conjugation, as the sp^3-hybridized silylene linkages allow for electronic delocalization through the σ-bonds, $p\pi - d\pi$ interactions between the conjugated segments via the unoccupied d-orbitals on silicon in addition to through-space interactions between the π-conjugated segments.[16-19] The later are considered the dominating in the literature. Scheme 1.2 illustrates these interactions.

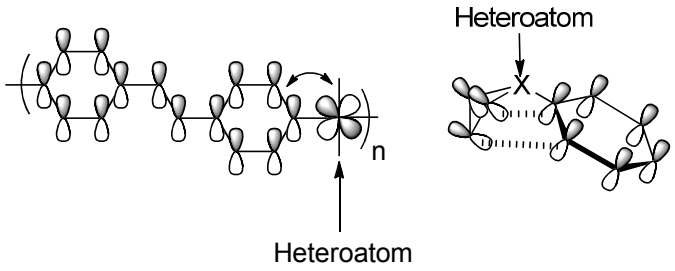

Scheme 1.2 pπ – dπ and through – space interactions in heteroatom containing system.

Incorporation of silicon into the main chain via hydrosilylation has been reported by Luh et al in 2005 as shown in Scheme 1.3.[20] In 2008, Kim et al reported the synthesis of conjugated block copolymers with silicon in the main chain.[21]

Hadziioannou and co-workers prepared oligothiophene-dibutylsilanylene copolymers whose emission maxima could be tuned between by altering the number of thiophene and silanylene units.[22] Silylene copolymers with other chromophores have been made by a similar route.[23-28]

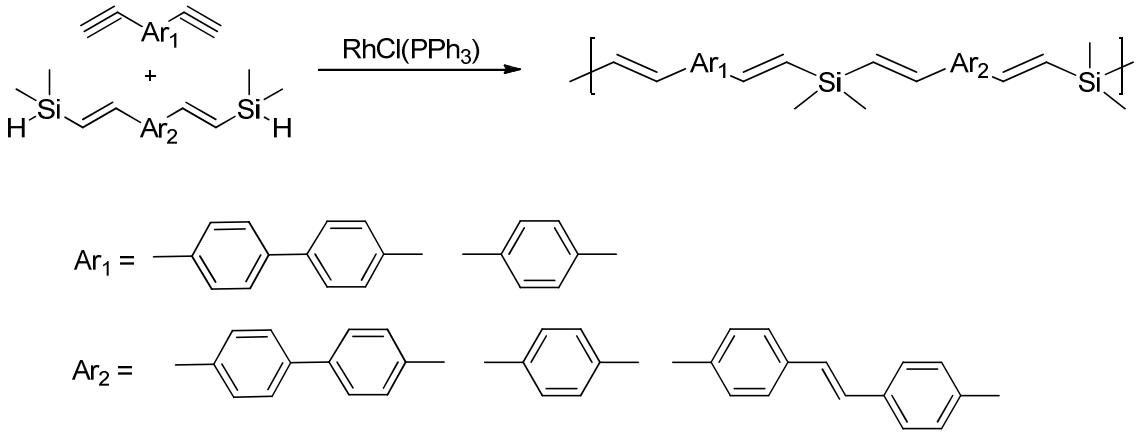

Scheme 1.3 Synthesis of conjugated organosilane systems

Boron containing polymers are studied because the vacant p – orbital on boron can be exploited in several different ways in order to develop polymers with linear and non-linear optical properties. For example, the electron deficient B can be incorporated in a linear polymer with an alternating aromatic system. Corriu et al reported the synthesis boron containing 2,5

diethynylthiophene system.[29] Chujo and co-workers reported the synthesis of linear conjugated systems with boron in the main chain via hydroboration of bifunctional alkynes with hindered aryl boranes as shown in Scheme 1.4.[30,31]

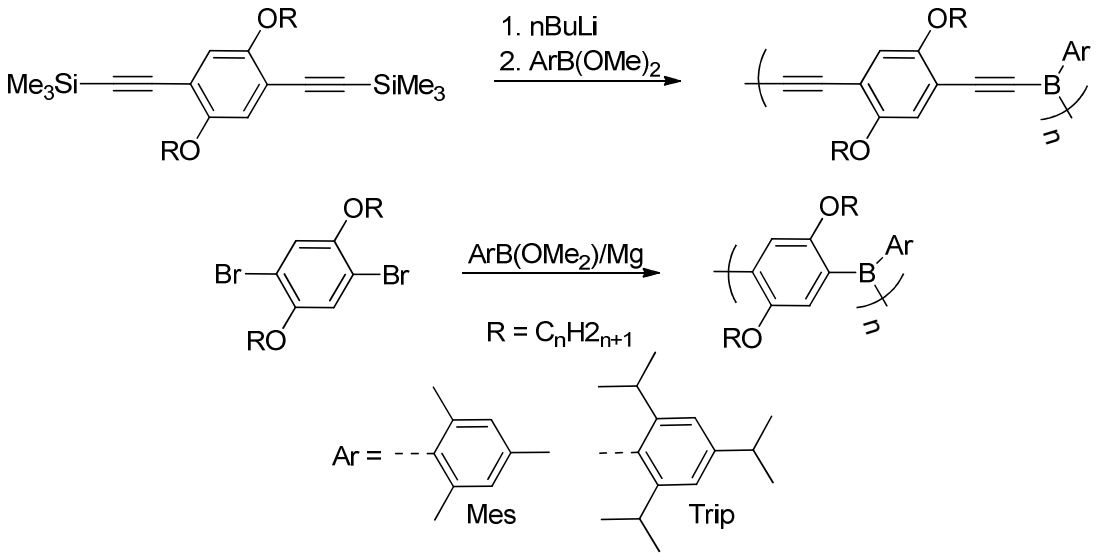

Scheme 1.4 Organometallic routes to conjugated organoboron polymers

In 2005, the Jäkle group reported the synthesis of boron containing polythiophene systems through tin – boron exchange reactions as shown in Scheme 1.5.[32] The photophysical properties of the polymers were controlled by varying the aryl substituent on the boron moiety.

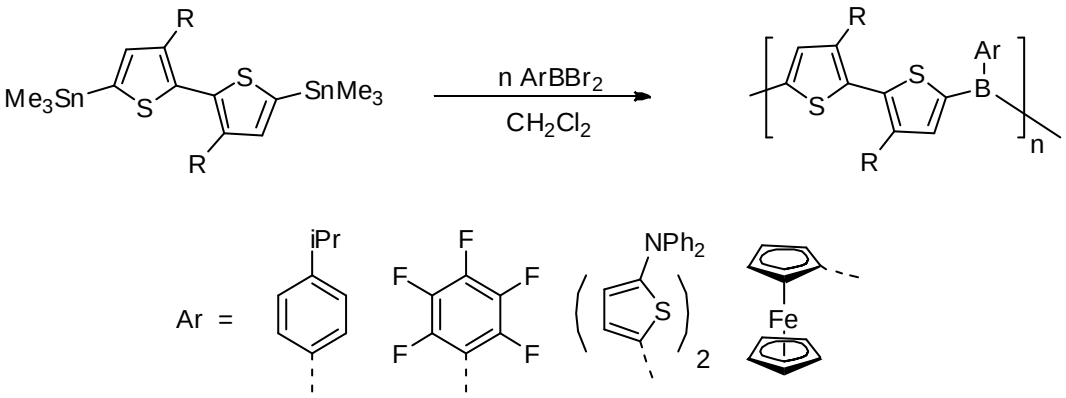

Scheme 1.5 Synthesis of boron-modified polythiophenes via tin–boron exchange[32]

Organoboron quinolates have gained lot of attention because of their relative stability and fluorescence efficiency compared to aluminium quinolate (AlQ_3).[33-36] The copolymerization of 8-hydroxyquinoline functionalized styrene via free radical polymerization was reported by Weck and co-workers.[37] In 2006, Jäkle group reported the synthesis of polystyrene based organoborane quinolate polymers with tunable photoluminiscent properties.[38] Polymers containing germanium, tin, and phosphorous are further examples of hybrid polymers synthesized via metathesis polymerization particularly,[39] acyclic diene metathesis (ADMET). For example, germanium-based polymers are of interest for applications in microlithography and as precursors for ceramics.[40]

While a great variety of different polymerization methods have been pursued for the preparation of various heteroatom containing polymers mentioned above, acyclic diene metathesis polymerization (ADMET) is attractive because the reaction conditions are typically quite mild, ethylene formed as only byproduct is readily removed under vacuum, and the resulting polymer structures are well-defined.

1.3 Olefin metathesis - Acyclic Diene Metathesis (ADMET)

The word "metathesis" originates from the Greek metatithenai (to transpose) [Meta (change) and Tithenai (to place)]. It involves an exchange of atoms or atom groups between two different molecules in a particular way. In olefin metathesis redistribution of carbon–carbon double bonds occur in the presence of metal carbene complexes.[41] If two identical olefins undergo metathesis, it is termed homometathesis and in case of different olefins reacting, it is termed cross metathesis.

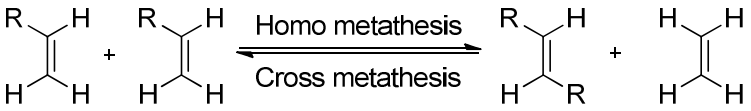

Scheme 1.6 Olefin metathesis

1.3.1 Mechanism

The mechanism of olefin metathesis was first predicted by Chauvin and Herisson in 1972. As shown in Scheme 1.7 the mechanism is associated with the formation of a metallacyclobutane ring (formed between an olefin and a metal carbene complex acting as the catalyst). This cyclic intermediate can break apart productively or non-productively either to generate new olefin or the starting materials respectively. The reaction is thermodynamically controlled, highly reversible, and equilibrium mixtures of olefins are obtained, often featuring linear and cyclic species.[42-44] The key step of the mechanism is shown in Scheme 1.7

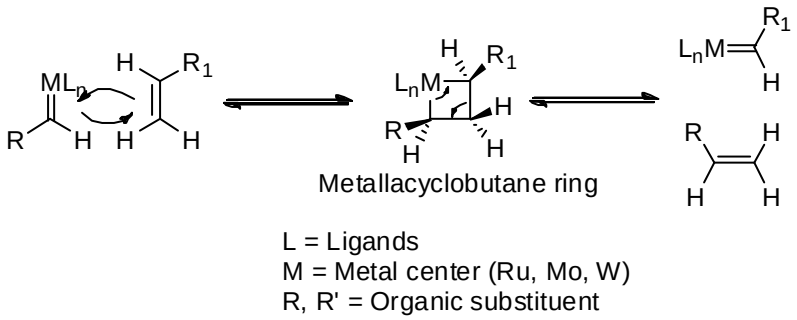

Scheme: 1.7 Metallacyclobutane – intermediate in olefin metathesis

Different modes of the metathesis reaction include ring opening metathesis, ring closing metathesis, cross metathesis, etc have been explored in various applications for several years.[45-47] Acyclic Diene Metathesis (ADMET) is a condensation reaction, leading to make oligomeric/polymeric materials, in which terminal divinyl (α, ω) functional monomers are polymerized using either Schrock or Grubbs type complexes.[48] Metathesis of α, ω dienes was proposed by Dall'Asta already in 1973,[49] however the term ADMET was popularized by Wagener et al in the 1980's. Other studies, e.g. by Doyle and Zuech without observed polymer probably are the result of the presence of competing side reactions.[50]

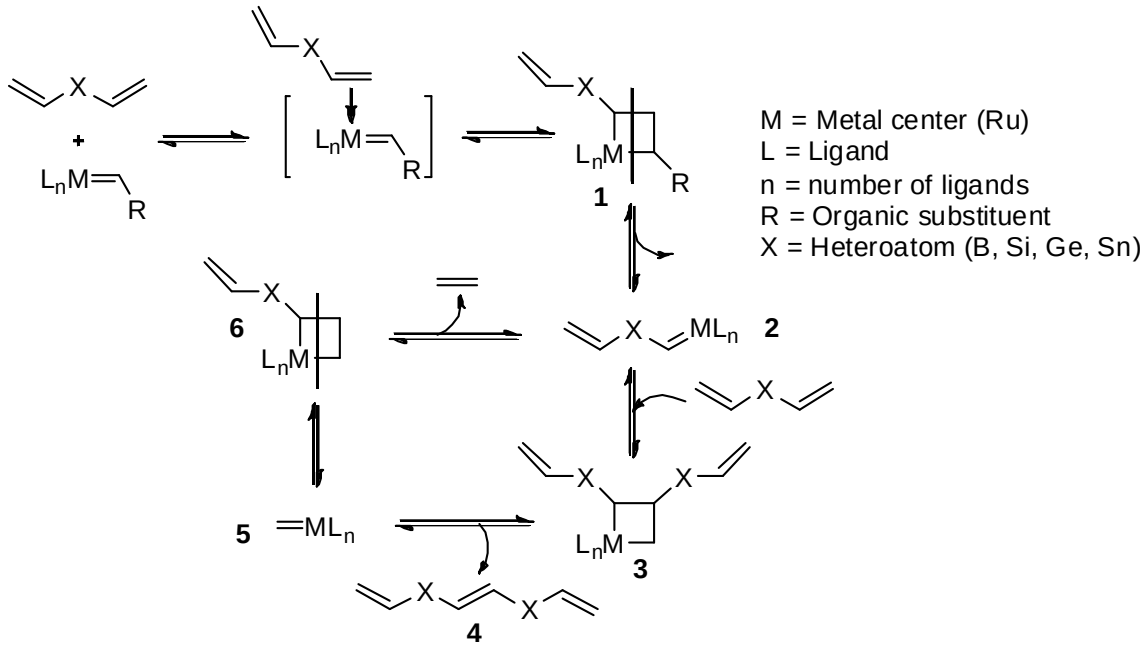

Scheme: 1.8 ADMET catalytic cycle

The first step of the ADMET cycle of is characterized by an initial activation of the vinyl bond of the monomer. In this step, a monomer fragment is transferred onto the metal-alkylidene system, resulting in the formation of metallacyclobutane ring. This ring cleaves in a productive way generating a new alkylidene complex **2** which is the propagating species for the polymerization. The reaction propagates in the presence of additional monomer giving rise to coupled polymers **4** with internal vinylene linkages. The methylidene catalyst **5** is regenerated every cycle. Each step in the reaction is a reversible and in equilibrium, and by removing the side product (usually ethylene) one can drive the reaction equilibrium to the product side, i.e. the polymer. This is generally done by intermittently applying vacuum. The "true catalyst" in the ADMET system is the methylidene complex **5**. Depending on the structures of monomer and the catalyst complex, ADMET can be employed for polymerization of an array of monomers with a wide varieties of

functional groups, producing well-defined linear, cyclic, olefin-containing, oligomers and polymers.

The presence of cyclic oligomers or polymers is also expected because, as the chain size increases, the chain growth reaction starts to compete with ring closing reaction in a chain/ring equilibrium as reported by Ruhland et al.[51]

1.3.2 Catalysts (Transition metal – alkylidene complex)

The catalysts are grouped into Schrock – type and Grubbs – type. In case of the Schrock type, the metal center is either molybdenum or tungsten.[52] Depending on the combination of metal center and ligands, the reactivity of the catalyst can be controlled.

The Grubbs – type systems are Ru – based alkylidenes developed in the1990's. The 1st generation system, the Ru metal center is bonded to two triphenyl phosphine ligands along with two metal-halogen and a Ru=C (benzylidene/vinylidene) linkages.[53] This system showed relatively low reactivity compared to Schrock systems. The 2nd generation catalyst was developed from the combination of the 1st Generation Catalyst and alkyloxy-protected 1,3-dimesityl-4,5-dihydroimidazol-2-ylidene.[54] One of the triphenyl phosphine ligands is replaced by a N-heterocyclic carbene (more basic and hence better σ donation-ability towards the metal center) in order to improve the reactivity. A 3rd generation Ru-based catalyst, (also known as Grubbs-Hoveyda 1st generation catalyst) replaces a triphenyl phosphine ligand by a *o*-isopropoxyphenylmethylene ligand. [55, 56] Scheme 1.9 represents an overview over the most important catalysts systems available to date.

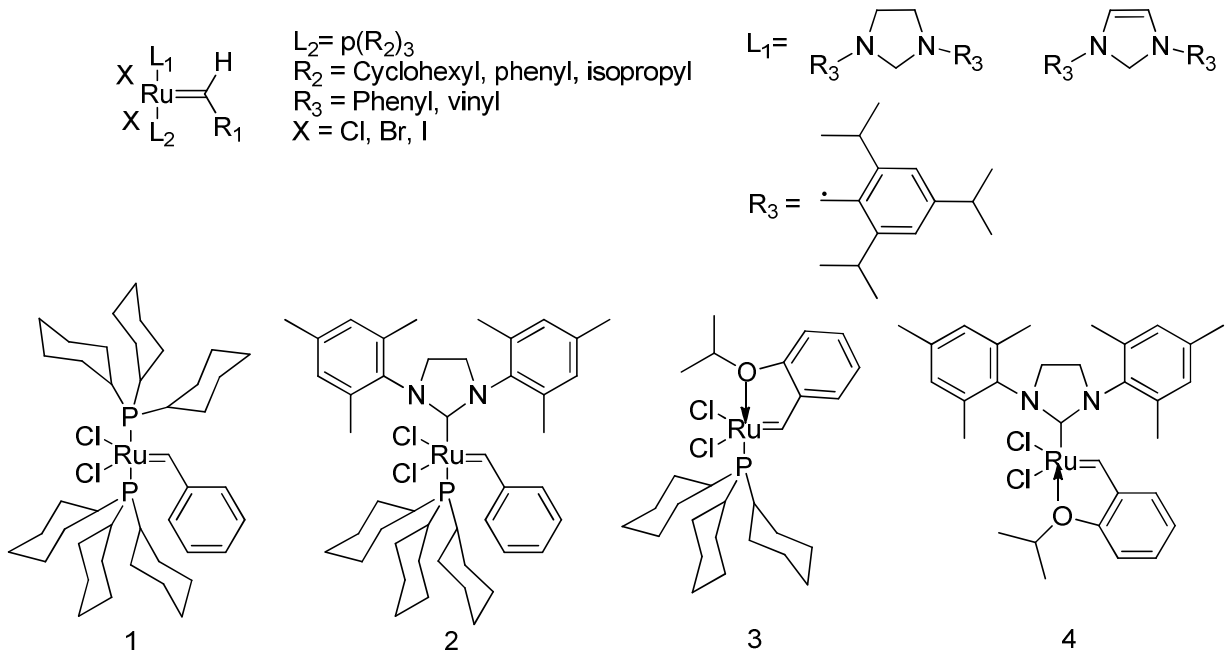

Scheme 1.9 General representation of Grubb's type catalyst. 1 Grubbs 1st generation; 2 Grubbs 2nd generation; 3 Grubbs-Hoveyda 1st generation; 4 Grubbs-Hoveyda 2nd generation catalyst

Grubbs – type systems are overall less reactive compared to Schrock catalysts but have become very important for a wide variety of metathesis reactions, they are also less costly and are easily available. In contrast to the Schrock systems, they can tolerate a wide range of polar functional/ pendent groups and solvents. Even a water soluble Grubbs catalyst has been reported. After reaction it can easily be removed by passing through a silica gel column.[57, 58]

1.4 ADMET - synthesis of heteroatom containing conjugated polymers

As indicated above, one particular opportunity of the Grubbs – systems was the access to functional and polar group containing conjugated polymers via ADMET. The synthesis of side-chain substituted PPV systems was reported by Thorn-Csanyi et al. and by Nomura et al,[59, 60] using Grubb's type catalysts. Over the last 10 years Wagener et al. have reported the synthesis of less well defined heteroatom (silicon) containing polymers using ADMET.[61, 62] Recently, cyclolinear carbosilane polymers made via ADMET have been reported by Interrante et al.[63] However, hardly any attention has been focused on the the synthesis of silicon/germanium/tin containing conjugated polymers via ADMET, as the vinyl derivatives of silicon compounds are very unreactive towards homometathesis due to steric and electronic effects originating from the silyl group, stimulating non-productive cleavage of the metallacyclobutane intermediate containing two silyl groups attached to adjacent carbon atoms.[64] Reports on the ADMET of silicon-containing monomers show ADMET dominated by side reactions: "silylative coupling", as reported by Marciniec et al., and radically cross – linked polymeric side products as reported by Bazan et al. are "exceptions" with no follow-up reports, probably due to unavoidable side-reactions.[65, 66] As discussed above, in silicon containing conjugated oligomers and polymer, the silicon moeity acts as a "spacer group" between the π-conjugation of the conjugated oligomer block, generating a well defined conjugation unit, usually with a band gap corresponding to a blue emission (difficult to make from inorganic counterparts).[67-69] In place of silicon, germanium and tin can also be used. Wagener reported the synthesis of polycarbostannanes *via* acyclic diene metathesis chemistry utilizing both a well-defined molybdenum akylidene and an aryloxo tungsten catalyst system.[70] Main chain boronate polymers were successfully synthesized by Wagener group by acyclic diene metathesis using both molybdenum and ruthenium based

catalytic systems.[71] In 2008, Mukherjee and Peetz reported the successfully synthesis of siloxane/silylene based macrocycle and polymers using Grubbs – type catalyst.[72] No significant side reactions were observed in this work. After this successful proof of principle, the established synthetic strategy was further explored to access a library of different heteroatom containing conjugated polymer, i.e. germanium and tin.

The core of this thesis lies in expanding the strategy to include the electron deficient boron and exploring different aromatic segments based on silicon, germanium and tin. This opens up a unified synthetic strategy to a vast library of heteroatom containing conjugated systems using boron, silicon, germanium and tin with a variety of aromatic segments.

2. A photoluminiscent Ge-containing conjugated macrocycle

2.1 Introduction

As mentioned earlier, macromolecules featuring alternating conjugated aromatic segments and heteroatoms in the backbone are of fundamental interest in both academic and industrial research. They often represent valuable candidates as electronic or photonic materials in advanced applications. Recently, we have reported on the synthesis of selective –Si-O-Si (siloxane) based ring structure with branched alkyl group on silicon via Acyclic Diene Metathesis along with silylene based linear chain architectures with well-defined microstructures (see above) The photophysical properties of these materials were further studied in order to understand the effect of the heteroatoms on these systems. However, homologous conjugated architectures with germanium have remained largely unexplored. The synthetic scope that we have already presented for the siloxane/silylene systems was further extended to the germanium systems in order to develop new architectures, particularly for a selective macrocycle based on germanium. The objective of this was to develop a unified synthetic strategy that can be utilized to generate a new class of conjugated aromatic systems based on different heteroatoms having well defined microstructure and conjugation path length.

2.2 Results and discussions

Here we describe the selective synthesis of a novel macrocycle containing two aromatic stilbene units that are connected by two –Ge-O-Ge (germoxane) linkages (Scheme 2.2). The synthesis involves olefin metathesis using the functional-group-tolerant Hoveyda-Grubbs type Ru-based initiators systems. As will be demonstrated, two germanium atoms stand in direct electronic conjugation with each aromatic segment causing a bathochromic shift in the optical spectra. Electron density is transferred from the oxygen atoms through the Ge orbitals into the aromatic segments. The optical properties are interpreted with the help of theoretical density functional theory (DFT) calculations using two basis sets: B3LYP/6-31G** and B3LYP/Lanl2dz. Using trans-stilbene as aromatic segment enables the results to be compared and interpreted based on a large body of literature on the physico-optical properties of isolated stilbene and derivatives.

The bisstyryl-containing germoxane monomer **1** (Scheme 2.1) was synthesized similarly to a siloxane homolog reported in a literature mentioned earlier. By carefully choosing the alkyl side – chain substitutions on Ge and optimizing the reaction conditions, especially monomer concentration and catalyst/monomer ratio, this olefin metathesis of **1** selectively yielded macrocycle **2** (Scheme 2.2) using Ru alkylidene complexes of the types “Grubbs 2^{nd} generation” and “Hoveyda Grubbs 2^{nd} generation”. Quantitative conversions were observed at reaction temperatures above ~50 ^{0}C. The olefin metathesis reaction mixtures remained homogeneous and a color change could be observed as the reaction progressed.

2.2.1 Monomer synthesis

The monomer **1** was synthesized according to Scheme 2.1 shown below. In the first step, *p* – bromostyrene was treated with magnesium in THF under reflux conditions for 6 h. The formed Grignard reagent was added dropwise to a solution of dibutyldichlorogermane in THF and the reaction was continued overnight at room temperature. The magnesium salt byproduct was first precipitated by adding hexane and then filtered off. To the hexane solution, water was added and the mixture stirred for 48 h. The hexane fraction was collected and treated with sodium sulfate. After evaporation of the hexane, a crude product was obtained as residue. This crude product was purified by column chromatography. Typical yields after purification were 75%

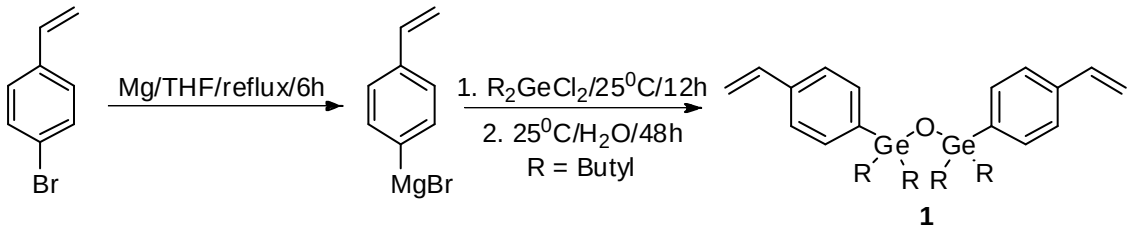

Scheme 2.1 Synthesis of monomer **1**

2.2.2 Olefin metathesis

The synthetic scheme for macrocycle **2** is shown in Scheme 2.2. Successful olefin metathesis was carried out in the presence of Hoveyda – Grubbs 2nd generation catalyst in toluene at 55 – 60^{0}C for 48 h under intermittent vacuum. The reaction mixture obtained was purified by column chromatography. The yield of isolated **2** after purification was 75%. Reaction optimizations included varying solvent, catalyst, catalyst/monomer ratios and temperature. Above reaction conditions represent the optimized conditions. Exploring different catalysts, Grubbs 2nd generation catalyst did not result in significant monomer conversion even at higher temperatures. With the Hoveyda – Grubbs 2nd generation catalyst reaction occurred at temperatures above

50^0C. Below 50^0C, no conversion was observed. Of the solvent systems tested, only pure toluene yielded product (tested solvents: THF, toluene, hexane, DCM and mixtures thereof).

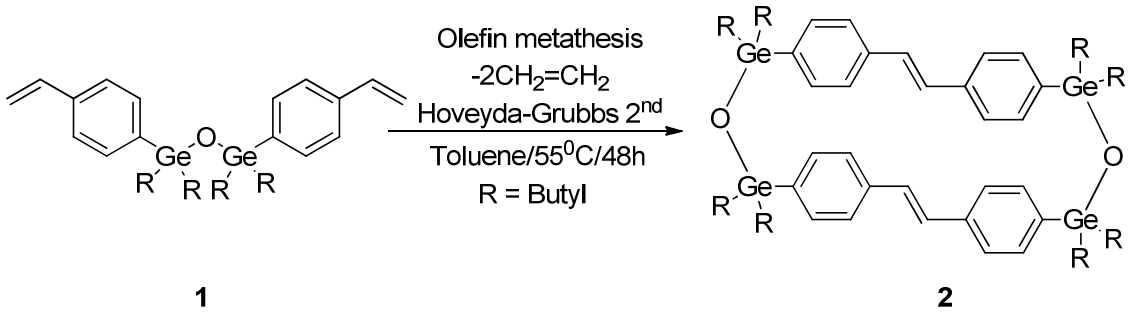

Scheme 2.2 ADMET of **1**

2.2.3 Characterization

2.2.3.1 NMR (Microstructure analysis)

The microstructure of both the monomer and the macrocycle were determined by ^{1}H and ^{13}C NMR spectroscopy as shown in Figures 2.1 – 2.4.

The proton resonances from the terminal vinyl group (–CH=C**H$_2$**) of the monomer appear as two doublets 5.28 (cis, $\mathbf{H_a}$, J = 11 Hz) and 5.79 (trans, $\mathbf{H_b}$, J = 17 Hz) ppm respectively. The –C**H$_c$**=CH$_2$, (J = 11 Hz) proton resonance appears as a doublet of doublets at 6.70 ppm. The resonances from the aromatic protons ($\mathbf{H_d}$ and $\mathbf{H_e}$) are centered around 7.46 ppm as two doublets. The chemical shifts of the aliphatic chain protons (butyl group) are observed around 0.89 – 1.50 ppm.

After completion of the formation of macrocycle **2**, the resonances from the terminal vinyl groups in **1** are no longer observed. A new singlet resonance at 7.13 ppm is assigned to the new internal trans vinylene protons (-C**H$_a$**,=C**H**-). No resonances for a cis-configured double bond were observed. Such resonance would be expected around 6.99 ppm[73]. The aromatic protons

appear as a resonance at 7.53 ppm. The protons from the butyl chains are observed in the range of 0.89 – 1.37ppm. The down field shift of the aromatic protons in **2** relative to **1** can be explained by the extended electron conjugation in the larger aromatic segments of the macrocycle compared to the monomer.

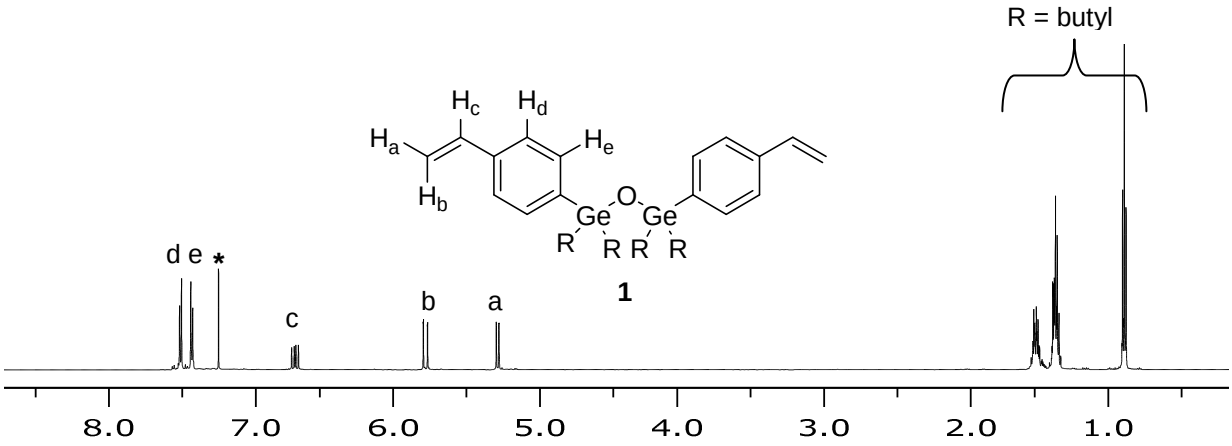

Figure 2.1 ^{1}H NMR (600MHz, $CDCl_3^*$) spectrum of **1**

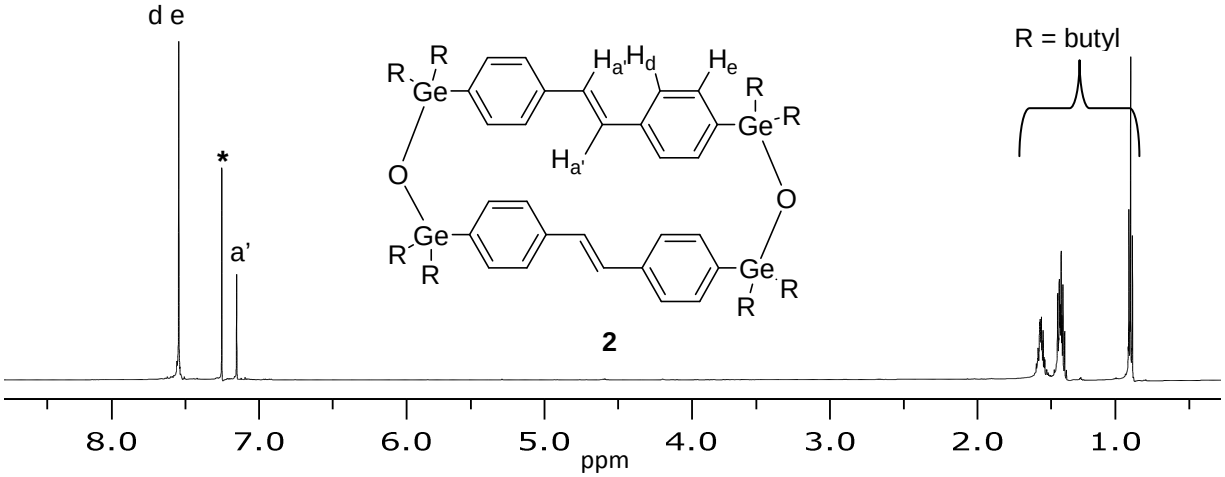

Figure 2.2 ^{1}H NMR (600MHz, $CDCl_3^*$) spectrum of **2**

In **1**, the carbon resonances associated with the terminal vinyl group (-$\underline{C_B}H=\underline{C_A}H_2$) are observed at 114.9 and 136.6 ppm respectively. The carbon resonances from the benzene ring are found at 126.1, 133.1, 137.1, 138.9 ppm. After metathesis, the carbon resonances of the terminal vinyl

group disappear and a new resonance around 129.2 ppm is observed, corresponding to the internal vinylene carbons (-$\mathbf{C}_{\mathbf{A}}$,H=**C**H-).The resonances of the carbons from the benzene rings are observed at 138.5, 126.5, 133.2 and 137.1 ppm. The complete ^{1}H NMR and ^{13}C NMR shifts and assignments of **1** and **2** are summarized in Table 2.1

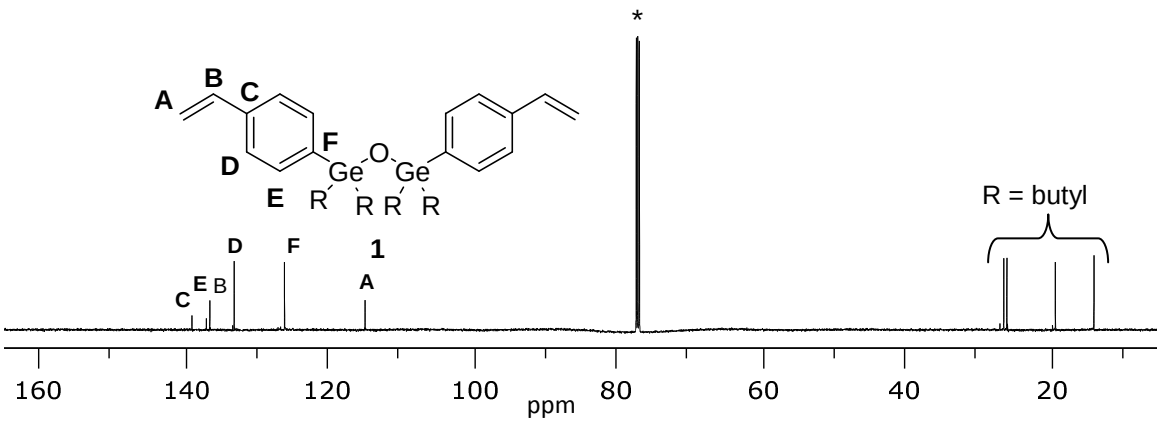

Figure 2.3 ^{13}C NMR (125MHz, $CDCl_3^*$) spectrum of **1**

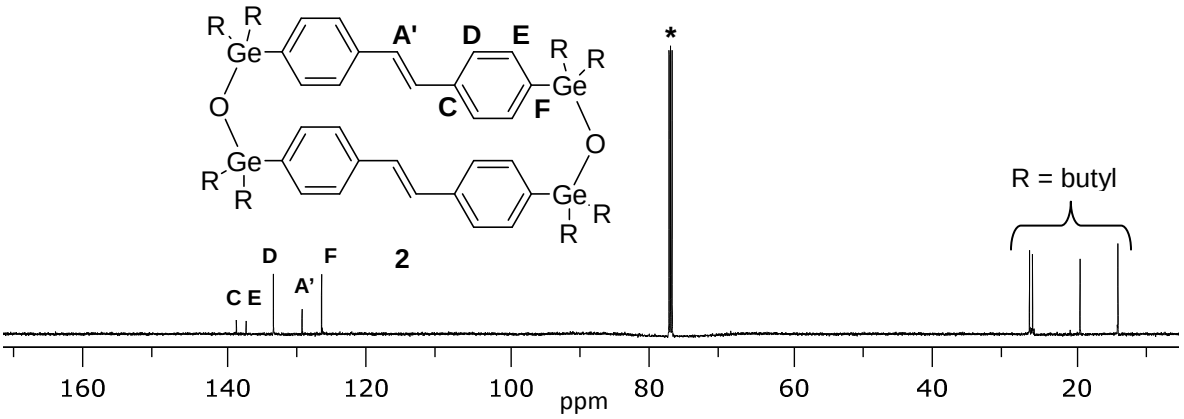

Figure 2.4 ^{13}C NMR (125MHz, $CDCl_3^*$) spectrum of **2**

Table 2.1 Summary of ^{1}H NMR and ^{13}C NMR assignments of **1** and **2**

				ppm			
Structure (^{1}H NMR)	**a**	**b**	**C**	**d,e**	**a'**		
1	5.28	5.79	6.70	7.46	-		
2	-	-	-	7.53	7.13		
Structure (^{13}C NMR)	**A**	**B**	**C**	**D**	**E**	**F**	**A'**
1	114.9	136.6	138.9	133.1	137.1	126.1	-
2	-	-	138.5	133.2	137.1	126.5	129.2

2.2.3.2 Size analysis (GPC and MALDI – TOF)

Figure 2.5 shows the gel permeation chromatograms of the monomer **1** and the macrocycle **2**. In case of the macrocycle a narrow monomodal distribution at 36.3 min is observed for the major product fraction in the system. Smaller amounts of higher molecular weight homologs are indicated by the shoulder at higher molecular weights (35 min), most likely a large macrocyclic byproduct. The tailing (31 – 34 min) indicates the possible presence of linear polycondensates, albeit in minor quantities. This is expected as ring closing always competes with chain growth in a ring/chain equilibrium typical for olefin metathesis; α, ω diolefins can undergo linear as well as cyclic polycondensation. The position of this equilibrium depends on thermodynamics and kinetics.[74] In this case, the conditions have been adjusted to almost exclusively lead to dimeric macrocycle.

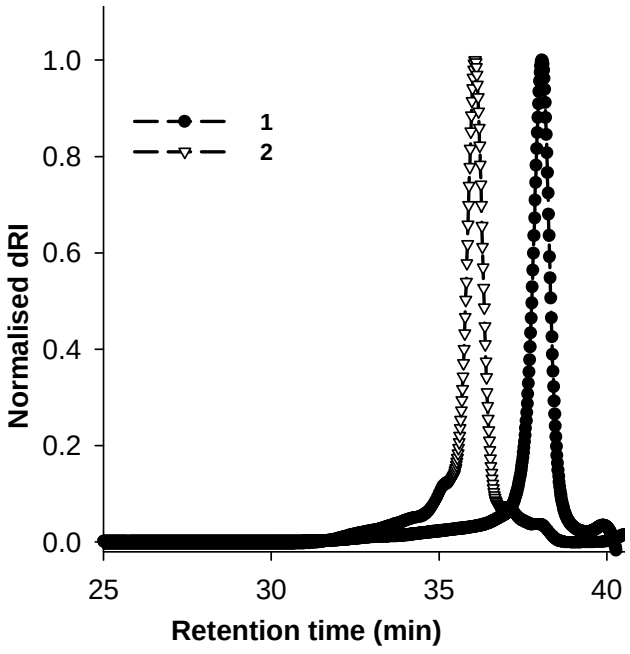

Figure 2.5 GPC chromatograms of **1** and **2** (THF)

MALDI – TOF of the monomer and the macrocycle was performed in the presence of dithranol as matrix and silver acetate. The observed isotope distributions of both **1** and **2** are in good agreement with the calculated spectra. The observed molar masses of monomer **1** and macrocycle **2** are 703 Da and 1350 Da respectively, which takes into account the atomic weights of one Ag^+ for monomer **1** and two Ag^+ for macrocycle **2**. The experimental molar mass of **2** proves the presence of the dimeric macrocycle is as expected.

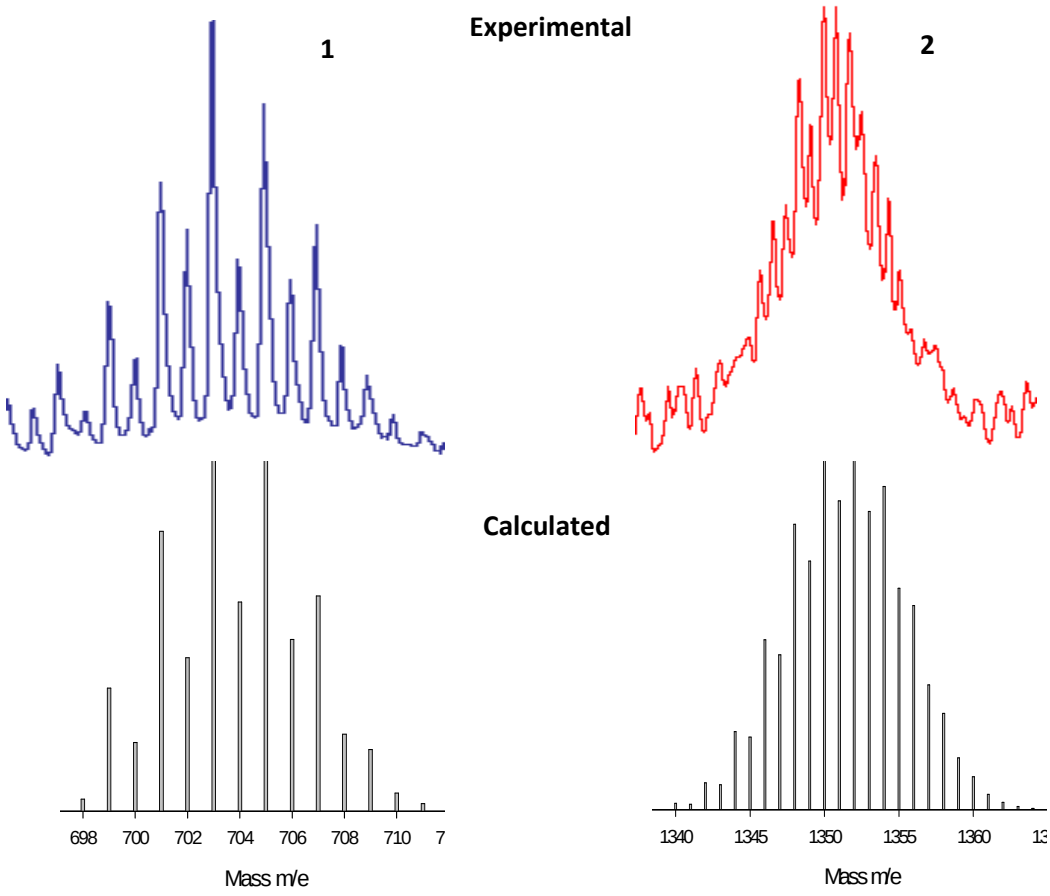

Figure 2.6 Isotope distributions of **1** and **2** (experimental and calculated)

2.2.3.3 Optical properties (UV/Vis and fluorescence spectroscopy)

UV/Vis absorption and emission spectra of hexane solutions of **1**, **2**, and *trans*- stilbene are shown in Figure 2.7. **1** and **2** show maxima for absorption at 256 nm and 320 nm and emission at 306 nm and 363 nm respectively. The absorption spectrum of **2** features two major components with maxima at 308 nm and 320 nm and a shoulder at 340 nm. Absorption and emission of **2** are structurally very similar to trans-stilbene, but 24 and 16 nm red shifted respectively. The red shift of the macrocycle **2** relative to **1** is expected and due to the extended conjugation. Compared to siloxane containing homologoues of **1** and **2** reported earlier the recorded absorption spectra are very similar however the emission spectrum is red shifted by 3 – 4 nm compared to the siloxane homologs (mentioned earlier). The shorter Ge – O bond length (1.776 A) accounts for higher electron density over the germanium atoms present in **2**, as a result of which the HOMO of the system is raised leading to a decrease in the HOMO – LUMO gap.[75] The fluorescence quantum yield of **2** was determined as ~40% in hexane, relative to pure trans-stilbene (5% yield in hexane).[76] Two stilbene units are tied through Ge-O-Ge linkages on both sides, preventing a photo-induced cis – trans isomerization of the vinylene bond usually observed in isolated trans-stilbene. As a result, **2** features a lesser number of nonradiative pathways for the relaxation of the excited states compared to stilbene.[77] Consequently, a higher fluorescence quantum efficiency is observed.

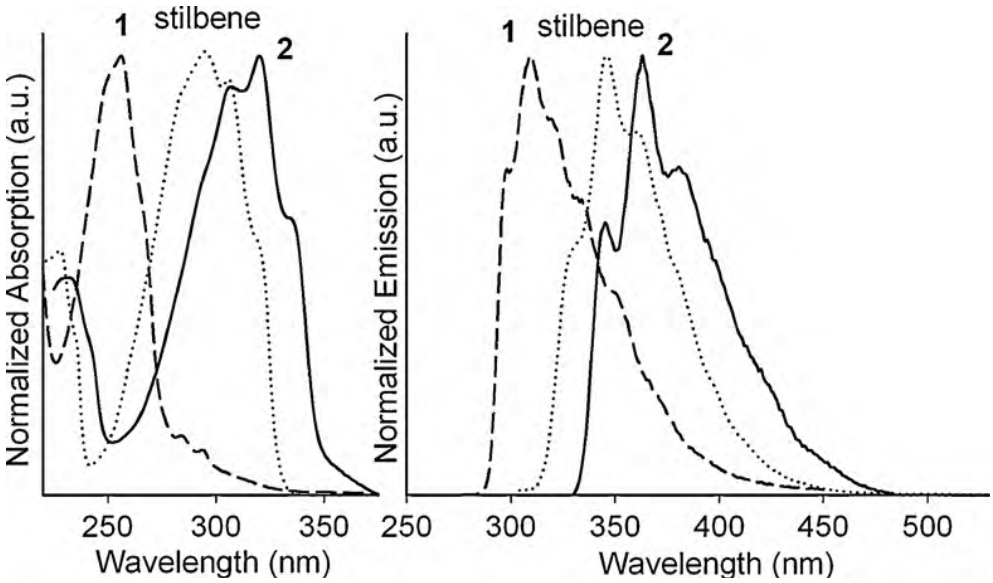

Figure 2.7 Absorption and emission spectra of **1**, **2** and trans – stilbene (in hexane)
[1] = [2] = [trans-stilbene] = 3.1x10^{-6}M
Excitation in absorption maxima: 256 nm for **1** and 320 nm for **2**

2.2.3.3.1 Theoritical calculations

To investigate both the red shift and high quantum efficiency in more detail, we used theoretical calculations to understand the influence of the heteroatoms and structural confinements on the electronic system of the trans-stilbene segment which acts as the fluorophore. A large body of experimental and theoretical literature on isolated trans-stilbene served as reference.[78-82] In a first step, the structures for R = methyl were optimized at the DFT level using B3LYP/6-31G** and B3LYP/Lanl2dz. The methyl group was chosen in place of butyl groups for reasons of reduced calculation time. No significant consequences are to be expected, as the basis set 6-31G** treats the polarizations of -CH_3 and extended alkyl chains similarly.[83] The first basis set 6-31G** adds polarization to both carbon and hydrogen. However, to understand the effect of heavier atoms like germanium, we also need a, second basis set, Lanl2dz, which places double zeta function over the valence shell of the heavier atom, whereas the inner shells are represented by electron core potential (ECP).[84] Identical calculations were carried out for **1**, **2**, and trans-stilbene. With the optimized structures, molecular orbitals were calculated based on time dependent density functional theory (TDDFT). For **1**, **2** and trans-stilbene, the optimized structure and the molecular orbitals associated with the main transitions for the absorption of **2** are illustrated in Figure 2.8 Calculated HOMO-LUMO energy gaps and absorption maxima are listed in Table 2.2, together with the observed values for absorption.

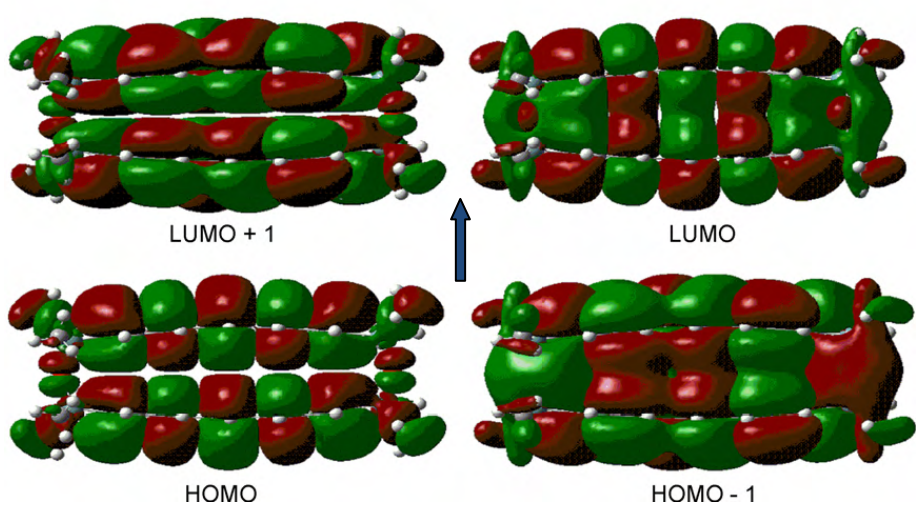

Figure 2.8 Two dominant absorptions i.e.: HOMO to LUMO + 1; HOMO - 1 to LUMO

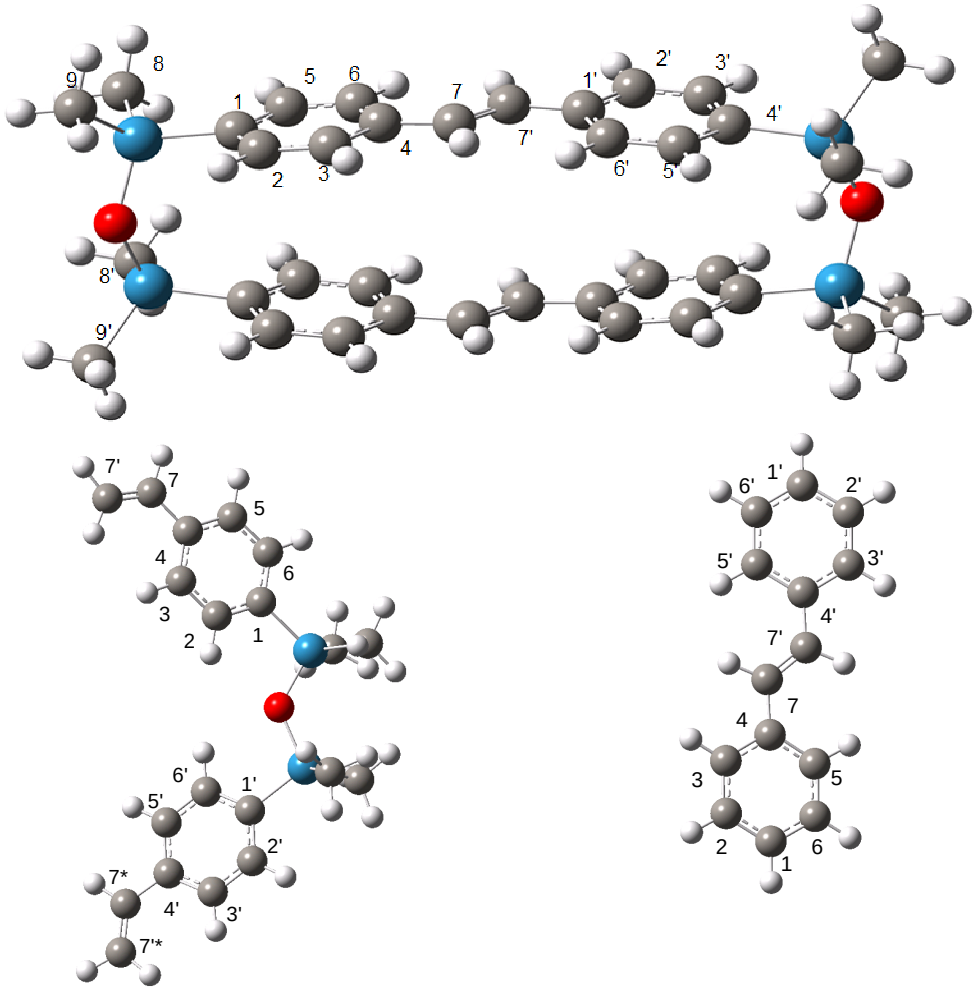

Figure 2.9 Optimized stuctures of **1**, **2** and trans-stilbene

Table 2.2 Absorption data of **1** and **2** along with HOMO – LUMO gap

Molecule	**Experimental**	**Calculated***	
	λ_{max} **(nm)**	λ_{max} **(nm)**	**HOMO-LUMO(eV)**
1	256	257	5.05
2	320	330	3.82
trans-stilbene	294	309	4.16

* based on B3LYP/6-31G** structure

Table 2.3 Geometrical Parameters for full geometry optimized **2**

Parameters	**Value[a,b]**	
d(C7-C7')	1.348	1.360
d(C7-C4)	1.468	1.472
d(C4'-C7')	1.468	1.472
d(C3-C4)	1.409	1.417
d(Ge-C1)	1.960	1.970
d(Ge*-C1)	1.970	1.970
d(Ge-O)	1.799	1.776
α (C7'-C7-C4)	123.3	126.8
α (Ge-O- Ge*)	133.1	160.4
α (C1- Ge-O)	110.4	109.3
α (C1- Ge*-O)	110.4	109.3
α (C9- Ge-O)	104.3	107.2
α (C9'- Ge-O)	104.3	107.2
α (C'-C7'-C4'-C3')	178.9	178.4
α (C4-C7-C7'-C4')	174.5	174.0

[a] d in Å; α in degrees ^{o}; [b] left value on B3LYP/6-31G** level right value on B3LYP/Lanl2dz level based calculations

Table 2.4 Geometrical Parameters for full geometry optimized **1** and **trans-stilbene**

trans-stilbene			**1**		
Parameters	**Value[a, b]**		**Paremeters**	**Value[a, b]**	
d(C7-C7')	1.348	1.36	d(C7-C7')	1.359	1.353
d(C7-C4)	1.466	1.47	d(C7-C4)	1.471	1.479
d(C4'-C7')	1.466	1.47	d(C4'-C7')	1.405	1.479
d(C3-C4)	1.41	1.42	d(C3-C4)	1.403	1.415
α (C7'-C7-C4)	127.1	126.9	d(Ge-C1)	1.930	1.966
α (C7-C7'-C4'-C3')	179.7	180.0	d(Ge-O)	1.793	1.770
α (C4-C7- C7'- C4')	174.9	180.0	α (C7'-C7-C4)	127.6	127.5
			α (C7-C7'-C4'-C3')	179.9	179.5

[a] d in Å; α in degrees ^{o}; [b] left value on B3LYP/6-31G** level right value on B3LYP/Lanl2dz level based calculations

Geometrical Parameters for the full geometry optimized **2** are summarized in Table 2.3 along with **1** and *trans* – stilbene in Table 2.4. The distance between two Ge atoms of one Ge-O-Ge link was calculated as 3.3 Å, well within the typical ππ stacking distance as reported by Dufresne et al. in the case of diamino stilbene derivatives,[85] whereas the distance between the two vinylene bonds was calculated as 4.4 Å (Figure 2.9).

Based on the calculated Mulliken charges, every stilbene segment carries a net partial charge of -0.478 concentrated on the vinylene bond. The partial negative charge over the vinylene bonds comes from the two oxygen atoms that carry partial positive charge.The high electron density results in repulsion, causing an outward deformation of the stilbene units away from each other. This repulsion also leads to an opening of the GeOGe angle to 133.1^{o} (160.4^{o} on the B3LYP/Lanl2dz level). In silicon based compounds, a more linear SiOSi angle is widely accepted to result in more favorable orbital interactions between the lone pairs of the O and the empty orbitals of Si. In the case of the presented macrocycle, a favorable through – space orbital interaction between oxygen and stilbene or the involvement of d-orbitals of the germanium atom would provide an explanation for the mechanism of moving electron density to the aromatic segments, and the red shift relative to isolated trans-stilbene. The calculated absorption results are in excellent agreement with experimental values (λ_{max}).The observation of two major emission components at 308 nm and 320 nm are also supported by the calculations (calc. absorption: 330 nm). HOMO and LUMO show very different symmetries. TDDFT calculations suggest two about equally important absorptions involving transitions (HOMO-1)/LUMO (transition at 308 nm) and HOMO/(LUMO+1) (transition at 319 nm) with relative contributions of ~40% and ~47%, respectively (see also Figure 2.8). Ongoing theoretical investigations are

aimed at optimizing the structure of the excited state and providing a detailed comparative study involving the homologous siloxane and germoxane containing macrocycles.

2.3 Conclusion

The synthetic approach presented potentially allows access to a variety of structural homologues with different aromatic segments in direct electronic conjugation to Ge or other heteroatoms. This will enable detailed structure/property investigations into electronically intriguing systems with significant practical importance in organic light emitting devices (OLED) and photovoltaic cells.

2.4 Experimental

General Information

All of the experiments using air/moisture sensitive materials were carried out in a nitrogen filled Labconco protector glove box and/or by the use of dry argon filled dual manifold (inert gas/ vacuum) using standard Schlenk line techniques. All glassware was cleaned and dried for at least 16 h in an oven at 120 ^{0}C prior to use.

Chemicals

Magnesium turnings, sodium sulfate and Grubbs-Hoveyda (2nd Generation) catalyst were obtained from Aldrich. *p*-bromostyrene (98%) was obtained from Alfa Aesar and dichlorodibutylgermane was obtained from Gelest Inc. Magnesium turnings was flame dried under high vacuum prior to use. Solvents e.g. tetrahydrofuran (THF), toluene, hexane came from Fisher Scientific. All solvents were dried and degassed by a "Pure Solv" solvent purification system (using activated alumina, copper catalyst, molecular sieves column when appropriate) by Innovative Technology Inc. before use. All other chemicals were used as received.

Instrumentation

^{1}H NMR (600 MHz) and ^{13}C NMR spectra were recorded in $CDCl_3$ on Varian Unity NMR instruments. $CDCl_3$ was used as an internal deuterium lock for the spectra. All of the signals in the NMR spectra are reported in ppm, multiplicity (s = singlet, d = doublet, t = triplet, q = quadruplet, m = multiplet, dd = doublet of doublet).

UV-Visible absorption spectra were recorded using a Perkin Elmer Model 650 UV Spectrophotometer with 1-cm path length cells. The samples were prepared with HPLC grade hexane ("Spectrasolv") in a sample cell.

Photoluminescence spectra were recorded using a Horiba Jobin Yvon Fluoromax-3 spectrofluorometer with 1-cm path length cells. The samples were prepared with HPLC grade hexane ("Spectrasolv") in a sample cell.

GPC analysis was carried out on an Alliance GPCV 2000 (Waters) instrument equipped with four Waters Styragel HR columns, i.e. HR-1, HR-3, HR-4, and HR-5E. HPLC grade THF was used as eluent, at a flow rate of 1.0 mL/min at 40 ^{0}C. Measurements are relative to a calibration with polystyrene standards and third order relative calibration curve was used to measure the molecular weight of unknown samples.

Computer time for the theoretical calculations was provided by City University of New York's High Performance Computing Research Center.

Synthesis of monomer 1

p-Bromostyrene (12.1 mmol) was dissolved in 25 ml THF. To this solution 24.2 mmol flame dried magnesium was added. The reaction mixture was refluxed for 6 h under argon. The solution was separated from unreacted magnesium and added dropwise to 11.2 mmol of di-n-butyldichlorogermane in 15 ml dry THF under argon at room temperature. The reaction was continued for 12 h. After 12 h 60 ml pentane was added dropwise to the reaction mixture until precipitation seized. The mixture was immediately filtered. To the filtrate 15 ml of distilled water was added and stirred at room temperature for two days. The organic layer was collected and dried. The product was then dissolved in dichloromethane and filtered through treated silica column. Yield: 60%.^{1}H NMR (600MHz, $CDCl_3$): δ = 7.46 (dd, 8H, aromatic –CH), 6.70 (dd, 2H, -C**H**=CH_2), 5.28 and 5.79 (d, 4H, -CH=C**H$_2$**), 1.50 (m, 8H, –CH_2), 1.36 and 1.45 (m, 16H, -CH_2), 0.886 (t, 12H, -CH_3).

Synthesis of macrocycle 2

Monomer 1 (0.366 mmol) was dissolved in 2ml of dry toluene. To this solution $9.25x10^{-3}$ mmol of Grubbs-Hoveyda 2nd generation catalyst was added [12]. The solution was stirred for 48 h under argon at 55 ^{o}C. Completion of reaction was indicated by ^{1}H-NMR (dissappearance of resonance from vinyl-protons versus appearance of resonances from vinylene-protons). The crude product was washed in hexane. The hexane layer was separated and then evaporated. The product was dissolved in DCM and then passed through silica column to purify the product. Yield: 75%.^{1}H NMR (600MHz, $CDCl_3$): δ = 7.53 (br, s, 16H, aromatic –CH), 7.13 (br, s, 4H, -CH=CH-), 1.54 (m, 16H, $–CH_2$), 1.35 and 1.37 (m, 32H, $-CH_2$), 0.886 (t, 24H, $-CH_3$),

3. Boron and silicon containing conjugated macromolecules

3.1 Introduction

Silicon and boron-containing conjugated materials are of much current interest for their potential use in organic light-emitting diodes, photovoltaics, and in sensory applications (see above also).[86] While a great variety of different polymerization methods have been pursued for their preparation, acyclic diene metathesis polymerization (ADMET) is attractive because the reactions conditions are typically mild, the ethylene formed as a byproduct is readily removed under vacuum, and the resulting polymer microstructures are well-defined.

We have recently demonstrated that silylene-containing conjugated polymers can be accessed via ADMET of conjugated silanes that feature two styryl moieties. A red shift in the emission spectra of the products compared to isolated stilbene showed the participation of silicon in the conjugation. In related work, Interrante and coworkers reported the preparation of photocurable and photoluminescent polycarbosilans.[87] The polymer films were thermally or photochemically cross-linked to yield blue-photoluminescent films. Polymers containing germanium, tin, and phosphorous are further examples of inorganic polymers synthesized via ADMET polymerization. For example, germanium-based polymers are of interest for applications in microlithography and as precursors for ceramics.[88]

To our knowledge, conjugated boron polymers with boron in the backbone and participating in the conjugation have not been reported to date. In fact, the only example of incorporation of boron-monomers into polymers by ADMET has been reported by Wagener and coworkers, who studied the polymerization of α,ω-vinyl-functionalized boronates.[89] Although the boronate monomers were metathesis active, ligand-exchange reactions among the boronate functional

groups and ring formation in solution prevented isolation and characterization of the polymers. The presence of these scrambling processes was confirmed via NMR spectroscopy.

This thesis describes the extension of the ADMET synthetic strategy that we have discussed earlier to Lewis acidic boron containing systems. The main objective was to develop and synthesize well-defined boron containing homopolymers and co-polymers (with silicon monomers) with high structural purity, and under the ADMET conditions that we have already established so far, thereby generating a new class of polymeric and co-polymeric systems having valuable photophysical properties arising from Lewis acidic boron in the case of homopolymers or both boron and silicon in the case of co-polymers.

We describe here the preparation of two different luminescent distyrylborane monomers and the successful preparation of the first conjugated organoborane homopolymers and random copolymers with organosilicon monomers. One of the boron-containing monomers features the 8-hydroxyquinolato (q) chelate ligand, where the access to the otherwise very reactive boron center is limited by tetrahedral co-ordination of boron with the quinolate moiety in order to make the systems stable under the ADMET conditions. A second luminescent monomer was prepared in which the boron is tri-coordinated but in which access to the boron center is sterically hindered using a sterically demanding tri-isopropyl phenyl ligand (Trip), thus making it less acidic and more stable.

3.2 Results and discussions

The bisstyryl-containing silylene monomer **1** (Scheme 3.1) was synthesized according to literature mentioned earlier. Olefin metathesis of **1** and **2(a,b)** using Ru alkylidene complexes of the types "Hoveyda Grubbs 2nd generation" to generate homopolymers **p2a**, **p2b** via homo-metathesis and random co-polymers **p12a**, **p12b** via cross metathesis is summarized in Scheme 3.2. Quantitative conversions were observed at reaction temperatures above ~55^{0}C. Below 55^{0}C no conversion was observed. The olefin metathesis reaction mixtures remained homogeneous (except in the case of **p2b**) and a color change could be observed as the reaction progressed.

3.2.1 Monomer synthesis

The general strategy for the synthesis of the monomers is shown in Scheme 1. Reaction of two equivalents of monoacetal of *p*-bromobenzaldehyde with dichloro dioctyl silane via lithiation resulted in the formation of silylene bis-acetal product which was further hydrolyzed to form silylene bis-dibenzaldehyde. Wittig reaction of bis-benzaldehyde led to the formation of co-monomer **1**. This monomer was purified by passing through silica gel using hexane as the eluent and was obtained as colorless oil. The experimental molecular weight was 288 g/mole (measured by GPC) which is in good agreement with the theoretical molecular weight 264 g/mole. The synthesis of the boron monomers started with *p*-chlorostyrene, which was converted into the Grignard reagent. Reaction of two equivalents of this Grignard with $B(OR)_3$ (R = Me or Bu) in THF gave distyrylalkyloxyborane, $Sty_2B(OR)$. Subsequent treatment with a small excess of triisopropylphenyl Grignard led to the formation of monomer **2a** in 25% isolated yield, whereas reaction with 2-*n*-hexyl-8-hydroxyquinoline gave the tetracoordinate monomer **2b**. The monomers were purified by column chromatography using hexanes as the eluent and isolated by recrystallization from hexanes. Both monomers showed excellent solubility in common organic

solvents such as CH_2Cl_2, THF, and toluene. The described synthesis for **2a** and **2b** was developed and carried out by Dr. Ami Doshi of Rutgers University.

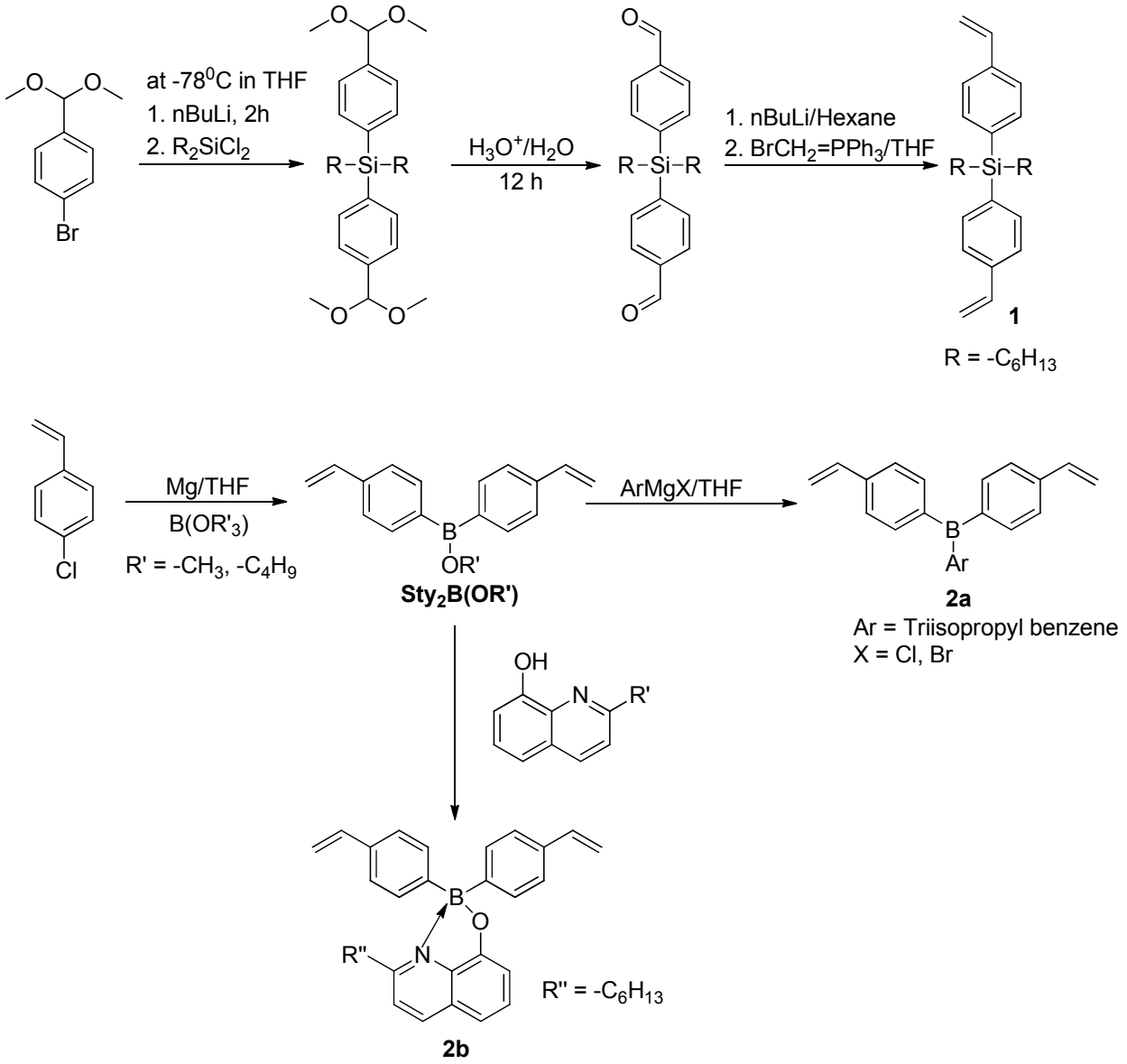

Scheme 3.1 Synthesis of Boron and Silicon containing monomers

3.2.2 ADMET polycondensation

The synthetic scheme for homopolymers **p1**, **p2a**, **p2b** and copolymers **p12a**, **p12b** is shown in Scheme 3.2. Successful olefin metathesis was carried out in the presence of Hoveyda – Grubbs 2nd generation catalyst in toluene at 55 – 60^{0}C for 48 h under vacuum. The reaction mixtures obtained were purified by column chromatography. In the case of homopolymers **p1** and **p2a** the isolated yields were around 70-75% after purification. However, in case **p2b**, the polymerization was stopped after 45 min due to the formation of insoluble precipitate which was not characterized further. The yield of isolated copolymers **p12a and p12b** after purification were ~70 - 75%. Reaction optimizations included varying solvent, catalyst and temperature. Above reaction conditions represent the optimized conditions. Exploring different catalysts, Grubbs 2nd generation catalyst did not result in significant monomer conversion even at higher temperatures. With the Hoveyda – Grubbs 2nd generation catalyst reaction occurred at temperatures above 55^{0}C.Below ~50^{0}C no conversion was observed. The ratio of concentration of monomer to catalyst ([monomer]/[catalyst]) in a typical homopolymerization/copolymerization was around 28:1. Of the solvent systems tested, only pure toluene yielded product (tested solvents: tetrahydrofuran (THF), toluene, hexane, dichloromethane (DCM) and mixtures thereof).

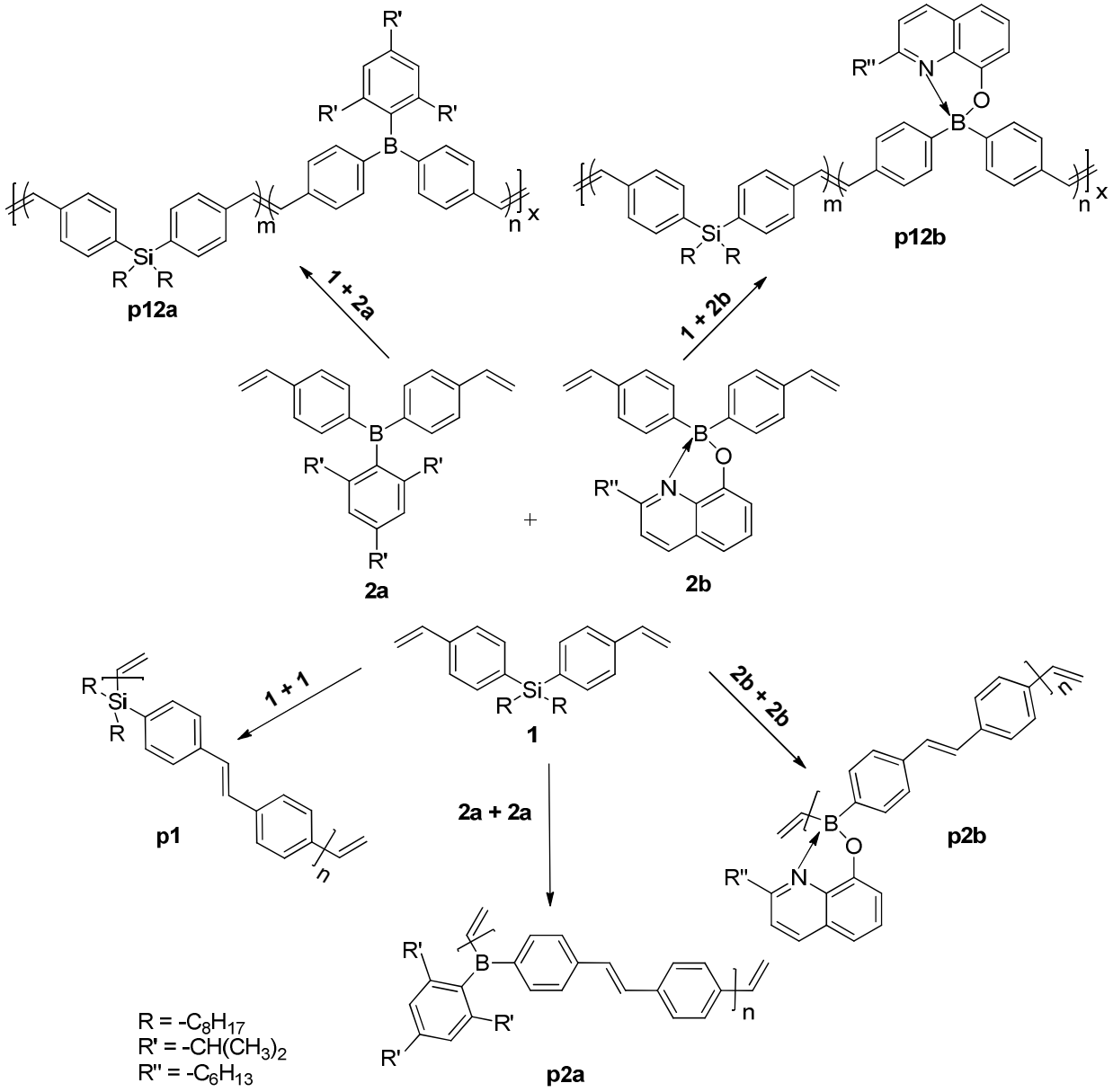

Scheme 3.2 Syntheses of homopolymers and copolymers via ADMET

3.2.3 Characterization

3.2.3.1 Size analysis

Molecular weights (M_n) of the ADMET polycondensation products were determined by gel permeation chromatography (GPC) relative to polystyrene standards. Traces for the differential refractive index (dRI) detector responses are shown for **p1**, **p2a**, **p12a**, and **p12b** (Figure 3.1).

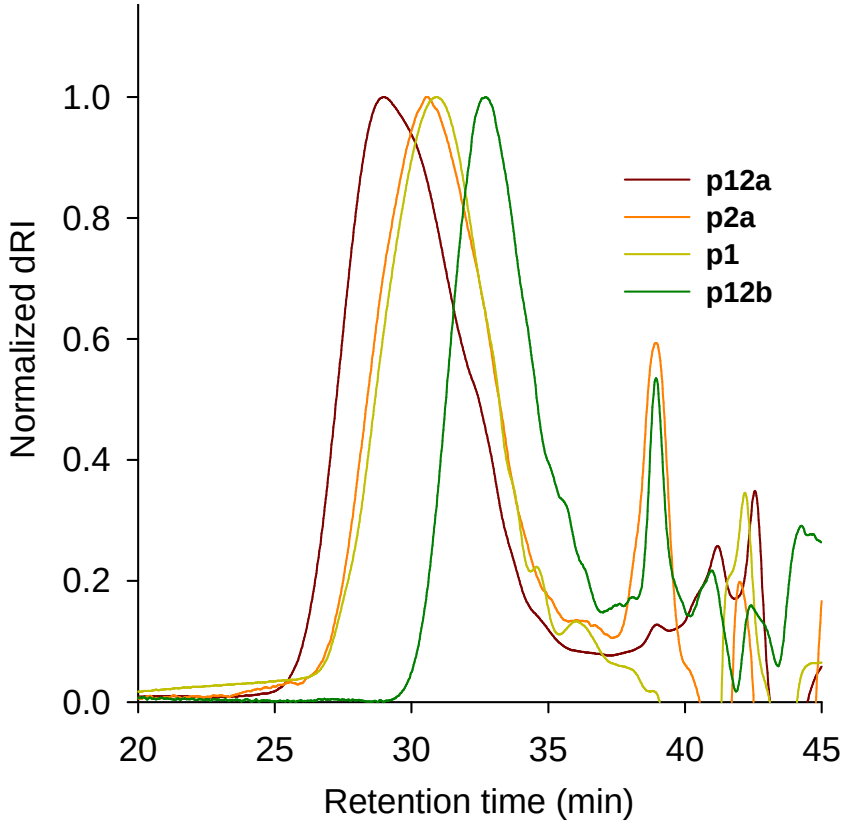

Figure 3.1 GPC traces of **p12a**, **p2a**, **p12b** and **p1**

Table 3.1 summarizes representative M_n (GPC and NMR results) and polydispersities (M_w/M_n) for **p1**, **p2a**, **p12a**, and **p12b** synthesized under similar reaction conditions. The calculated M_n values based on NMR were calculated by end group analysis (integrals of signals from chain end vinyl protons vs. chain internal vinylene protons, see also NMR discussion below). The presented results characterize representative polycondensates synthesized in toluene at 60 ^{o}C

after 48 h reaction time. The homopolymers **p1** and **p2a** showed M_n ~ 3,900 and 5,440 g/mol in the GPC analysis and 6,260 and 7,070 g/mol in the NMR analysis respectively. Due to some insoluble residue (~15%) the observed M_n for **p2a** most likely underestimates the real value. Polydispersities were in the range of 1.7 – 2.2. Since monomer **2b** was only partially soluble, a GPC analysis was not performed.

Polymerization of **2b** resulted in an insoluble precipitate after 1-2 h reaction time and was not investigated further with regard to molecular weight or structure. GPC analysis of **p12a** and **p12b** yielded M_n of 7,480 and 2,240 g/mol, NMR yielded M_n ~ 14,850 and 7,790 g/mol respectively.

Lower reaction temperatures generally resulted in lower conversions, higher reaction temperatures in an increase of insoluble precipitate, particularly in the case of **p2a**. Reaction temperatures below 50 ^{o}C did not yield any product at all, regardless of catalyst used. Higher ratios of [monomer]/[catalyst] resulted in lower conversions, and lower ratios of [monomer]/[catalyst] in increased precipitation of insoluble byproduct in the case of **p2a**. Among the solvents investigated, pure toluene yielded the best results and pure THF resulted in no conversion, using mixtures of toluene and THF resulted in low conversion.

As the chain size increases with conversion, it is expected that the chain growth reaction starts to compete with ring closing, in an equilibrium described above.[74] Thus it is possible that small fractions of the polymeric products consist of cyclic macromolecules. This might explain some of the shoulders on the low molecular weight side of the distributions in the GPC traces as well as the fact that end-group calculations based on well-resolved NMR spectra yielded significantly higher molecular weights than GPC analysis.

Table 3.1 ADMET polycondensation results and molecular weights

Sample	Reaction Conditions[1]		M_n g/mole		M_w/M_n
	[Monomer] mM	[Catalyst] mM	GPC	NMR	
p1	200	4*	3900	6260	1.75
p2a	70	2.5	5440	7070	2.23
p2b[2]	70	2.5	n.d.	n.d.	n.d.
p12a	40, 40 ([1],[2a])	2.3	7480	14850	2.03
p12b	50, 50 ([1],[2b])	3.2	2240	7790	1.68

[1] T = 60 °C/ t = 48 h/ toluene; [2] insoluble precipitate after 1-2 h reaction time, n.d. = not determined); * Grubbs 2nd generation catalyst – all other entries: Grubbs-Hoveyda catalyst.

3.2.3.2 NMR (Microstructure analysis)

The silylene monomer **1** was characterized earlier by ^{1}H, ^{13}C and ^{29}Si NMR spectroscopy in our group in a literature mentioned earlier. The boron monomers **2a** and **2b** were fully characterized by ^{1}H, ^{13}C and ^{11}B NMR spectroscopy in a separate report.[90] In the case of **2a**, the presence of a broad ^{11}B NMR signal at 70 ppm (frequency at half width, $w_{1/2}$ = 1900 Hz) is typical of tricoordinate triarylborane species. In contrast, the hydroxyquinoline monomer **2b** shows a relatively sharp signal at 11.7 ppm (frequency at half width, $w_{1/2}$ = 610 Hz) that is strongly upfield shifted, which is consistent with tetra-coordinated boron. The ^{1}H NMR spectra of the new distyrylborane monomers showed the expected vinyl peak patterns. The vicinal protons $=CH_2$ exhibit two characteristic doublet resonance at around ~5.7 and ~5.1 ppm and the –CH proton showed a double doublet at around 6.7 ppm. Integration of the ^{1}H NMR spectra of the monomers confirmed the 2:1 ratio expected for the styryl groups with respect to those of the aromatic protons of the tri-isopropylphenyl and quinolate groups, respectively.

The microstructures of the polymeric products **p12a** and **p12b** were determined by means of ^{1}H-NMR, Nuclear Overhauser Effect Spectroscopy (NOESY), Heteronuclear Single Quantum Coherence (HSQC) and Correlation Spectroscopy (COSY) techniques. Figure 3.2 displays an overlay of the ^{1}H NMR spectra of **p12a**, **p2a** and **p12b**. Details for **p12a** and **p12b** are enlarged separately in Figures 3.3 and 3.4, respectively, together with their respective structural assignments.

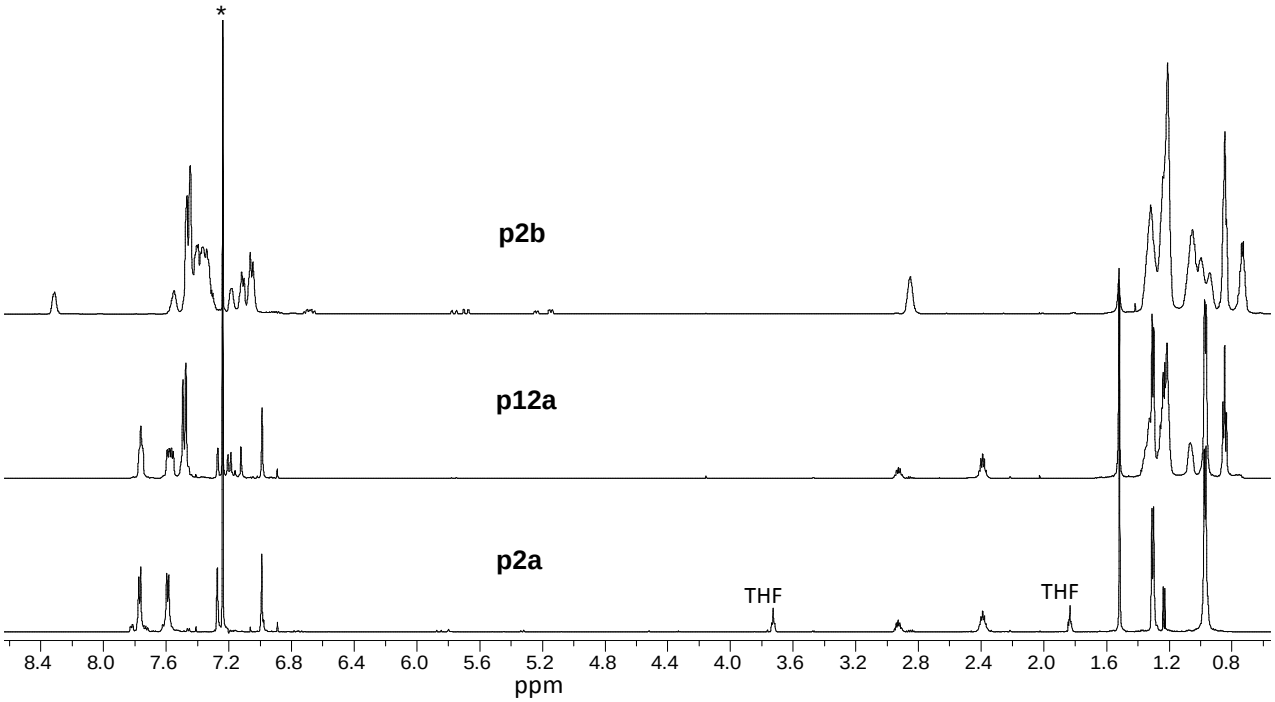

Figure 3.2 ^{1}H NMR (600 MHz, $CDCl_3^*$) spectral overlay of **p12b**, **p12a** and **p2a**

Homopolymerization of **2a** resulted in the formation of linear conjugated system **p2a** with internal vinylene linkages. The internal vinylene proton resonance of **p12a** appeared around 7.27 ppm. The aromatic protons from the stilbene unit appeared as two doublets centered around 7.76 ppm. The aromatic protons from the Trip moiety appeared as a singlet around 6.99 ppm. In the event of partial degradation of **p2a** after the reaction work up a doublet around 1.22 ppm was observed which arose from a free Trip moiety. The co-condensation of two monomers, **1** with **2a** or **1** with **2b**, lead to random co-polymers with three possible coupling modes, giving rise to three distinct vinylene bonds. Coupling of the two monomers always led to the formation of trans – stilbene type repeat unit, either reaction of a Si monomer with another Si monomer or Si with a boron monomer or boron with another boron monomer. Integration of the proton-NMR resonances of these three vinylene types arising from the Si – Si homocoupling, B –B

homocoupling and Si – B heterocoupling, gave a ratio of 1:1:2 respectively in the case of **p12a**. This ratio proved the randomness of coupling vinyl groups, regardless of co-monomer structures. This is only possible if both monomers and resulting chain ends have similar reactivities. This fact is also supported by the observation, that both the monomer systems undergo homo- and co-polymerization under identical experimental conditions. The detailed assignments for **p12a** are illustrated in Figure 3.3 in a representative drawing of a polymer chain segment showing the three possible coupling modes, giving rise to three resonances ‘d’ (Si on both sides of stilbene), ‘e’ (B on both sides of stilbene), and ‘a’ with ‘b’ (Si and B on alternate stilbene sides). They are observed at 7.12ppm, 7.28ppm and as a quartet centered around 7.20ppm respectively. The aliphatic protons from the octyl and the isopropyl groups show resonances in the range of ~ 0.88 – 3.0ppm. Resonances from the vinyl protons from the chain end around 5.29 and 5.78ppm are very small. Integration of these resonances vis-à-vis the resonances from the vinylene protons allowed to calculate a number average molecular weight of ~14,850 g/mol. This is about twice the weight determined by GPC (Table 3.1). One explanation could be the possible formation of macrocycles by “back-biting” of the reactive chain ends (vide supra) as indicated by a shoulder at 32 min in the GPC trace. Such macrocycles are common components in the complex ADMET equilibria (see above). Another possible explanation could be lower hydrodynamic volume of **p12a** in the GPC column.

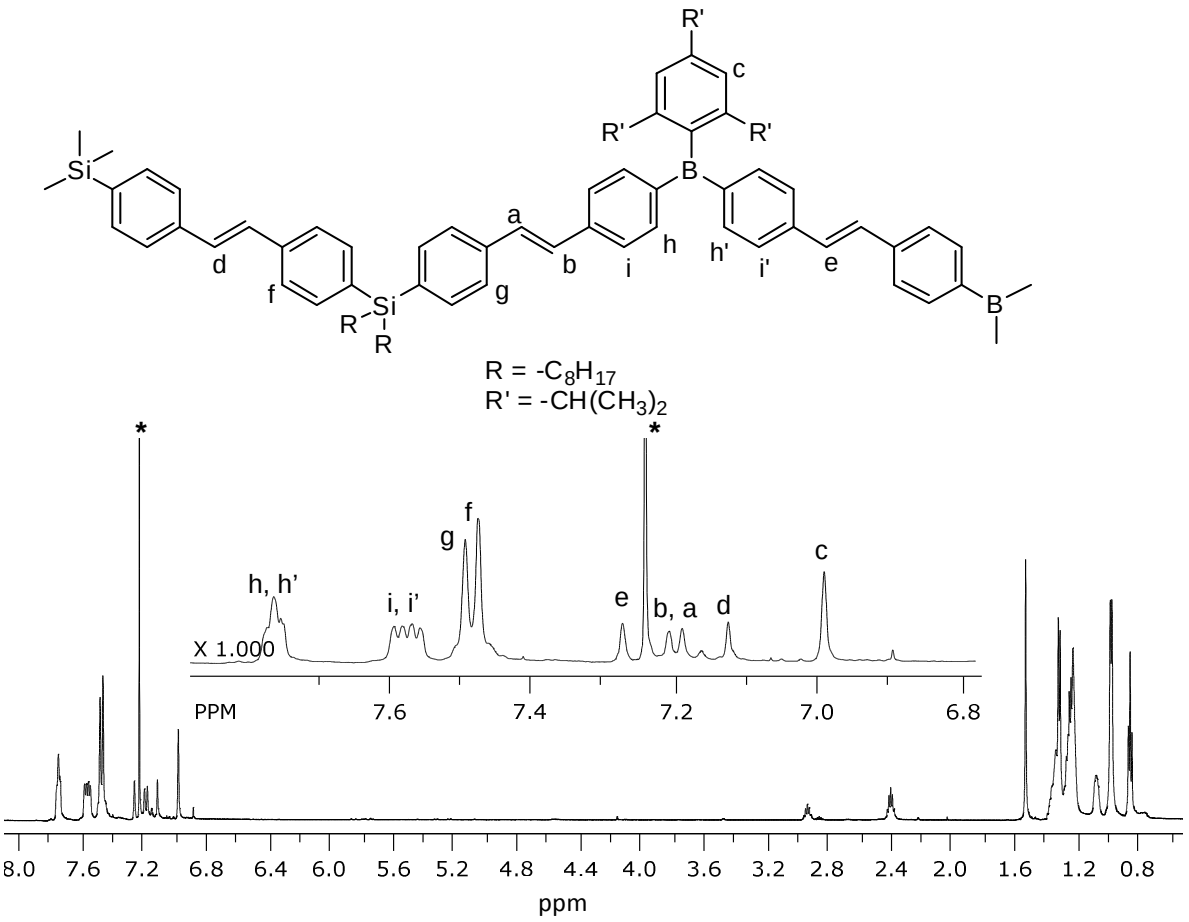

Figure 3.3 ^{1}H NMR (600 MHz, $CDCl_3^*$) spectrum of **p12a** with assignments

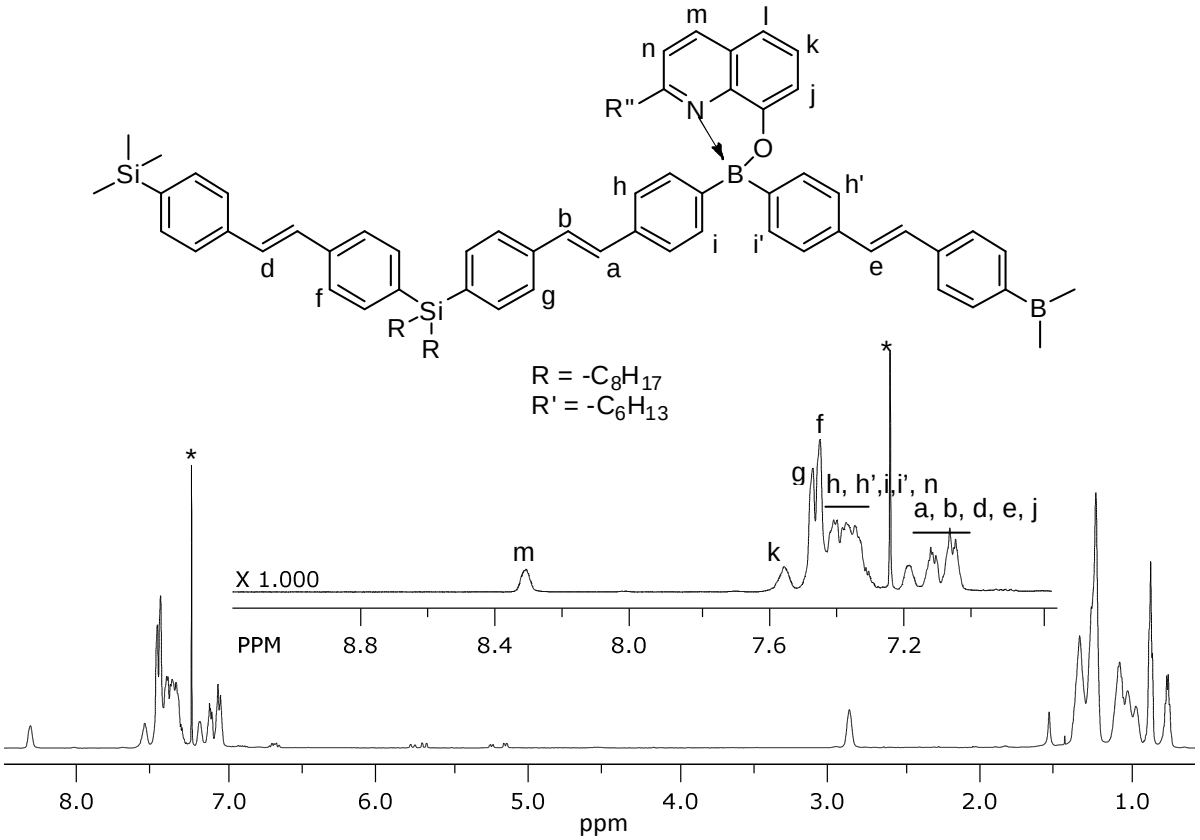

Figure 3.4 ^{1}H NMR (600 MHz, $CDCl_3^*$) spectrum of **p12b** with assignments

The NMR spectrum of **p12b** (Figure 3.4) shows the absence of vinyl groups for both the Si-monomer **1** (doublets at 5.79 and 5.26 ppm) and B-monomer **2b** (doublets at 5.71 and 5.12 ppm) upon copolymerization. The new resonances observed around together with 5.76 ppm and 5.24 ppm together with 5.68 ppm and 5.14 ppm arise from the two different chain-end vinyl functions (attached to either a B- or Si- repeat units respectively).

As in the case of **p12a**, resonances from three distinct vinylene groups are observed at 7.27, 7.22, 7.18, and 7.12 ppm (e, b, a, and d respectively, Figure 3.3). A quantification of their relative amounts via integral ratios was not possible in this case. The resonances could be assigned with the help of HSQC, NOESY, and COSY experiments. Figures 3.5 and 3.6 represent selected

regions from the HSQC spectra of **p12a** and **p12b** respectively. The resonances from the alkyl protons (hexyl group of the B repeat unit and octyl group of the Si-repeat unit) lie in the range 0.7 – 1.7ppm. Table 3.2 and 3.3 representatively summarize the NMR observations leading to the assignments in **p12a** and**p12b**.

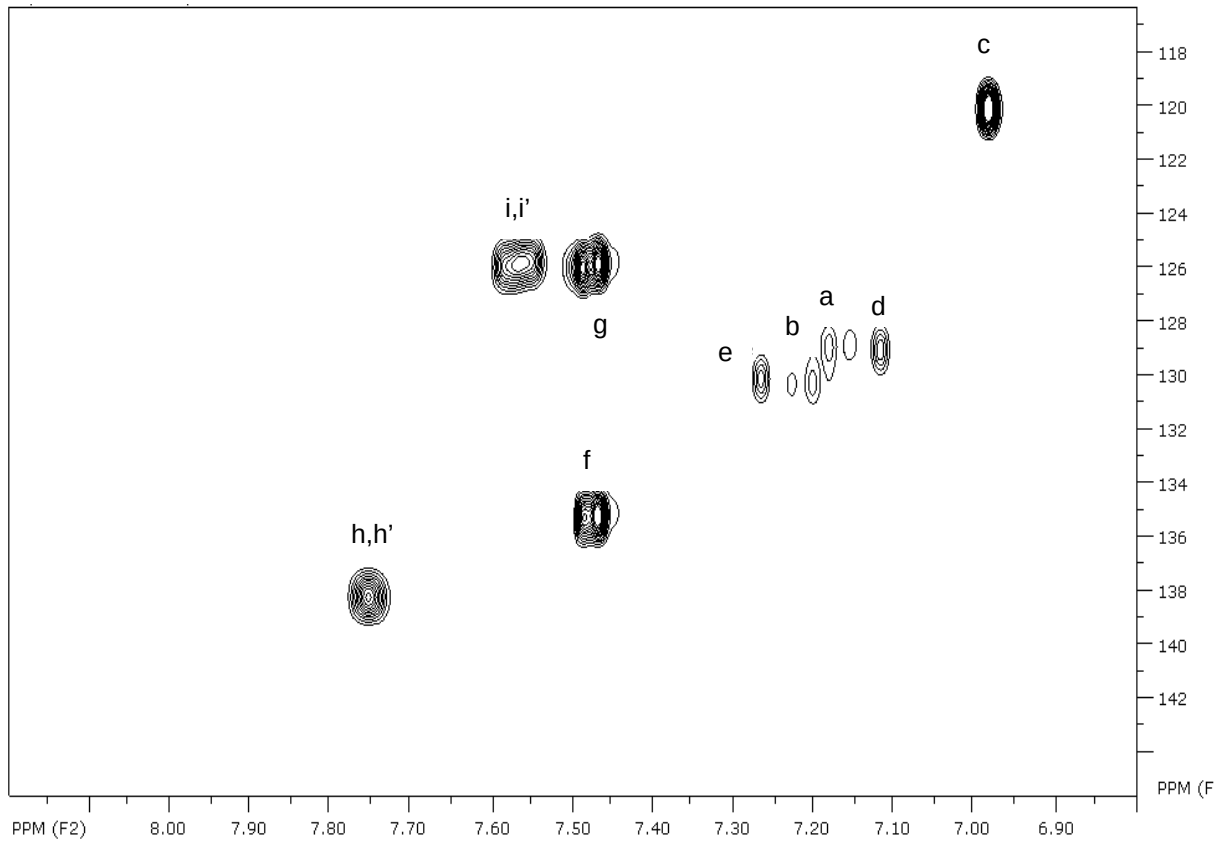

Figure 3.5 HSQC spectrum of **p12a** (assignments in Table 3.2)

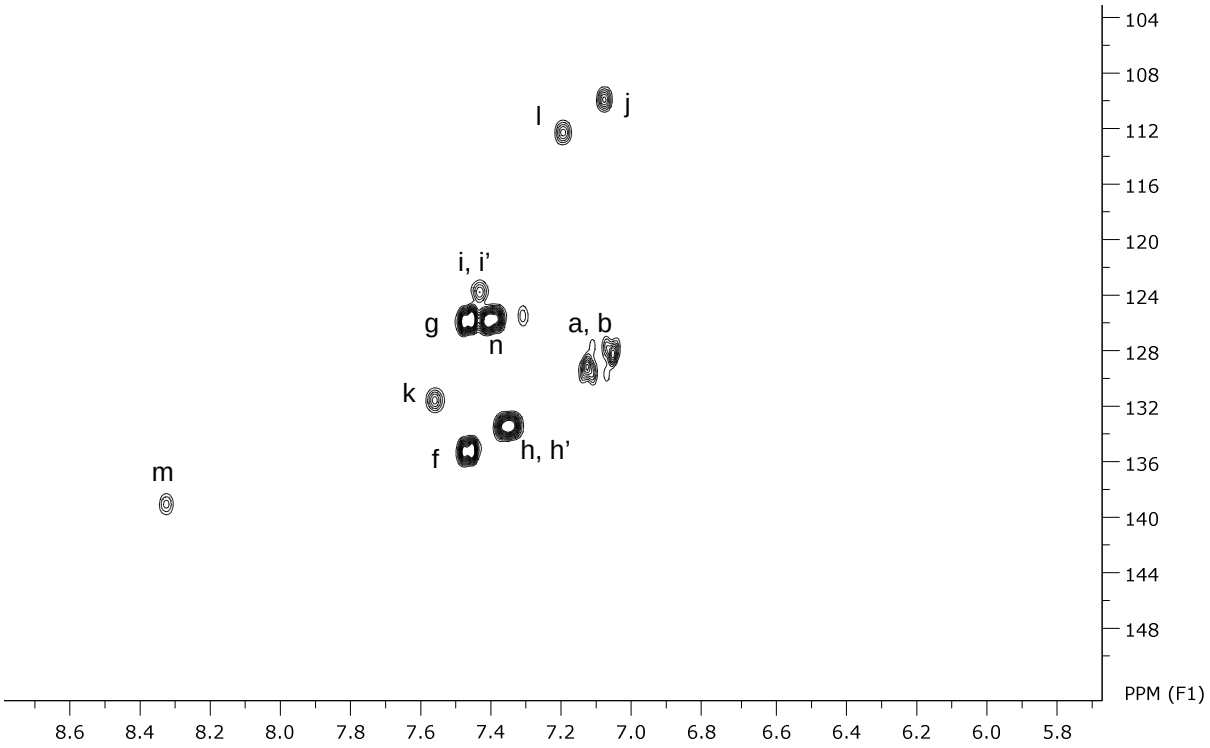

Figure 3.6 HSQC spectrum of **p12b** (assignments in Table 3.3)

Table 3.2 NMR assignments in **p12a** using HSQC and NOESY

Proton	^{1}H-NMR shift(ppm)	HSQC with ^{13}C(ppm)	NOESY with ^{1}H(ppm)
a	7.18	128.88	7.25, 7.56, 7.49
b	7.22	130.25	7.18, 7.56, 7.49
c	6.99	119.95	6.99, 2.39, 2.94
d	7.12	128.98	7.18, 7.20
e	7.27	130.1	7.27, 7.58, 7.76
f	7.47	135.12	7.12, 7.47
g	7.49	125.9	7.49, 7.18
h, h’	7.76	138.25	7.76, 7.56, 2.39
i	7.56	125.76	7.56, 7.20, 7.76
i’	7.58	125.76	7.58, 7.76, 7.27

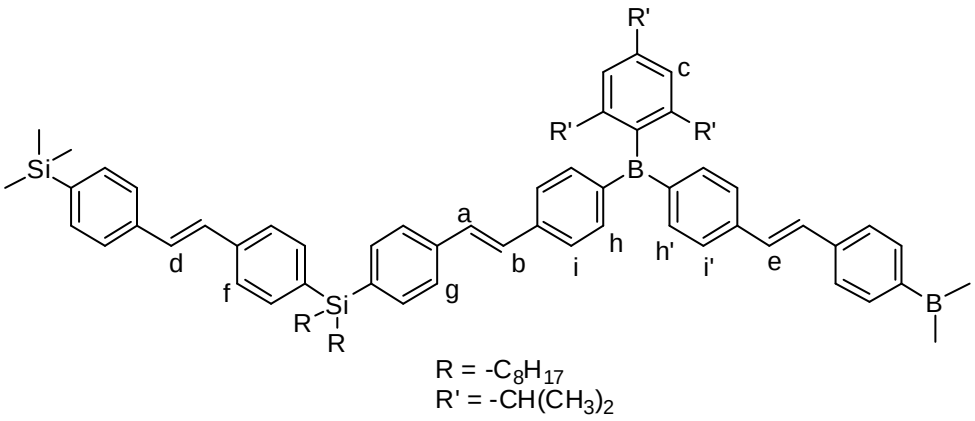

Table 3.3 NMR assignments in **p12b** using HSQC and NOESY

Proton	^{1}H-NMR shift(ppm)	HSQC with ^{13}C(ppm)	NOESY with ^{1}H(ppm)
j	7.08	109.56	7.55
k	7.55	131.39	7.2, 7.08
l	7.19	112.03	7.57
m	8.33	138.87	7.42
n	7.42	125.6	7.06(weak), 8.33
f	7.45	135.09	7.12
g	7.47	125.6	7.11, 7.06
h,h'	7.35	133.23	7.11, 7.07,7.43, 7.04
i,i'	7.43	123.68	7.10(weak), 7.35
a	7.11	129.1	7.46, 7.35
b	7.07	128	7.46, 7.35
d	7.12	128	7.45
e	7.04	128	7.35

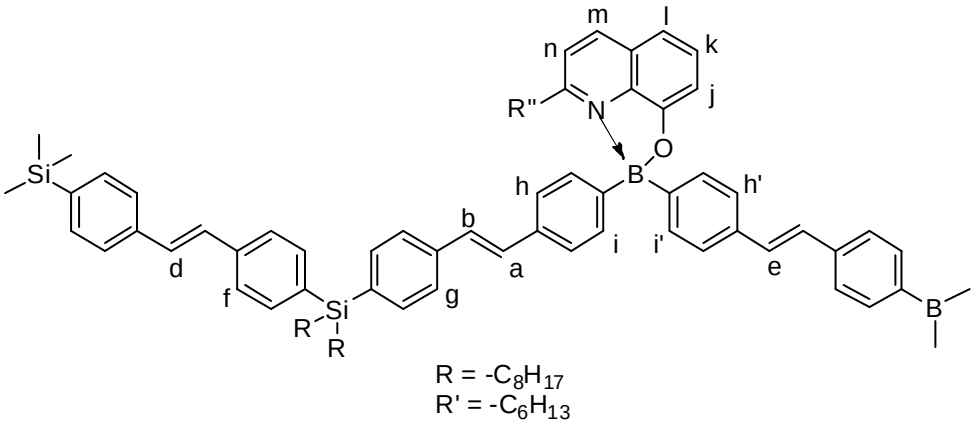

3.2.3.3 Optical properties (UV/Vis and Fluorescence spectroscopy)

The absorption and emission properties of all products were characterized as solutions in dichloromethane. As expected, the absorptions of all macromolecular homo- and co-poly condensates are red-shifted compared to the respective monomers. This is different for the emission characteristics. The polycondensates based on **2a** show emissions that are similar to the emission of **2a**. Isolated trans-stilbene in dichloromethane absorbs at 295 nm and emits at 347 nm. A comparison between the boron polymer and the respective monomer is illustrated in Figure 3.7. The absorption spectrum of the polymer **p2a** in THF shows a band with vibronic structure and a maximum at approximately 405 nm that is red-shifted by approximately 80 nm relative to that of the monomer **2a**. This bathochromic shift is attributed to the extended conjugation through the boron moiety (p-π overlap). The emission data for **2a** is quite similar to that of the polymer **p2a** with $\lambda_{em\ max}$ = 423 nm, however the polymeric material shows two distinct peaks at 423 and 448 nm, which are 0-0 and 0-1 intrachain singlet transitions, where the 0-0 transition is the most intense transition.[91] The perfectly mirrored absorption and emission bands and relatively small Stokes shift is indicating a highly rigid polymeric structure and has been observed for other rigid polymers.[92] The fluorescence quantum yield of the polymer **p2a** is also higher than that of the monomer **2a** due to the rigid polymer backbone, resulting in lesser vibrational losses along with non-radiative losses during relaxation in addition to the steric hindrance offered by Trip groups may prevent aggregation, thereby further reducing the probability of non-radiative decay. A similar enhancement of quantum efficiencies has been observed, for example, by Swager and co-workers upon incorporation of rigid pentiptycene moieties into polyphenylenevinylenes.[93-95]

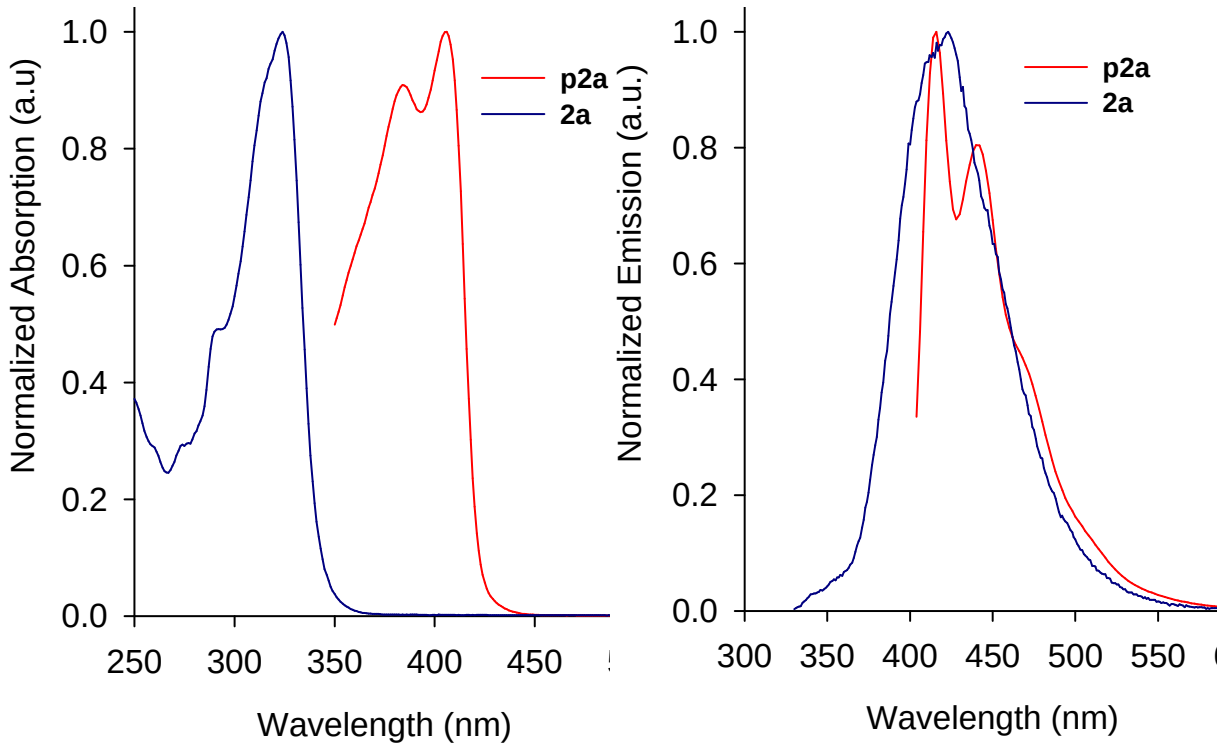

Figure 3.7 Comparison of Absorption and Emission Spectra of **2a** and **p2a** in THF

In the case of **p12a** (Figure 3.8) three absorptions are observed at 317, 350 and 381 nm corresponding to the three different chromophores present in the system. The homo-polycondensate **p2a** had the lowest energy absorption with a maximum at 406 nm and a less intense one at 381 nm. **p12b** showed an absorption with less half width and a maximum at 327 nm. However there is a energy band around 390 nm which can be assigned to intra-ligand charge transfer to pyridyl ring present within the quinolate system.[96] Although this band is lower in intensity in the absorption, the emission is centered almost entirely on this chromophore, which is why we see mostly emission at 494 nm.

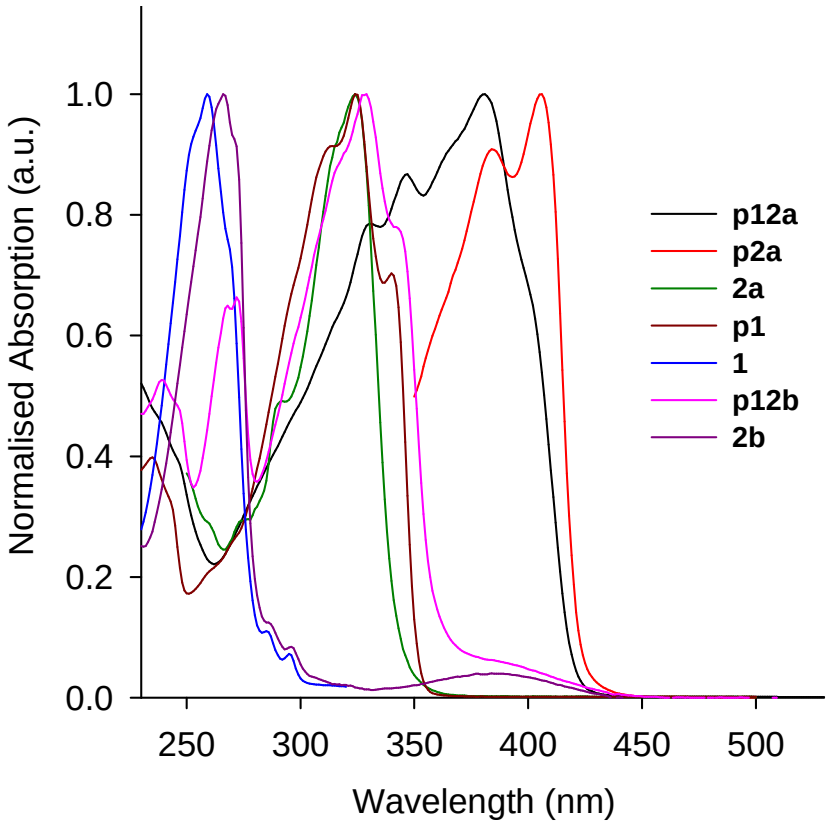

Figure 3.8 UV/Vis spectra of **1, 2a, 2b, p1, p2a, p12a, p12b** in DCM

The emission maxima of **p1**, **p2a**, **p12a**, and **p12b** were observed at 356, 416, 416, and 494 nm respectively (Figure 3.9). The emission maxima for **p2a** and **p12a** are very close to the maximum of **2a** at 424 nm. This emission behavior was also observed in the case of flourene based monomers,[97] which is attributed to charge transfer and aggregation resulting in large Stoke shift in case of the monomer **2a**. The maximum emission of **p12b** overlaps well with that of **2b** together less intensive emission around 356 nm that coincides with the emission of **p1**. It seems that the emission of B-containing polycondensate **p12b** is dominated by boron quinolate chromophore rather than the trans-stilbene units in the backbone, the latter however dominating the absorption behavior.

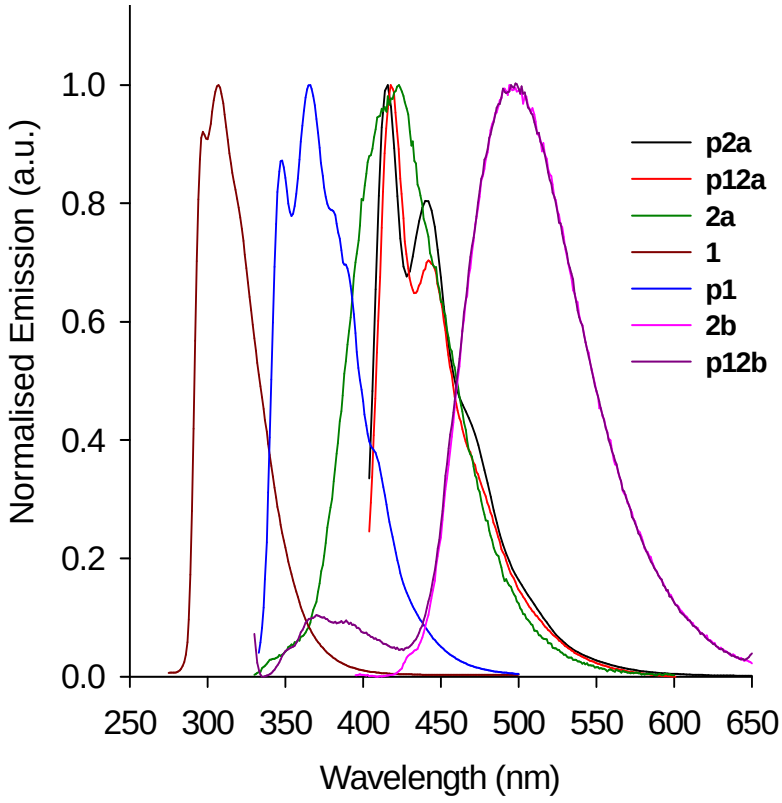

Figure 3.9 Emission spectra of **1, 2a, 2b, p1, p2a, p12a, p12b**

A possible explanation could be that the emission of the aromatic B-substituents is less easily quenched than the emission from the backbone. To support this, dilution experiments were carried out. Figure 3.10 details the emission of **p12b** solutions upon sequential dilution with additional solvent dichloromethane. With increasing dilution, the short wavelength emission maximum gradually becomes relatively stronger, until it finally dominates and the originally dominating emission with a maximum at 494 nm which now has been reduced to a shoulder. Upon dilution, the polycondensate backbones quench less likely, resulting in a stronger relative emission. However it is also possible that due to molecular interaction at high concentration there is a possibility of excimer formation resulting in intense emission around 494 nm upon excitation at a single wavelength.[98] There is also a possibility of intermolecular energy migration

from the backbone to the pyridyl ring of the quinolate chromophore at high concentration upon excitation at 324 nm.

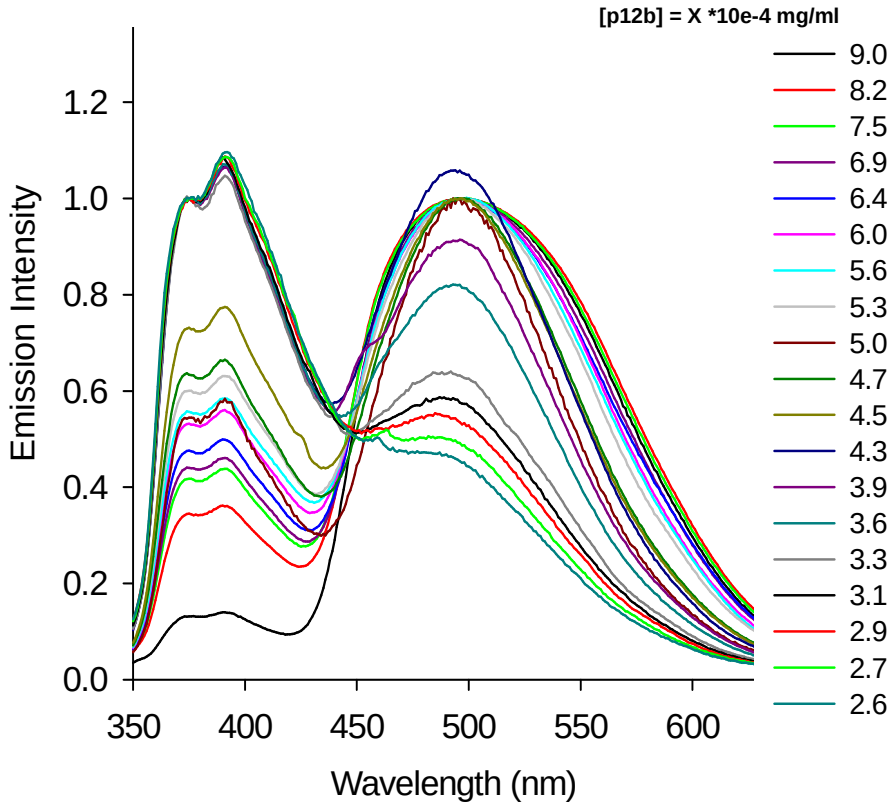

Figure 3.10 Effect of dilution on the emission behavior of **p12b** in DCM.
([**p12b**] = 9 x 10^{-4} g/ml)

A unique capability of tricoordinate B-containing conjugated systems with strong fluorescent characteristics is their ability to indicate the presence of Lewis donors (see above). In the presence of F^- ions (tetrabutylammonium fluoride), the fluorescence from **p12a** is quenched as shown in Figure 3.11, indicating the potential use of this system as a sensory material for nucleophiles. The binding of the fluoride ion to the vacant p-orbital at the boron center results in the disruption of the conjugation path and fluorescence quenching as a consequence. It is also observed that there is an abrupt reduction in fluorescence intensity at B/F^- ratio between 23 and 20 which might be due to polymer "co-operative effect" resulting in switch – off. This polymer

co-operative effect was further supported by reports from the Jäkle group[99] where similar co-operative effect was observed for boron containing styrene based polymers. The optical properties of the products are summarized in Table 3.4.

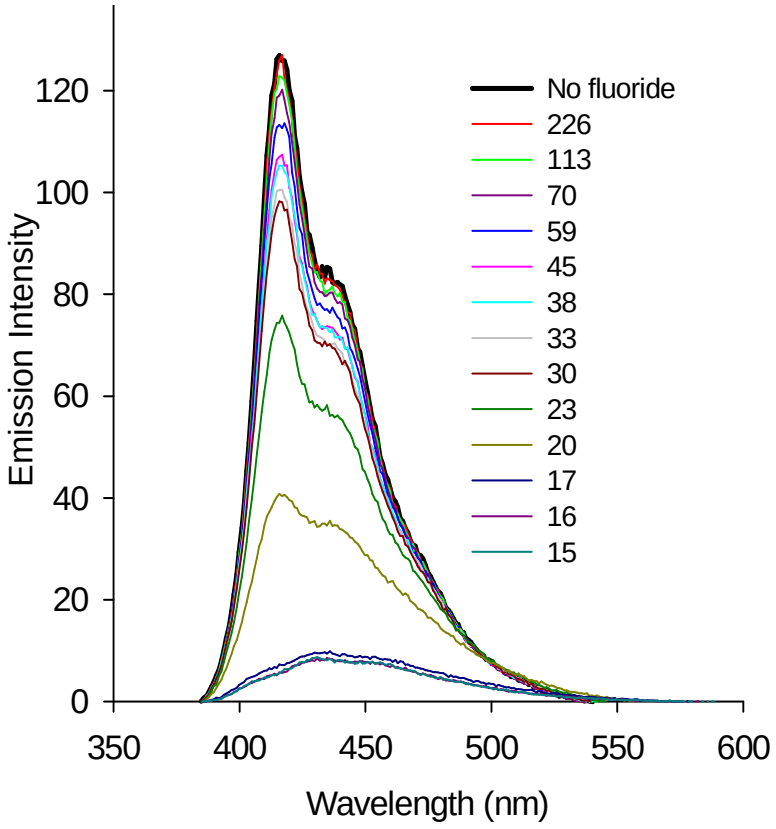

Figure 3.11 Titration of **p12a** with F^- ions in THF. [B] = 7.7 x 10^{-4} M and [F^-] = 8.5 x 10^{-4} M

Table 3.4 Experimental absorption and emission maxima values of the monomer and polymers

Sample	λ_{abs} (nm)	λ_{em} (nm)*	ϕ_{eff}
1	256	307	
2a	317	424	
2b	265, 381	494	
p1	324	356	0.25
p2a	406	416	0.30
p12a	381	416	0.28
p12b*	327, 385	494	[1]n.o.

*For λ_{em} the excitations wavelength for :**1** = 256 nm, **2a** = 317 nm, **2b** = 265 nm, **p1** = 324 nm, **p2a** = 406 nm, **p12a** = 381 nm, **p12b** = 327 and 385 nm, [1]not observed

3.2.3.4 Thermal stability (in N_2)

The degradation of **p12a** followed two-step degradation process compared to **p2a** which followed a one-step degradation process (Figure 3.12). In the case of **p12a**, the average repeat unit weight is 743 g/mol. The 1st step degradation resulted in a weight loss of 24-26% at 195^{0}C that corresponds to the fragmentation of triisopropyl benzene moiety (Trip group) whose exact mass is 203 g/mol. Rapid degradation of the polymeric backbone started at 290^{0}C. The observed residual weight of **p12a** and **p2a** were negligible, but in case of **p12b** the residual weight is considerable high around 18 – 20%. Considering the average repeat unit weight of **p12b** is around 810 g/mol, the residual weight mainly corresponds to the hydroxyquinolate moiety whose exact mass is 144 g/mol. Again, **p12b** has the highest stability compared to **p2a** and **p12a** (5% weight loss @ 290^0 – 300^{0}C) due to the added electron density around the boron center from the 8HQ moiety.

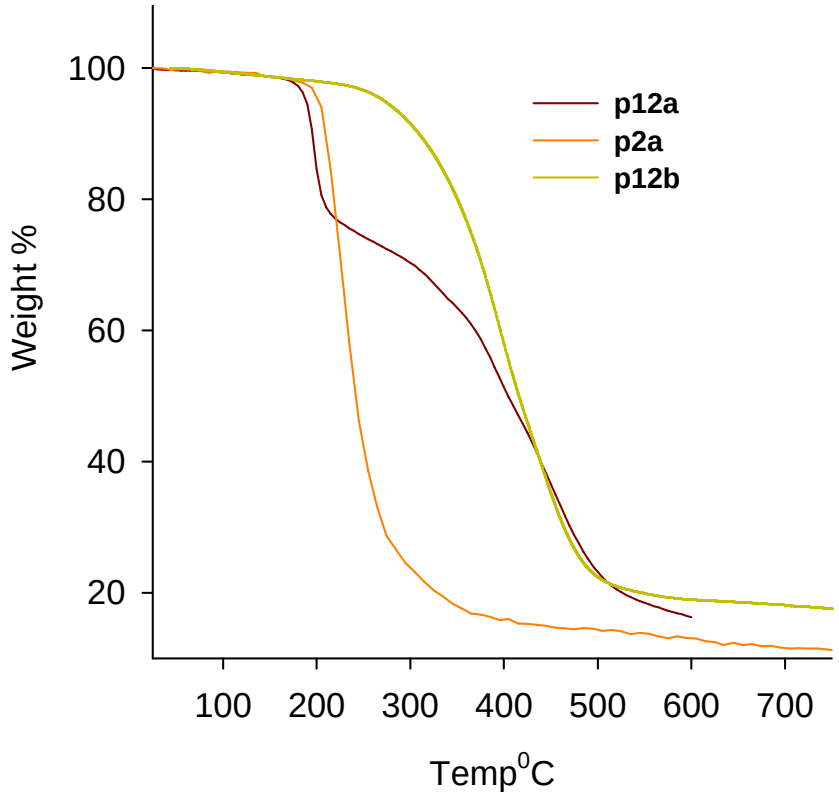

Figure 3.12 TGA curves for **p12a, p2a, p12b** (performed under nitrogen atmosphere)

3.3 Conclusion

The synthetic scope discussed in the previous chapter has been successfully extended for the development of copolymers based on boron and silicon. The copolymer **p12a** and **p12b** obtained are stable under ambient conditions and are potential candidates for application in the field of sensor materials and emissive materials. This will help to explore a wide range of organometallic materials based on Group 13 and 14. The discussed synthetic strategy can also extended for the development of intrinsic systems combining different organic heterocyclic systems with inorganic counterparts based on Group 13 and 14.

3.4 Experimental

General Information

All of the experiments using air/moisture sensitive materials were carried out in a nitrogen filled Labconco protector glove box and/or by the use of dry argon filled dual manifold (inert gas/ vacuum) using standard Schlenk line techniques. All glassware was cleaned and dried for at least 16 h in an oven at 120 ^{0}C prior

Chemicals

Mg (turnings), 8-hydroxyquinoline, trimethyl borate, and triisopropyl borate were purchased from Acros. 4-Chlorostyrene was purchased from Alfa Aesar. (2,4,6-triisopropylphenyl)magnesium bromide,[100] 2-butylquinolin-8-ol and 2-hexylquinolin-8-ol were prepared as previously reported.[101] Triphenylphosphonium methyl bromide, n-BuLi (2.5M) and Hoveyda – Grubbs 2nd Generation catalyst was purchased from Sigma - Aldrich were purchased from Sigma – Aldrich. Dibenzaldehyde dioctyl silylene was previously reported in a literature mentione above. Solvents such as tetrahydrofuran (THF), toluene, hexane, and diethyl ether were purchased from Fisher Scientific. Except for diethyl ether, all other solvents were dried and degassed by a “Pure Solv” solvent purification system (using activated alumina, copper catalyst, molecular sieves column.) by Innovative Technology Inc. before use. All other chemicals were used as received. Column chromatography was carried out on silica gel 60 (70-230 mesh) form EMD Chemicals Inc.

Instrumentation

^{1}H NMR (600 MHz) and ^{13}C NMR spectra were recorded in $CDCl_3$ on Varian Unity NMR instruments. $CDCl_3$ was used as an internal deuterium lock for the spectra. All of the signals in the NMR spectra are reported in ppm, multiplicity (s = singlet, d = doublet, t = triplet, q = quadruplet, m = multiplet, dd = doublet of doublet).

UV-Visible absorption spectra were recorded using a Perkin Elmer Model 650 UV Spectrophotometer with 1-cm path length cells. The samples were prepared with HPLC grade hexane ("Spectrasolv") in a sample cell.

Photoluminescence spectra were recorded using a Varian spectrofluorometer with 1-cm path length cells. The samples were prepared with HPLC grade hexane ("Spectrasolv") in a sample cell.

GPC analysis was carried out on an Alliance GPCV 2000 (Waters) instrument equipped with four Waters Styragel HR columns, i.e. HR-1, HR-3, HR-4, and HR-5E. HPLC grade THF was used as eluent, at a flow rate of 1.0 mL/min at 40 ^{0}C. Measurements are relative to a calibration with polystyrene standards and third order relative calibration curve was used to measure the molecular weight of unknown samples.

Synthesis of 1

To a suspension of 12.5g (35 mmol) of methyltriphenylphosphonium bromide in 100 mL of dry THF, 12 mL of *n*-BuLi [2.5 M in hexane, 30 mmol] were slowly added at 0 °C. The reaction mixture was stirred for 3 h. To the resulting solution, 4.64g (10 mmol) of dibenzaldehyde dioctylsilylene dissolved in 10 mL of dry THF were slowly added at 0 °C. The resulting mixture was stirred for 12 h and then washed with brine. The organic phase was extracted with diethyl ether twice, dried over sodium sulfate, and concentrated to yield the dioctyldistyrylsilylene as a

crude oil, which was purified by passing through a silica gel column using hexane as an eluent to obtain a colorless liquid. Yield: 66%. ^{1}H NMR (600 MHz, $CDCl_3$) δ = 7.47 (d, J = 7.8 Hz, 4H), 7.39 (d, J = 8.1 Hz, 4H), 6.72 (dd, J =11.2 Hz, 17.7 Hz, 2H), 5.79 (d, J = 17.7 Hz, 2H), 5.26 (d, J = 11.2 Hz, 2H), 1.2 – 1.5 (m, 24H), 1.0 – 1.2 (m, 4H), 0.88 (t, J = 7Hz, 6H). ^{13}C NMR (125 Mhz, $CDCl_3$) δ = 138.1, 136.9, 136.4, 135.1, 125.51, 114.2, 33.7, 31.9, 29.3, 29.2, 23.7, 22.7, 14.1, 12.6. ^{29}Si NMR ($CDCl_3$) δ = -6.84.

Synthesis of 2a

To a suspension of Mg (2.67 g, 0.11 mol) in 300 mL THF was added slowly 4-chlorostyrene (7.62 g, 0.055 mol) while maintaining the temperature below 60 °C. The reaction mixture was stirred at 60 °C for 2 h and allowed to cool to room temperature. The resulting styryl-Grignard solution was decanted to another flask using a cannula. Trimethylborate was then added slowly to the Grignard solution and the reaction was stirred for 3 h. The resulting distyrylborate solution was added slowly to a solution of (2,4,6-triisopropylphenyl)magnesium bromide in THF and refluxed for 36 h. The crude product was extracted using hexanes and passed through a silica gel column using hexanes as the eluent. The pure product was obtained via crystallization from hexanes as colorless crystals (2.5 g, 25 %). ^{1}H NMR (499.893 MHz, $CDCl_3$): δ = 7.75 (d, ^{3}J = 7.5 Hz, 4H, Ph-H2,6), 7.50 (d, ^{3}J = 7.5 Hz, 4H, Ph-H3,5), 7.00 (s, 2H, Tip-H3,5), 6.80 (dd, ^{3}J = 18.0 Hz, 2H, H9), 5.90 (d, ^{3}J = 18 Hz, 2H, H10), 5.37 (d, ^{3}J = 12 Hz, 2H, H11), 2.95 (sept, ^{3}J = Hz, 1H), 2.40 (sept, ^{3}J = Hz, 2H), 1.33 (d, ^{3}J = 7.0 Hz, 6H), 0.98 (d, ^{3}J = 12.0 Hz, 12H); ^{13}C (125.698 MHz, $CDCl_3$): δ = 149.1, 148.7, 142.4, 140.8, 140.8, 138.4, 138.4 137.1, 125.7, 120.3, 115.7, 35.7, 34.4, 24.4;^{11}B NMR (160.380 MHz, $CDCl_3$): δ = 70 ($w_{1/2}$ = 1900).

Synthesis of 2b

A solution of distyrylborate prepared as described above (29.0 mmol, 200 mL THF) was added slowly to 2-*n*-hexyl-8-hydroxyquinoline (5.0 g, 0.022 mol) in 50 mL THF and stirred for 24 h. Complete conversion was confirmed by ^{11}B NMR spectroscopy and the mixture was then quenched with chlorotrimethylsilane (1.8 g, 0.017 mol) to remove any unreacted Grignard. Insoluble salts were removed by filtration. The product was purified by crystallization from hexanes and obtained as a yellow solid (2.0 g, 32%). ^{1}H NMR (499.893 MHz, $CDCl_3$): δ = 8.35 (d, ^{3}J = 8.5 Hz, 1H, Q-H2), 7.58 (pst, ^{3}J = 8.5 Hz, 1H, Q-H6), 7.45 (d, ^{3}J = 8.5 Hz, 1H, Q-H3), 7.33 (dd, ^{3}J = 8.0 Hz and 12.0 Hz, 8H, Ph-H2,6 and Ph-H3,5), 7.21 (d, ^{3}J = 8.5 Hz, 1H, Q-H5), 7.09 (d, ^{3}J = 7.5 Hz, 1H, Q-H7), 6.70 (dd, ^{3}J = 11.0 Hz, 17.5 Hz, 2H, H9), 5.72 (d, ^{3}J = 17.5 Hz, 2H, H10), 5.18 (d, ^{3}J = 11.0 Hz, 2H, H11), 2.86 (t, ^{3}J = 7.0 Hz, 2H, Hex), 1.11 (m, 2H, Hex), 0.99 (m, 6H, Hex), 0.78 (t, ^{3}J = 7.0 Hz, 3H, Hex); ^{13}C (125.698 MHz, $CDCl_3$): δ = 158.7, 157.9, 145.6, 139.3, 137.5, 136.4, 133.5, 131.7, 126.9, 125.6, 124.0, 113.0, 112.4, 109.9, 34.8, 31.6, 29.5, 29.3, 22.6, 14.2; ^{11}B NMR (160.380 MHz, $CDCl_3$): δ = 11.7 ($w_{1/2}$ = 610).

Synthesis of p1

The silicon based homopolymer was prepared according to a literature procedure.[72]

^{1}H NMR (600 MHz, $CDCl_3$) δ = 7.57 (br, s, 8H), 7.13 (s, 2H), 6.6 – 6.9 (m, 2H), 5.78 (d, 2H), 5.26 (d, 2H), 0.88 – 1.38 (m, 34H). ^{13}C NMR (125 MHz, $CDCl_3$) δ = 138.2, 137.4, 133.8, 129.1, 125.9, 33.5, 31.9, 29.2, 23.0, 22.6, 15.8, 15.2, 14.1. ^{29}Si ($CDCl_3$) δ = -6.83.

Synthesis of p2a

60 mg (0.14 mmol) of **2a** were placed in an air-free reaction tube and dissolved in 2 mL of toluene. To the reaction tube 3.5 mg (0.0049 mmol) of Hoveyda-Grubbs 2nd generation catalyst was added. The reaction was carried out at 50-60 °C for 24h under vacuum. The crude product

was concentrated by removing the solvent, washed with methanol and centrifuged. The precipitate was collected and traces of solvent were removed under vacuum. The product was obtained as a solid. Yield: 75%. ^{1}H NMR (600 MHz, $CDCl_3$) δ = 7.76 (d, J = 7.5Hz, 4H), 7.58 (d, J = 8.4 Hz, 4H), 7.27 (s, 2H), 2.92 (m, 1H), 2.41 (m, 2H), 1.35 (d, J = 7 Hz, 6H), 0.95 (d, J = 6.15 Hz, 12H).

Synthesis of p12a

55 mg (0.12 mmol) of **1** and 50 mg of **2a** (0.12 mmol) were placed in an air-free reaction tube and dissolved in 3 mL of toluene. To the reaction tube were added 4.4 mg (0.0070 mmol) of Hoveyda-Grubbs 2nd generation catalyst. The reaction was carried out at 60 °C for 48h under vacuum. The crude product was concentrated by removing the solvent, washed with methanol, redissolved in dichloromethane and then passed through a short silica gel column with dichloromethane as the eluent. The product was obtained as a solid. Yield: 75%. ^{1}H NMR (600 MHz, $CDCl_3$) δ = 7.76 (br, 4H), 7.56 – 7.58 (dd, 4H), 7.49 (s, 4H), 7.47 (s, 4H), 7.27 (s, 2H), 7.18 – 7.2 (m, J = 11.1 Hz, 2H), 7.12 (s, 4H), 6.99 (s, 2H), 2.92 (m, 1H), 2.41 (m, 2H), 0.88 – 1.4 (m, 52H). ^{13}C NMR (125 MHz, $CDCl_3$, aromatic) δ = 138.3, 135.1, 130.3, 130.1, 129.0, 128.9, 125.9, 125.8, 120.0.

Synthesis of p12b

91 mg (0.20 mmol) of **1** and 96 mg of **2b** (0.22 mmol) were placed in an air-free reaction tube and dissolved in 4 mL of toluene. To the reaction tube were added 7.9 mg (0.013 mmol) of Hoveyda-Grubbs 2nd generation catalyst. The reaction was carried out at 60 °C for 48h under vacuum. The crude product was concentrated by removing the solvent, washed with methanol, redissolved in dichloromethane and then passed through a short silica gel column with dichloromethane as the eluent. The product was obtained as a solid. Yield: 70%. ^{1}H NMR (600

MHz, $CDCl_3$) δ = 8.33 (br, 1H), 7.55 (br, 1H), 7.47 (s, 4H), 7.45 (s, 4H), 7.43 (br, 4H), 7.42 (br, 1H), 7.35 (br, 4H), 7.19 (br, 1H), 7.12 (br, 2H), 7.11 (br, 1H), 7.08 (br, 1H), 7.07 (br, 1H), 7.04 (br, 2H), 2.84 (br, 2H), 0.8 – 1.3 (m, 45H). ^{13}C NMR (125 MHz, $CDCl_3$, aromatic) δ = 138.9, 135.1, 133.2, 131.4, 129.1, 127.8, 125.6, 123.7, 112.0, 109.6.

4. Heteroatoms containing conjugated thiophene based polymer –Synthesis and photophysical properties

4.1 Introduction

Polythiophenes are a class of compounds of conjugated systems that have gained considerable attention over the past decades due to their potential application in photoharvesting systems. Because of their versatile synthetic approach with facile functionalizations the electronic properties can be easily tuned.[102] Oligothiophenes or polythiophenes are also candidates for applications in organic thin film transistors and LEDs, in addition to photovoltaic cells.[103] Several classes of thiophene - based polymers and oligomers have been reported. Poly (alkylthiophene) (PAT) systems in general,[104] have been reported for applications as solar cell materials. Several copolymers based on thiophene have also been reported, e.g., alternating phenylene – thiophene copolymer by Salaneck, et al.[105] In another case, thiophene – fluorene copolymers were used to fine tune HOMO - LUMO band gaps,, resulting in the improvement of charge injection and transport.[106] Apart from the aforementioned copolymers and homopolymers, poly/oligo-2,5- thienylvinylenes are a class of thiophene – based materials that show long average conjugation lengths and small band gap values,[107] however poly (2,5-thienylenevinylene)s (PTV) have not been investigated deeper. More recently, Lecrec and coworkers synthesized a 2, 7-carbazolylenevinylene – thienylenevinylene copolymer and studied their electronic properties.[108] Integration of a heteroatom (Si) within the polymeric backbone of thiophene systems was reported by Hadziioaannou and co-workers.[109] The polymers were found to have a very well defined conjugation length because of the interruption offered by the silanylene units. Later, Yoshino et al. reported similar block copolymers based on thiophene and silanylene units, controlling the conjugation length and thus the emission characteristics.[110]

Bazan et al, reported the synthesis of poly[(silanylene)dithienylethylene] derivatives via acyclic diene metathesis using a Schrock type catalyst and attempted to study the structure – property relationship.[111] But the report describes the predominant formation of free radical side products which prevented further investigations. The following report describes the ADMET synthesis of conjugated poly(dithienylethylene) systems incorporating with Group 14 elements, particularly Si, Ge and Sn via acyclic diene metathesis, using a Grubbs 2nd generation catalyst. The heteroatoms stand in direct electronic conjugation with the dithienylethylene units. Structural investigations were carried out to understand the effect of the heteroatom on the overall molecular structure and properties. This report then also attempts a preliminary structure/property study with regard to the effect of the heteroatom on the absorption and emission of the chromophore.

4.2 Results and discussions

The report involves first the synthesis of the homologous silicon, germanium and tin containing monomers and then their subsequent ADMET polycondensation.

The heteroatom containing thiophene based monomers were synthesized in a two – step synthetic strategy starting with a Wittig reaction followed by a lithiation reaction. The detailed synthetic strategy for the monomers is described in Section 4.2.1. Olefin metathesis of the monomers was carried out in the presence of Grubbs 2nd generation catalyst at temperatures around 60 – 90^{0}C for 2 – 6 days in toluene. The olefin metathesis reaction mixtures remained homogeneous and a color change could be observed as the reaction progressed. The polymerization was also carried out in the presence of Hoveyda – Grubbs 2nd generation catalyst under the same reaction conditions; however no considerable conversion was observed.

4.2.1 Monomer synthesis

2-bromo 5-vinylthiophene **2** which was used as a monomer precursor was synthesized from 5-bromothiophene 2-carbaldehyde **1** via Witting reaction as shown in Scheme 4.1.

All homologues monomers **3a, 3b, 3c** were prepared by the same strategy, regardless of heteroatom (see Scheme 4.1). 2-bromo 5-vinylthiophene **2** was lithiated at -78^{0}C for 2 h in a solvent mixture of THF and diethylether. The lithiated thiophene solution was coupled with a difunctional Si, Ge, or Sn building block (R_2SiCl_2/R_2GeCl_2/R_2SnCl_2) at -78^{0}C and left to react for a time period of 12 h while the temperature slowly rose to room temperature. The reaction product was isolated by removing THF and ether under vacuum. The residue was then re-dissolved in hexane and washed with water. The hexane fraction was collected and removed. Product was obtained as a residue. and further purified by column chromatography. Representative product yield were 75%, 72% and 67% for **3a**, **3b**, **3c** respectively after purification.

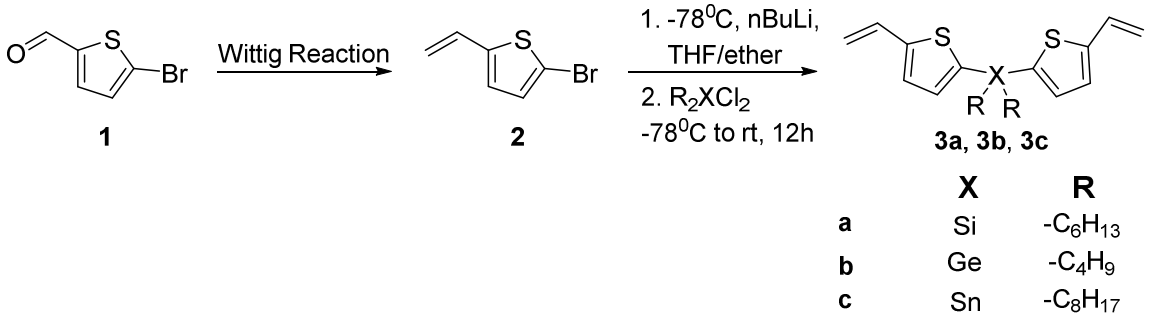

Scheme 4.1 Synthesis of **3a - c**

4.2.2 ADMET polycondensation

The synthetic scheme for polymers **p3a** – **c** is shown in Scheme 4.2 below. The ADMET polycondensation of **3a – c** was carried out in the presence of Grubbs 2nd generation catalyst in toluene at temperatures in the range of 65^0 – 90^0C for a period of 2 – 6 days under intermittent removal of vacuum. The reaction mixtures obtained were purified by column chromatography. The yields of isolated polymers **p3a** – **c** were ca. 67 – 75%. Reaction optimizations included variation of solvent, catalyst and temperature. Above reaction conditions represent representative optimized conditions. Using Hoveyda - Grubbs 2nd generation catalyst did not result in significant monomer conversion even at higher temperatures. With the Grubbs 2nd generation catalyst, reaction occurred at temperatures in the range of 65^0 - 90^0C. Monomer conversion was achieved at 90^0C in the case of **3c**. In general, higher monomer conversions were observed only at higher temperatures and after longer time. However, at temperatures above 90^0C side reactions and deactivation of catalyst started to compete with the ADMET reaction. Of the solvent systems tested, only pure toluene yielded product. (tested: THF, DCM and mixtures). The ADMET polycondensation results and molecular weights (M_n via NMR) are summarized in Table 4.1.

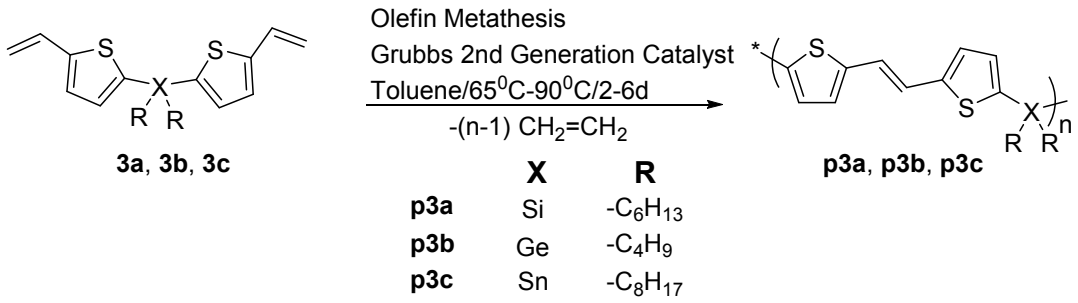

Scheme 4.2 ADMET synthesis of **p3a - c**

4.2.3 Characterization

4.2.3.1 Size analysis

Molecular weights (Mn) of the ADMET polycondensation products were determined by gel permeation chromatography (GPC) relative to polystyrene standards. Traces for the differential refractive index (dRI) detector are shown in Figure 4.1.

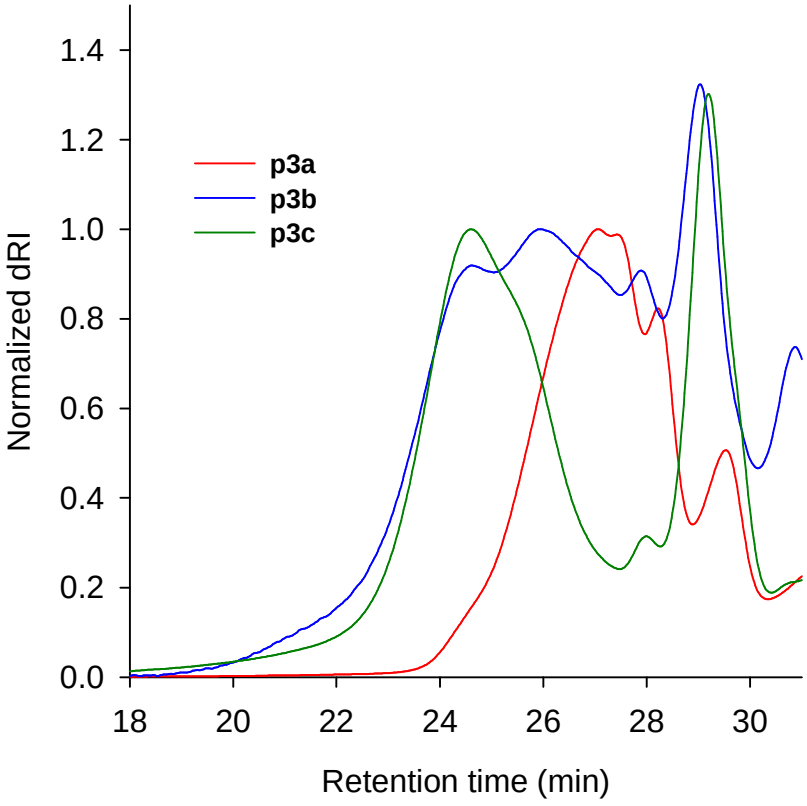

Figure 4.1 GPC traces of **p3a**, **p3b** and **p3c**

Table 4.1 summarizes reaction conditions, representative M_n (GPC and NMR results) and polydispersities (M_w/M_n) for **p3a – c**. The M_n values based on NMR were calculated by end group analysis (integrals of signals from chain end vinyl protons vs. chain internal vinylene protons).

Table 4.1 ADMET polycondensation results and molecular weights

Sample	Reaction Conditions		M_n (g/mol)		M_w/M_n
	[Monomer] mM	[Catalyst] mM	NMR	GPC	
p3a[1]	160.0	8.0	12000	2726	1.8
p3b[2]	80.0	5.7	4000	3820	2.5
p3c[3]	123.3	11.9	5000	7326	2.2

[1]T = 65^0C/t = 55 h, [2]T = 70^0C/t = 96 h, [3]T = 90^0C/t = 6 d. All polycondensations were carried out in 3 ml of toluene.

In an end group analysis, the ratio of integrals of the terminal vinyl protons to that of the internal vinylene protons yielded M_n of the polymers **p3a – c**. For **p3a**, the M_n was 12000 g/mol with a degree of polymerization (D.P.) of 34. For **p3b**, the M_n was 4000 g/mol with a D.P. of 11 and for **p3c**, the M_n was 5000 g/mol with a D.P. of 9.

The M_n values determined by GPC were 2726 g/mol, 3820 g/mol and 7326 g/mol for **p3a**, **p3b** and **p3c** respectively. Polydispersities were in the range of 1.8 – 2.5. The molecular weights determined by GPC were found to be very different compared to the results obtained from NMR. In the case of **p3c**, relatively higher temperatures and longer reaction times were required in order to achieve significant conversion.

Lower reaction temperatures generally resulted in lower conversions. Reaction temperatures below 60^0C did not yield any product at all, regardless of catalyst or monomer used. Higher [monomer]/[catalyst] ratios resulted in lower conversion in all the three cases. Among the solvents investigated, pure toluene yielded the best results.

4.2.3.2 NMR (Microstructure analysis)

The microstructures of the monomers (**3a**, **3b**, **3c**) were characterized by ^{1}H NMR and ^{13}C NMR. Figure 4.2 represents an overlay of the proton NMR spectra of the three monomers.

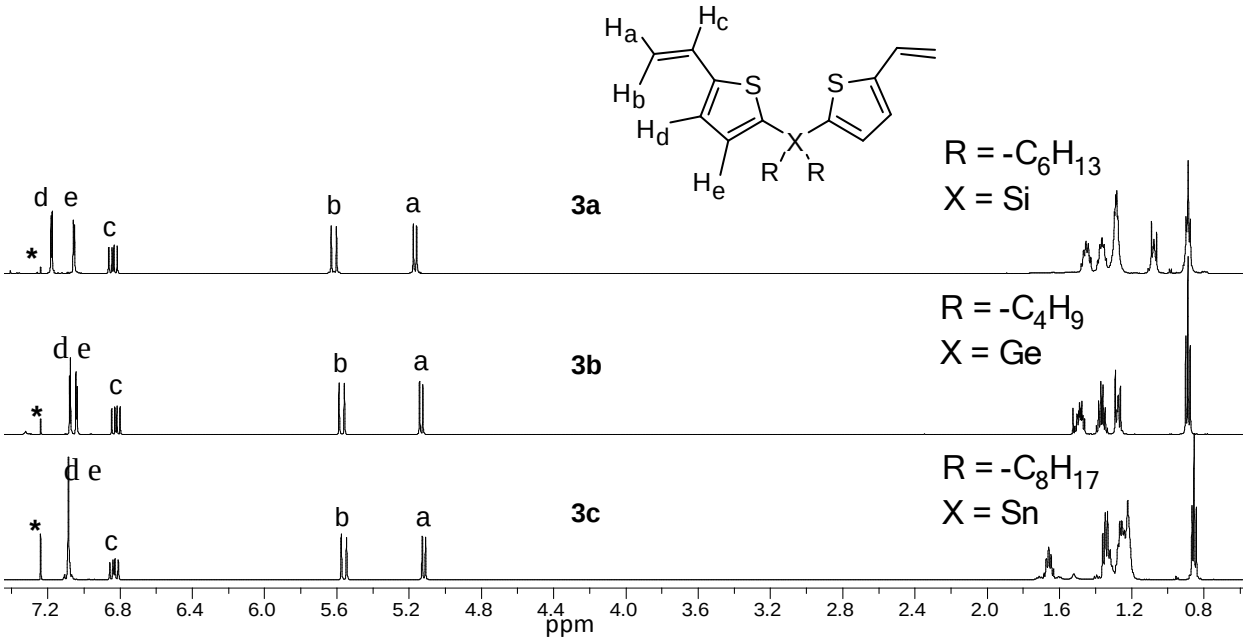

Figure 4.2 ^{1}H NMR (600 MHz, $CDCl_3^*$) of **3a - c**

The proton resonances from the terminal vinyl group –CH=C**H₂** of the monomers appear as two doublets $\mathbf{H_a}$ (cis) and $\mathbf{H_b}$ (trans) around 5.16 and 5.61 ppm, 5.13 and 5.57 ppm, 5.12 and 5.56 ppm for **3a**, **3b** and **3c** respectively. It is to be noted that there is an upfield shift of the resonance signals of the terminal vinyl protons from **3a** to **3c.** The "cis" resonance gradually changes from 5.16 ppm to5.13 ppm to 5.12 ppm for **3a**, **3b** and **3c** respectively. The "trans" resonance gradually changes from 5.61 ppm to 5.57 ppm to 5.56 ppm for **3a**, **3b**, **3c** respectively indicating increase in shielding effect with increase in size of the heteroatoms on the terminal vinyl protons.

The –C**H$_c$**=CH$_2$ proton appears as a double doublet at 6.84ppm, 6.82ppm and 6.83ppm for **3a**, **3b**, **3c** respectively. The resonances from the aromatic protons appear at 7.18 and 7.06 ppm as a double doublet in the case of **3a**. For **3b** the signals are observed at 7.07 and 7.04ppm. For **3c** only one resonance at 7.08 ppm is observed. The proton resonances from the aliphatic chain are observed around 0.88 – 1.80 ppm.

Figure 4.3 represents an overlay of ^{13}C NMR of the monomers **3a**, **3b** and **3c**.

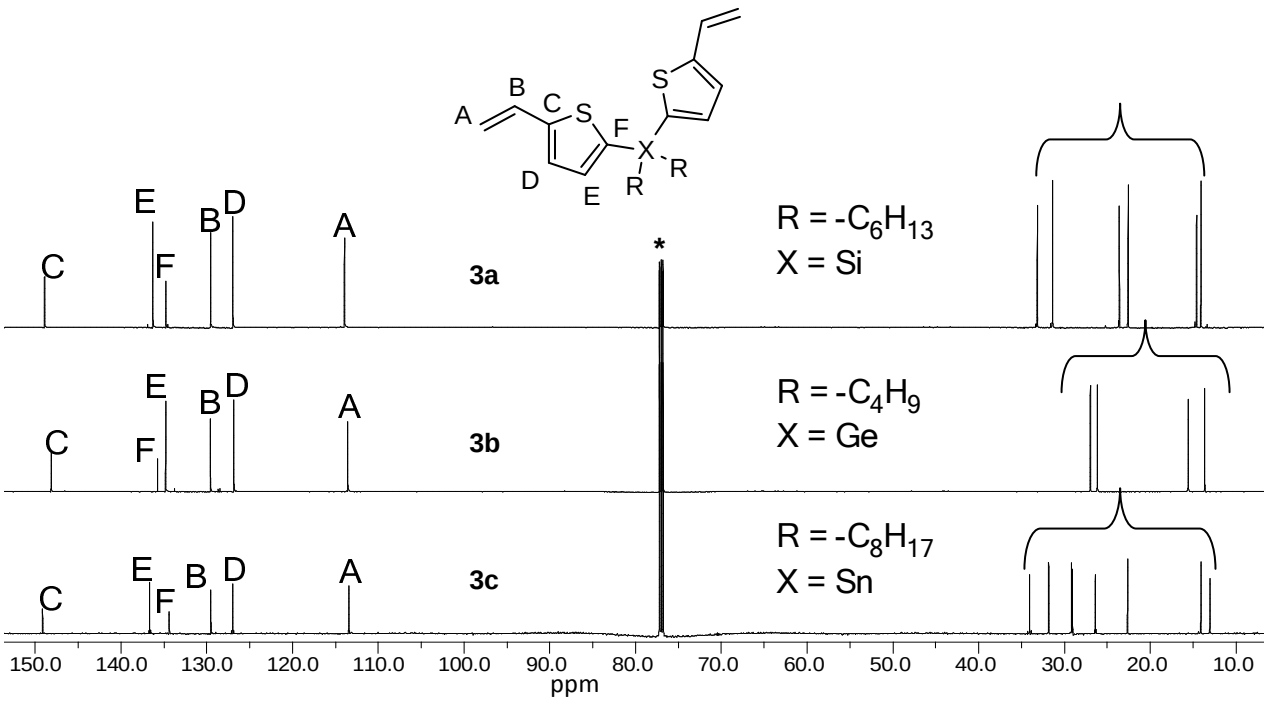

Figure 4.3 ^{13}C NMR (125 MHz, $CDCl_3^*$) overlay of **3a**, **3b**, **3c**

The carbon resonances associated with the terminal vinyl group (-**C$_B$**H=**C$_A$**H$_2$) are observed at 113.99(**C$_A$**) and 129.56(**C$_B$**) ppm for **3a**. In the cases of **3b** and **3c**, the carbon resonances associated with the terminal vinyl group (-**C$_B$**H=**C$_A$**H$_2$) are observed at 113.5(**C$_A$**) and 129.58(**C$_B$**) ppm and 113.43(**C$_A$**) and 129.52(**C$_B$**) ppm respectively. The entire proton and carbon assignment are summarized in Table 4.2 and Table 4.3 respectively with structures.

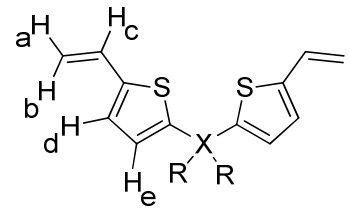

	X	R
3a	Si	$-C_6H_{13}$
3b	Ge	$-C_4H_9$
3c	Sn	$-C_8H_{17}$

	ppm				
Entry	a, b	c	d	e	**R**
3a	5.16, 5.61	6.84	7.18	7.06	$-C_6H_{13}$ = 0.88 – 1.6
3b	5.13, 5.57	6.82	7.07	7.04	$-C_4H_9$ = 0.88 – 1.6
3c	5.12, 5.56	6.83	7.07 (broad)		$-C_8H_{17}$ = 0.8-1.8

Table 4.2 ^{1}H NMR assignments of **3a**, **3b** and **3c**

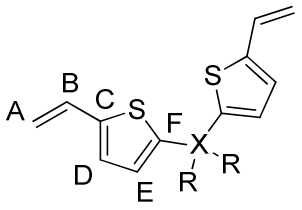

	X	R
3a	Si	$-C_6H_{13}$
3b	Ge	$-C_4H_9$
3c	Sn	$-C_8H_{17}$

	ppm						
Entry	A	B	C	D	E	F	**R**
3a	113.99	129.56	148.93	126.99	136.33	134.77	$-C_6H_{13}$ = 15 - 36
3b	113.53	129.58	148.14	126.80	134.80	135.78	$-C_4H_9$ = 13 - 28
3c	113.43	129.52	149.15	126.88	136.66	134.39	$-C_8H_{17}$ = 13 - 35

Table 4.3 ^{13}C NMR assignments of **3a**, **3b** and **3c**

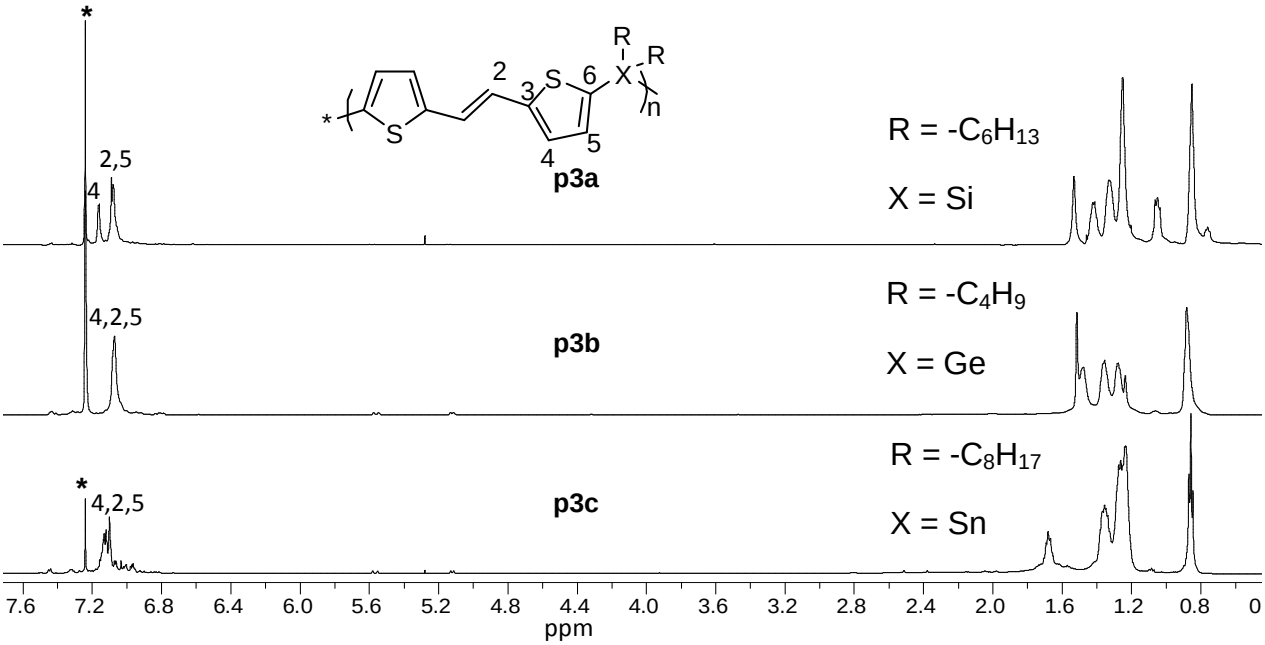

Figure 4.4 ^{1}H NMR (600 MHz, $CDCl_3^*$) overlay of **p3a**, **p3b** and **p3c**

An ^{1}H NMR overlay of all three polymers **p3a** – **c** is shown in Figure 4.4. After polymerization, resonance signals from the terminal vinyl protons from the chain ends were observed but none of the vinyl protons from the monomer. The aromatic protons appeared as broad signals around 7.08 ppm and 7.17 ppm for **p3a**, 7.08 ppm and 7.09 ppm for **p3b**, 7.07 ppm and 7.09 ppm for **p3c**. The newly formed internal vinylene protons appeared as resonances around 7.09 ppm, 7.07 ppm and 7.05 ppm for **p3a**, **p3b** and **p3c** respectively. This resonance experiences a gradual upfield shift as the heteroatom changes from Si to Sn. The presence of free radical based side products was not observed in any of the three cases which is supported by the absence of resonance signals in the range of 2.2 – 2.7 ppm.[112] Complete ^{1}H NMR and ^{13}C NMR assignments are summarized in Table 4.4

Figure 4.5 represents a ^{13}C NMR overlay of the ADMET polycondensates (**p3a** – **c**).The resonance signal from the terminal vinyl carbon $C_{\mathbf{A}}$ disappear after polymerization and a new peak $C_{\mathbf{A}}$ – related peak appears for the chain and terminal vinyl. The same is observed for the

signals from the terminal vinyl carbon C_B; shifted from 129.56 ppm to 121.81 ppm, 129.58 ppm to 121.51 ppm, 129.52 ppm to 121.20 ppm for **p3a**, **p3b** and **p3c** respectively. The resonance signal from the internal vinylene carbon formed is dependent on the heteroatom: In the sequence **p3a** – **c** (Si, Ge, Sn), the resonance is found gradually more upfield (Table 4.4).

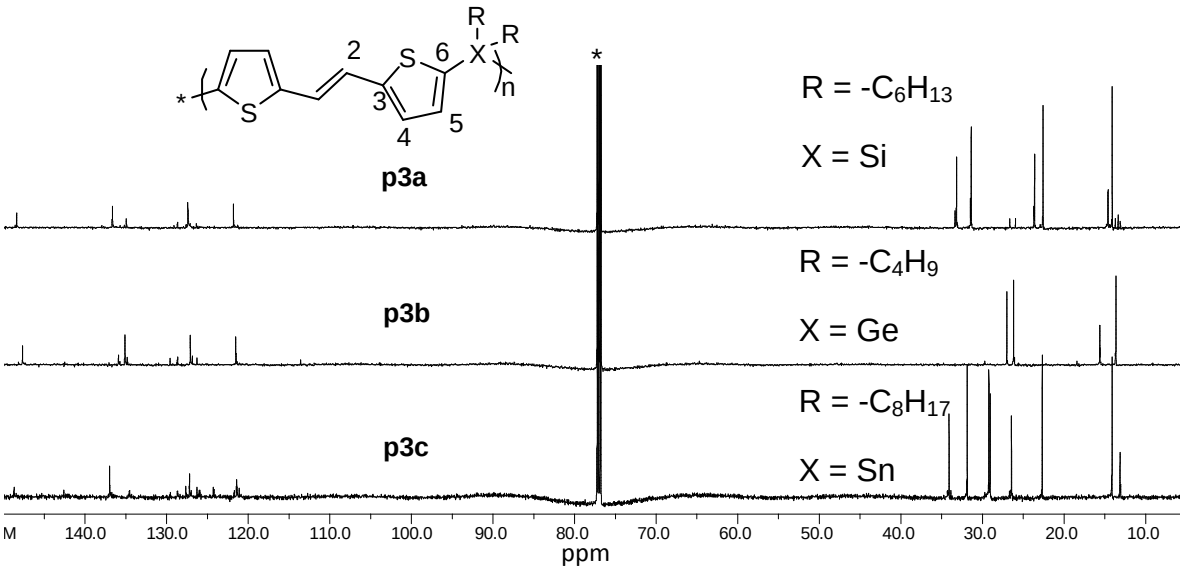

Figure 4.5. ^{13}C NMR (125 MHz, $CDCl_3^*$) overlay of **p3a**, **p3b** and **p3c**

In the case of **p3c**, both the proton and the carbon spectra revealed the presence of several additional resonances to the product. This might be explained by the tendency of tin compounds to undergo penta-valent coordination at higher temperatures giving rise to side products. Regardless of the systems, from the ^1H NMR and the ^{13}C NMR the structures of the polycondensates were found to be in "*all trans*" configuration with regard to the vinylene bond. In order to prove the microstructure of the polymers suggested above, correlation spectroscopy, particularly HSQC and COSY, was performed.

4.2.3.2.1 HSQC analysis of p3a, p3b and p3c

Correlation spectroscopy (HSQC) of the three polymers **p3a - c** indicated very strong and distinct C – H couplings from the aromatic part. In each of the three cases, three distinct signals were observed from the aromatic part, which can be accounted for two C – H coupling from the thiophene unit (C_4-H_4 and C_5-H_5) and one C – H coupling from the internal vinylene part (C_2-H_2). All these different couplings are summarized in Table 4.4.

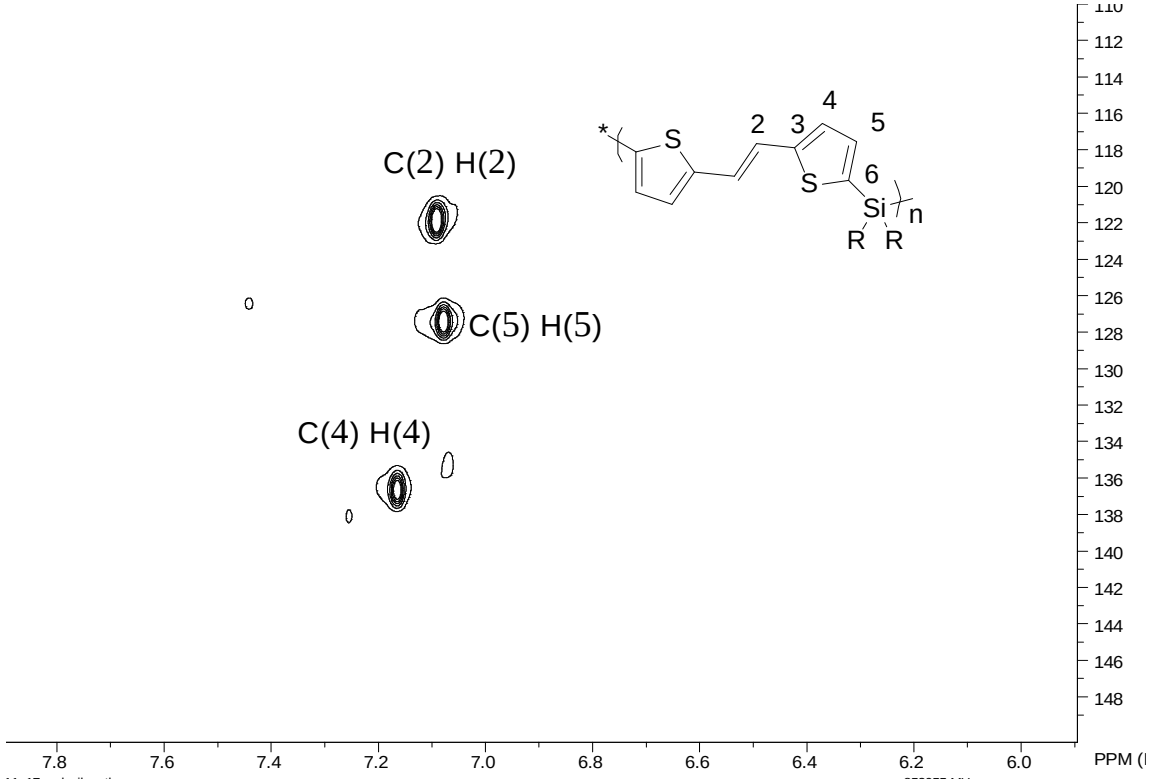

Figure 4.6 HSQC spectrum of **p3a** (selected region)

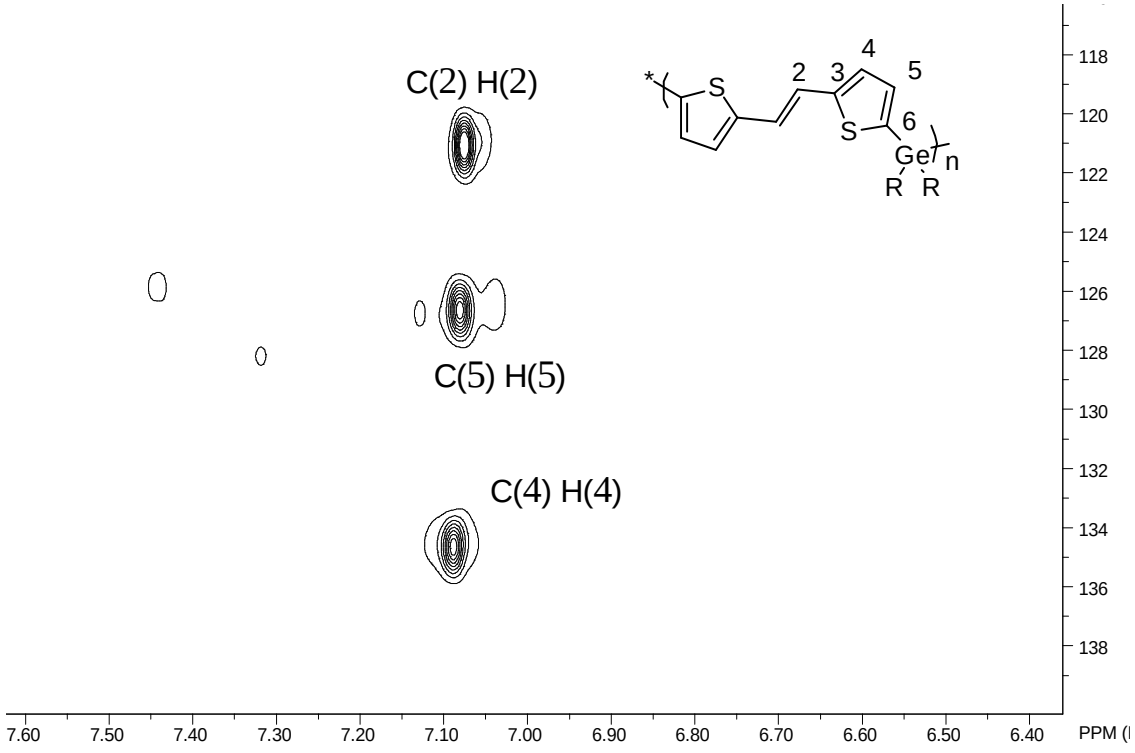

Figure 4.7 HSQC spectrum of **p3b** (selected region)

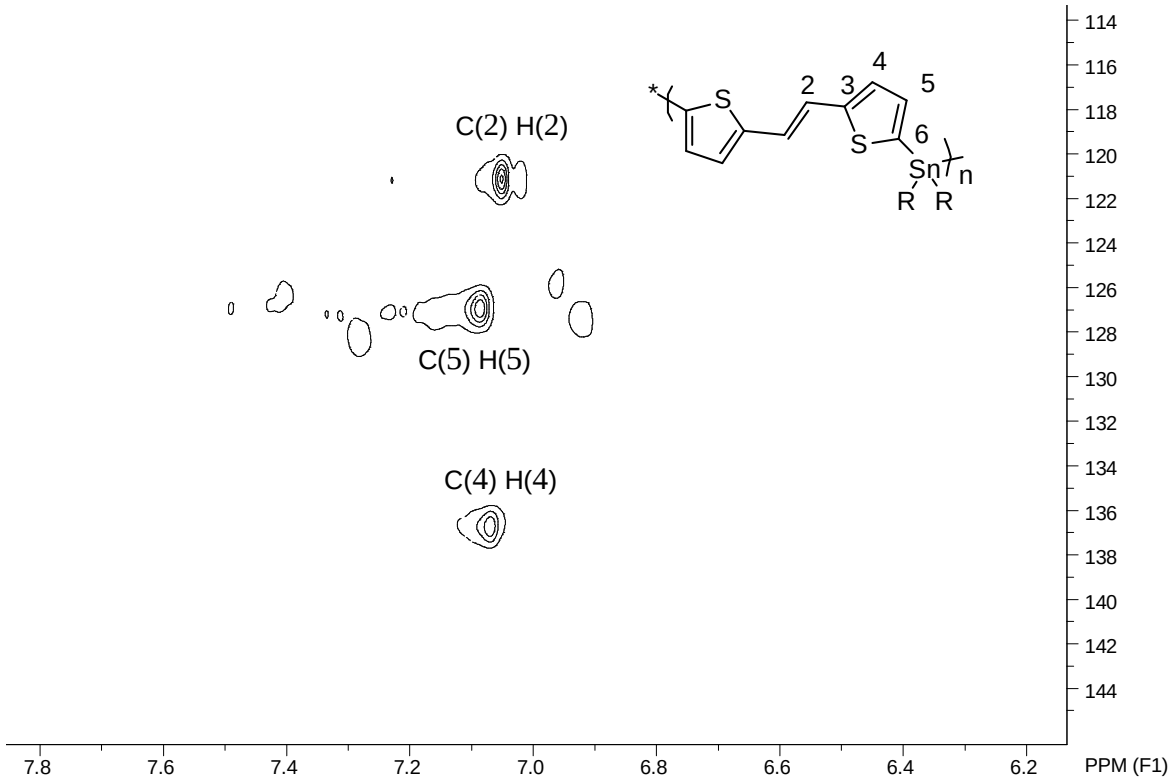

Figure 4.8 HSQC spectrum of **p3c** (selected region)

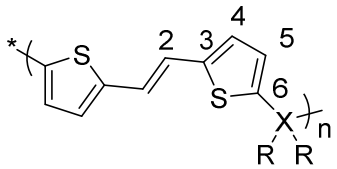

	X	R
p3a	Si	$-C_6H_{13}$
p3b	Ge	$-C_4H_9$
p3c	Sn	$-C_8H_{17}$

	Assignment	HSQC – coupling observed between	
		^{13}C (ppm)	^{1}H (ppm)
p3a	2	121.81	7.09
	5	127.43	7.08
	4	136.77	7.17
	6	134.94	n.o.
	3	148.38	n.o.
p3b	2	121.51	7.07
	5	127.07	7.08
	4	135.09	7.09
	6	135.89	n.o.
	3	147.65	n.o.
p3c	2	121.20	7.05
	5	127.00	7.09
	4	136.83	7.07
	6	134.50	n.o.
	3	148.70	n.o.

[1]not observed

Table 4.4 Structural assignments based on HSQC and ^{13}C and ^{1}H NMR

4.2.3.3 Optical properties (UV/Vis and Fluorescence spectroscopy)

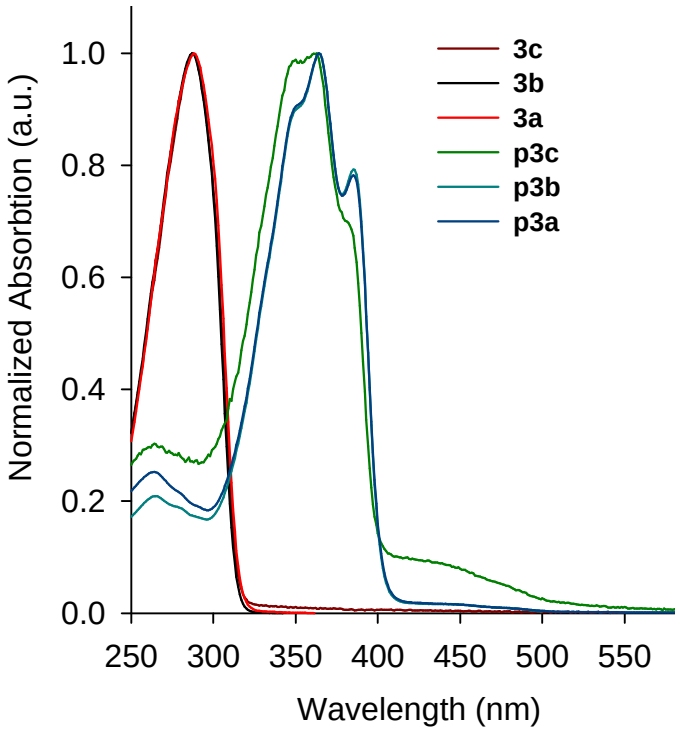

Figure 4.9 Absorption spectra of **3a-c** and **p3a-c** ([**3a - c**] ~ 10^{-4} M, [**p3a - c**] ~ 10^{-4} M)

UV/Vis absorption spectra of hexane solutions of monomers (**3a** – **c**) and polymers (**p3a** – **c**) are shown in Figure 4.9. The monomers showed absorption maxima at 283 – 284 nm. The absorption maxima of the polymers **p3a** – **c** were observed in the range of 361 – 363 nm. In the cases of **p3a** and **p3b**, the absorption spectra featured two major components with maxima ~363 nm and ~396 nm (shoulder peak). This shoulder peak is greatly reduced in the case of **p3c**, instead a low energy band with relatively weak intensity around 448 nm is observed. A possible explanation of such low energy component in **p3c** could be the presence of aggregated species.

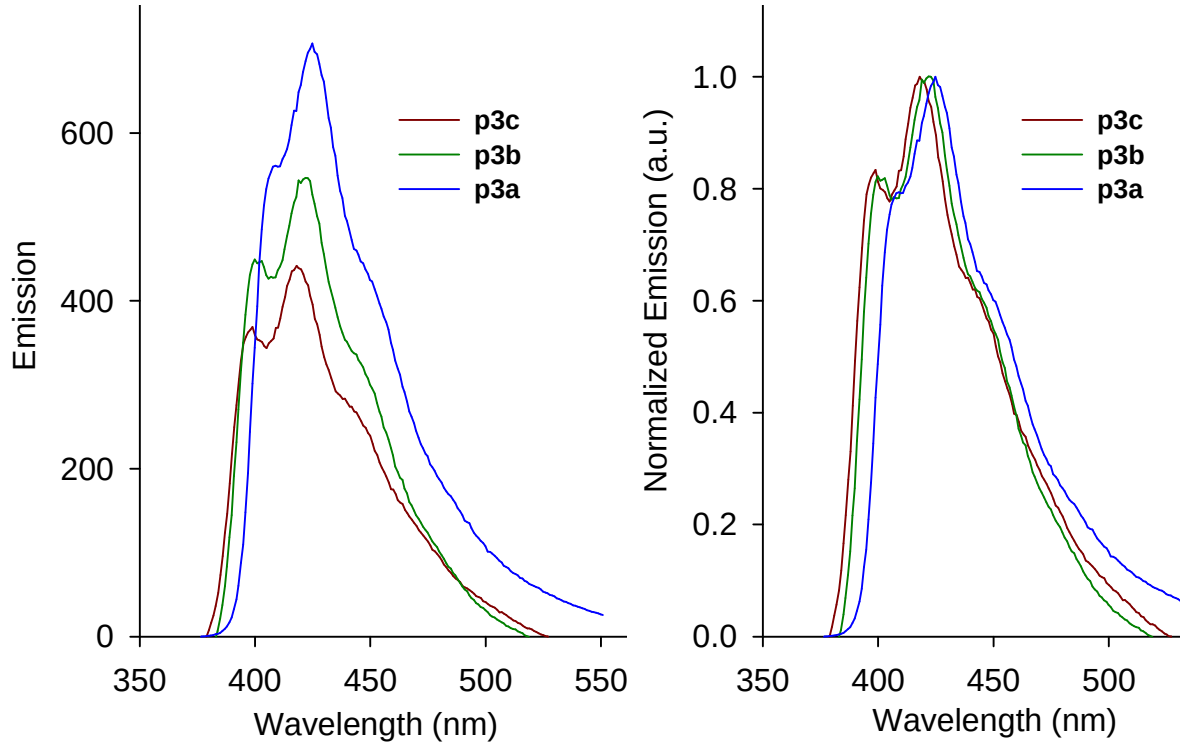

Figure 4.10 Emission spectra of **p3a** – **c** ([**p3a** – **c** = 2.0 x 10^{-5} M])

Figure 4.10 represents the unnormalized emission spectra of polymers in hexane with identical concentration. It is to be mentioned that monomers did not show any emission due to the spin – orbital coupling effect exerted by sulfur over the structure of the monomer resulting in the formation of triplet states[113], whereas the polymers are strongly fluorescent in the blue region, with emission maxima are recorded in the range of 419 – 423 nm.

Gradually more quenching of fluorescence was observed from **p3a** ⟶ **p3c** in similar concentrations (2 x 10^{-5} M) in hexane. It is possible that the increase in size of the heteroatom from Si to Sn (hetero-atom effect) is responsible for the transfer of the excited electrons to a triplet state via intersystem crossing resulting in the observed quenching of fluorescence; although lifetimes of the excited states have not been measured here but decrease in quantum efficiency has been observed. A gradual blue shift of the emission maxima was also observed from **p3a** to **p3c**. As the size of the heteroatoms increases from **p3a** to **p3c** (Si [117 pm] Ge [122

pm], Sn [140 pm]),[114] the through – space interaction between the π - conjugated segments decreased resulting in the observed blue shift.

Table 4.5 summarizes the absorption and the emission data of the monomers and the polymers.

Table 4.5 Absorption and emission data of **3a - c**, **p3 - c**.

Sample	$\lambda_{max\ (abs)}$ **(nm)**	$\lambda_{max\ (em)}$ **(nm)**	$*\phi_{eff}$
3a	284	-	
3b	283	-	
3c	284	-	
p3a	363	423	0.25
p3b	362	421	0.18
p3c	360	419	0.11

* referenced to the repeat units via NMR M_n, relative to trans-stilbene

4.2.3.3.1 Effect of concentration on the emission of p3a, p3b, p3c.

The effect of concentration on the emission behavior of the polymers was studied and is shown in Figure 4.11.

The fluorescence spectrum of **p3a** exhibited a shoulder at 440 nm which seems to remain unchanged even when the concentration is increased. The long hexyl chains on the silicon moiety prevent aggregation of the polymeric backbone. As a result, the intensity of the lower energy band around 440 nm did not increase with the increase in concentration or the emission at 440 nm is simply not related to aggregates.

For **p3b**, the shoulder at 440 nm increases insignificantly with the concentration range studied supporting the conclusion drawn from **p3a**. There is however some tailing observed at longer wavelengths, indicating the possible presence of aggregates. The shorter butyl chains on the germanium atom may allow for an easier aggregation. Formation of these weakly emissive aggregated species in solution may also responsible for the reduction in emission intensity compared to **p3a**.[115]

In the case of **p3c**, the concentrations are very similar to the **p3b** case. This observation is despite of the presence of the longer octyl chains on the tin atom. These aggregated species seems to reduce the luminescence intensity compared to both **p3a** and **p3b**.

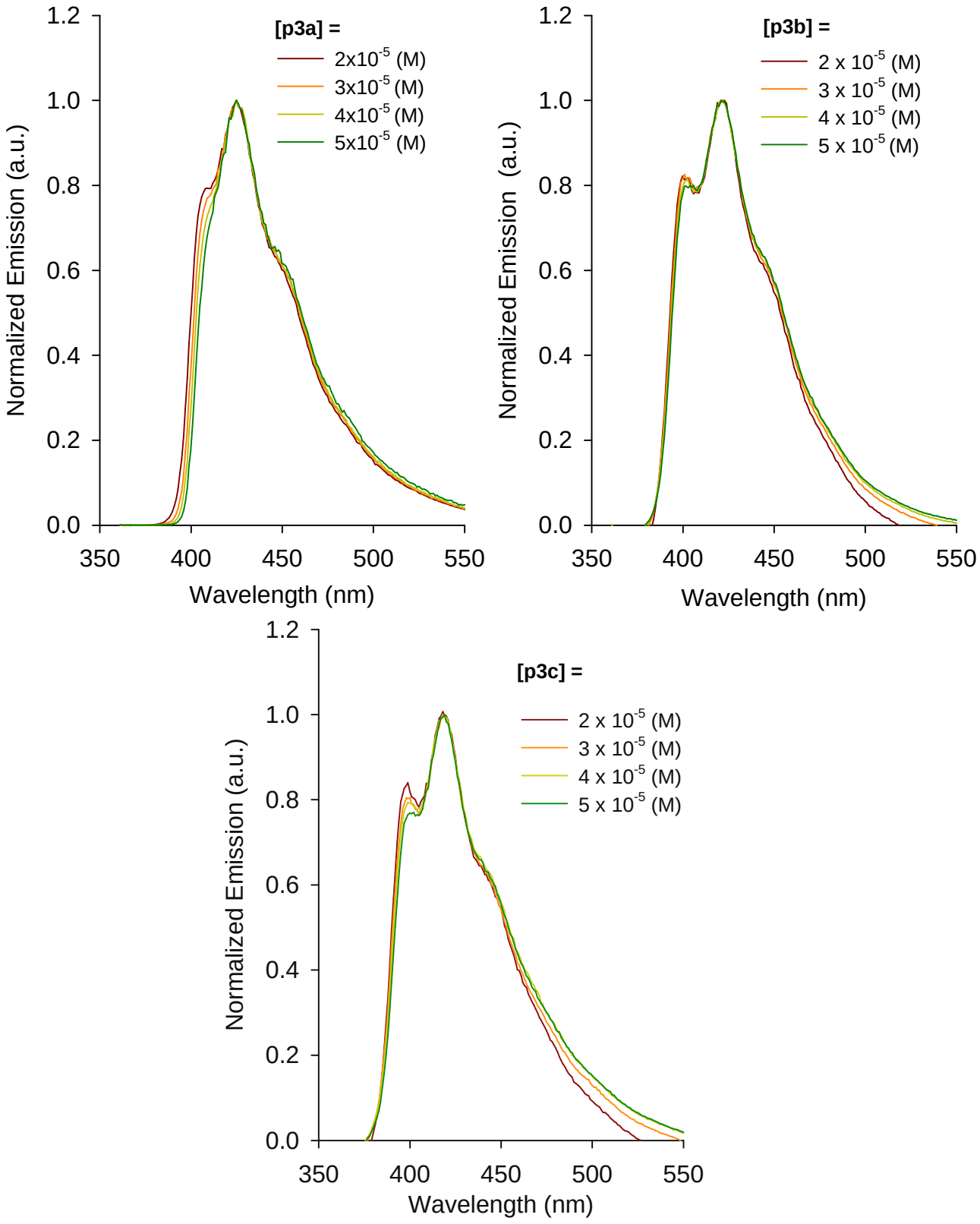

Figure 4.11 Effect of concentration on the emission characteristics of **p3a - c**

4.2.3.4 Thermal Analysis of p3a, p3b and p3c (in N_2)

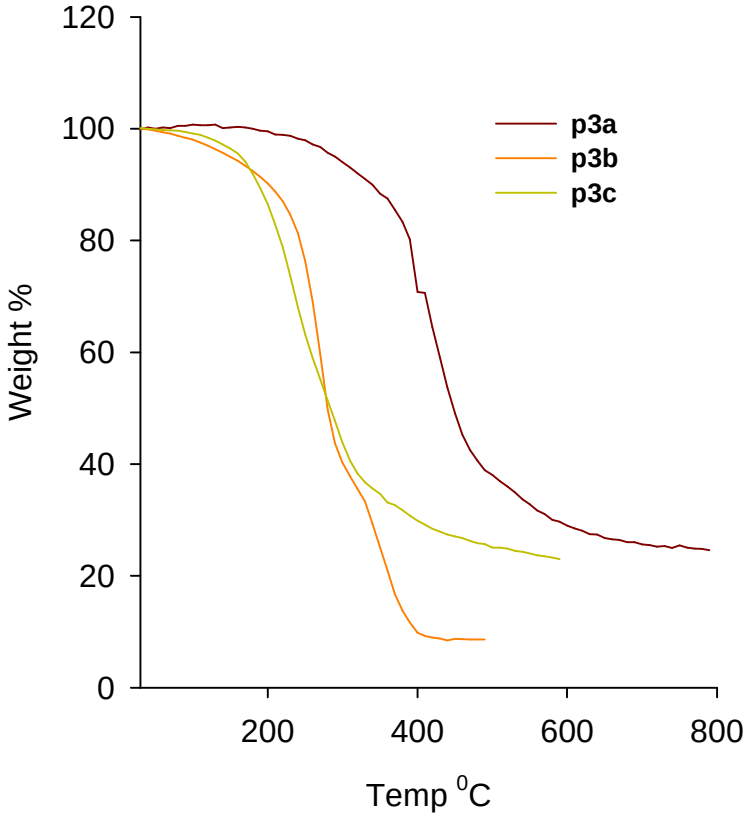

Figure 4.12 TGA curves for **p3a - c**

The thermo-gravimetric curves of **p3a – c** are shown in Figure 4.12. Table 4.6 summarizes the 5% wt loss temperatures of the polymers. Out of the three polymers, **p3a** showed the highest stability as 5% weight loss occurred at 290^{0}C. For **p3b** and **p3c** the backbone starts to decompose at earlier stage around 150^0 – 160^{0}C. In case of **p3c**, a residual mass of 22% was observed, whereas in case of **p3a**, a residual mass of 24% was observed.

Table 4.6 5% weight loss temperatures of **p3a – c**

Entry	5%wt loss temp (^{0}C)
p3a	290
p3b	150
p3c	160

4.3 Conclusion

In conclusion, the synthesis of heteroatom (Si, Ge and Sn) containing thiophene based polymers has opened a new window for the development of electron rich heteroatom containing aromatic conjugated systems and comparison of their photophysical properties. The polymers developed are structurally pure i.e "all – trans" configuration at the vinylene as indicated by the NMR. No free radical based product was observed under ADMET conditions studied.

Further studies can be carried out on the aggregation behavior of these systems to understand comprehensively the quenching phenomenon involved at high concentration in solution. Electrochemical studies of these materials may provide further information for potential applications of these systems.

4.4 Experimental

General Information

All of the experiments using air/moisture sensitive materials were carried out in a nitrogen filled Labconco protector glove box and/or by the use of dry argon filled dual manifold (inert gas/ vacuum) using standard Schlenk line techniques. All glassware was cleaned and dried for at least 16 h in an oven at 120 ^{0}C prior to use.

Chemicals

nBuLi (2.5 M in hexane), sodium sulfate and Grubbs (2nd Generation) catalyst, 5-bromothiophene 2-carbaldehyde (98%) were obtained from Sigma Aldrich. Dichlorodihexylsilane, dichlorodioctyltin were obtained from Gelest Inc and dichlorodibutylgermane was obtained from Arcos Chemicals. Solvents e.g. tetrahydrofuran (THF), toluene, hexane were purchased as HPLC grade from Fisher Scientific. All solvents were dried and degassed by a "Pure Solv" solvent purification system (using activated alumina, copper catalyst, molecular sieves column when appropriate) by Innovative Technology Inc. before use. All other chemicals were used as received.

Instrumentation

^{1}H NMR (600 MHz) and ^{13}C NMR spectra were recorded as solutions in $CDCl_3$ on Varian Unity NMR instruments. $CDCl_3$ was used as an internal deuterium lock for the spectra. All of the signals in the NMR spectra are reported in ppm, multiplicity (s = singlet, d = doublet, t = triplet, q = quadruplet, m = multiplet, dd = doublet of doublet).

UV-Visible absorption spectra were recorded using a Perkin Elmer Model 650 UV Spectrophotometer with 1-cm path length cells. The samples were prepared with HPLC grade hexane ("Spectrasolv") in a sample cell.

Photoluminescence spectra were recorded using a Varian spectrofluorometer with 1-cm path length cells. The samples were prepared with HPLC grade hexane ("Spectrasolv") in a sample cell.

GPC analysis was carried out on an Alliance GPCV 2000 (Waters) instrument equipped with four Waters Styragel HR columns, i.e. HR-1, HR-3, HR-4, and HR-5E. HPLC grade THF was used as eluent, at a flow rate of 1.0 mL/min at 40 ^{0}C. Measurements are relative to a calibration with polystyrene standards and third order relative calibration curve was used to measure the molecular weight of unknown samples.

Thermogravimetric Analysis was carried out on a Hi –Res TGA 2950 Thermogravimetric Analyzer from TA instruments using platinum with a heating rate 10^{0}C/min under continuous flow of nitrogen. Elemental analyses were performed in Atlantic Microlab. Inc.

Synthesis of 2-bromo 5-vinylthiophene (2)

6.2 mmol of triphenylphosphonium methyl bromide was suspended in 30 ml dry THF. To this suspension 5.7 mmol of nBuLi (2.5 M in hexane, 2.3ml) was added dropwise at 0^{0}C. The reaction mixture was stirred for 3h. To this resulting solution 5.2 mmol of 2-bromo 5-thiophene carbaldehyde (1) dissolved in 10ml of dry THF were added slowly at 0^{0}C. The resulting solution was stirred for 12h at room temperature and then concentrated under reduced pressure followed by washing with hexane. The hexane layer was kept over sodium sulfate and then filtered. The organic phase was then concentrated under reduced pressure to yield the crude product. Further purification was carried by column chromatography with hexane-dichloromethane (7:3) solvent mixture as the eluent to obtain a reddish yellow liquid. Yield 65%.

^{1}H NMR (600MHz, $CDCl_3$) δ = 6.89 (d, 2H), 6.69 (d, 2H), 6.67 (q, 2H), 5.45 (d, 2H, J = 17.43 Hz), 5.13 (d, 2H, J = 10.99 Hz)

Synthesis of 3a

1.25 mmol of **2** was dissolved in a THF/diethylether solvent mixture (3/0.5). To this resulting solution 1.25 mmol of nBuLi (2.5 M in hexane, 0.5ml) was added at -78^{0}C. The reaction mixture was stirred for 3h at -78^{0}C. To the resulting solution, 0.6 mmol of dichlorodihexylsilane was added dropwise at -78^{0}C. The reaction mixture was then allowed to warm up to room temperature over a period of 12h. The reaction mixture was then concentrated under reduced pressure. The crude product was then dissolved in hexane and washed with water. The hexane layer was collected and kept over sodium sulfate and then filtered. The hexane layer was further concentrated under reduced pressure to obtain a yellowish residue. Purification of the residue was carried out by column chromatography using hexane/DCM (7:3) as the solvent mixture to obtain a yellowish liquid. Yield 75%.

^{1}H NMR (600MHz, $CDCl_3$) δ = 7.18 (d, 2H, J = 3.51 Hz), 7.05 (d, 2H, J = 3.32 Hz), 6.84 (q, 2H), 5.62 (d, 2H, J = 17.46 Hz), 5.17 (d, 2H, J = 11.07 Hz), 0.89 – 1.45 (m, 26H).

^{13}C NMR (125 MHz, $CDCl_3$) δ = 148.9, 136.3, 134.8, 129.6, 127, 114, 33.2, 31.4, 23.6, 22.6, 14.6, 14.1.

Elemental analysis: 68.13% C, 8.51% H, 14.59% S.

Synthesis of 3b

0.96 mmol of **2** was dissolved in THF/Diethylether solvent mixture (3/0.5). To this resulting solution 0.96 mmol of nBuLi (2.5 M in hexane, 0.38ml) was added at -78^{0}C. The reaction mixture was stirred for 3h at -78^{0}C. To the resulting solution 0.45 mmol of dichlorodibutylgermane was added dropwise at -78^{0}C. The reaction mixture was then allowed to warm up to room temperature over a period of 12h. The reaction mixture was then concentrated under reduced pressure. The crude product was then dissolved in hexane and washed with water.

The hexane layer was collected and kept over sodium sulfate and then filtered. The hexane layer was further concentrated under reduced pressure to obtain a yellowish residue. Purification of the crude residue was carried out by column chromatography using hexane/DCM (7:3) as the solvent mixture to obtain a yellowish liquid. Yield 72%.

^{1}H NMR (600MHz, $CDCl_3$) δ = 7.08 (d, 2H, J = 3.35 Hz), 7.04 (d, 2H, J = 3.35 Hz), 6.82 (q, 2H), 5.57 (d, 2H, J = 17.52 Hz), 5.13 (d, 2H, J = 10.86), 0.89 – 1.48 (m, 18H).

^{13}C NMR (125 MHz, $CDCl_3$) δ = 148.1, 135.8, 134.8, 129.6, 126.8, 113.5, 26.9, 26.2, 15.6, 13.6.

Synthesis of 3c

1.69 mmol of **2** was dissolved in THF/Diethylether solvent mixture (3/0.5). To this resulting solution 1.69 mmol of nBuLi (2.5 M in hexane, 0.675ml) was added at -78^{0}C. The reaction mixture was stirred for 3h at -78^{0}C. To the resulting solution 0.84 mmol of dichlorodioctyltin was added dropwise at -78^{0}C. The reaction mixture was then allowed to warm up to room temperature over a period of 12h. The reaction mixture was then concentrated under reduced pressure to obtain a crude product. The crude product was dissolved in hexane and washed with water. The hexane layer was collected and kept over sodium sulfate and then filtered. The hexane layer was further concentrated under reduced pressure to obtain a yellowish residue. Purification of the crude residue was carried out by column chromatography using hexane/DCM (7:3) as the solvent mixture to obtain a yellowish liquid. Yield 68%.

^{1}H NMR (600MHz, $CDCl_3$) δ = 7.08 (br, 4H), 6.83 (q, 2H), 5.56 (d, 2H, J = 17.39 Hz), 5.12 (d, 2H, J = 11.02 Hz), 0.85 – 1.66 (m, 34H).

^{13}C NMR (125 MHz, $CDCl_3$) δ = 149.1, 136.7, 134.4, 129.5, 126.9, 113.4, 34.1, 31.9, 29.2, 27.8, 26.4, 22.7, 14.1, 13.1.

Elemental analysis: 57.04% C, 7.41% H, 10.28% S.

Synthesis of p3a

0.48 mmol of **3a** was dissolved in dry toluene. To the solution 0.024 mmol of Grubbs 2nd generation catalyst was added. The reaction mixture was stirred for 48 – 55h at 70^{0}C. The reaction progress was monitored by observing the intensity of the terminal vinyl peaks using ^{1}H NMR. At the end of the reaction, the mixture was concentrated under reduced pressure, re-dissolved in hexane and passed through a silica gel column using small volume of DCM as a co-eluent. Yield 70%

^{1}H NMR (600 MHz, $CDCl_3$) δ = 7.08 (br, 4H), 6.83 (q, 2H), 5.59 (d, 2H), 5.14 (d, 2H), 0.76 – 1.42 (m, 26H).

^{13}C NMR (125 MHz, $CDCl_3$) δ = 148.4, 136.8, 134.9, 127.4, 121.8, 33.2, 31.4, 23.6, 22.6, 14.6, 14.1.

Synthesis of p3b

0.24 mmol of **3b** was dissolved in dry toluene. To the solution 0.017 mmol of Grubbs 2nd generation catalyst was added. The reaction mixture was stirred for 96h at 80^{0}C. The reaction progress was monitored by observing the intensity of the terminal vinyl peaks using ^{1}H NMR. At the end of the reaction, the mixture was concentrated under reduced pressure, re-dissolved in hexane and passed through a silica gel column using small volume of DCM as a co-eluent. Yield 70%

^{1}H NMR (600 MHz, $CDCl_3$) δ = 7.09 (br, 2H), 7.08 (br, 2H), 7.07 (br, 2H), 5.56 (d, 2H), 5.12 (d, 2H), 0.88 – 1.48 (m, 18H).

^{13}C NMR (125 MHz, $CDCl_3$) δ = 147.7, 135.9, 135.1, 127.1, 121.5, 27.1, 26.2, 15.6, 13.7.

Synthesis of p3c

0.37 mmol of **3c** was dissolved in dry toluene. To the solution 0.035 mmol of Grubbs 2nd generation catalyst was added. The reaction mixture was stirred for 6d at 70^0-80^{0}C. The reaction progress was monitored by observing the intensity of the terminal vinyl peaks using ^{1}H NMR. At the end of the reaction, the mixture was concentrated under reduced pressure, re-dissolved in hexane and passed through a silica gel column using small volume of DCM as a co-eluent. Yield 65%

^{1}H NMR (600 MHz, $CDCl_3$) δ = 7.09 (br, 2H), 7.07 (br, 2H), 7.05 (br, 2H), 5.57 (d, 2H), 5.12 (d, 2H), 0.86 – 1.68 (m, 34H).

^{13}C NMR (125 MHz, $CDCl_3$) δ = 148.7, 136.8, 134.5, 127, 121.2, 34.1, 31.9, 29.2, 29.1, 26.5, 22.7, 14.1, 13.1.

5. Synthesis and characterization of alkyloxy side – chain substituted SiPPV systems

5.1 Introduction

As mentioned earlier, silicon containing stilbene (SiPPV), 2, 5-thienylene vinylene (Si thiophene) based polymeric systems are promising materials for application in LEDs and photovoltaic systems.

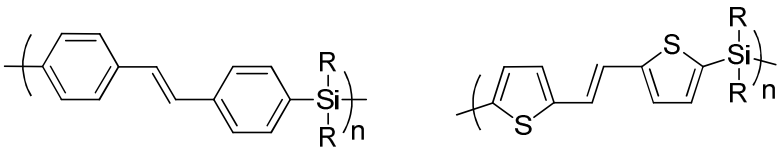

SiPPV Si thiophene

Scheme 5.1 Representative SiPPV and Si thiophene systems

Possible size - effects were seen in heteroatom containing thiophene based polymers resulting in decrease in emission intensity with an increase in size. To have a better understanding on interactions between a heteroatom like silicon and a π – conjugated system, we developed electron rich heteroatom containing polymeric systems. The objective of this work lies in designing such an electron rich monomer based on silicon containing a bistyryl system with electron donating alkyloxy-substitution on the styryl moieties and its corresponding polymer using the synthetic strategy we have discussed earlier and evaluate structure/property correlation with respect to photo – physical properties in the context of this earlier work. The monomer developed was expected to be more radically active compared to the stilbene systems because of the presence of electron donating alkyloxy substituent. The challenge lies in achieving a structurally pure polymeric system via ADMET and no free radical based product under the reaction condition for the metathesis.

5.2 Results and discussions

The alkyloxy – substituted distyryl containing silylene monomer **6** was prepared by following a five – step synthetic strategy starting from hydroquinone. Olefin metathesis of the monomer was carried out using Grubbs 2nd generation catalyst and Hoveyda – Grubbs 2nd generation catalyst under similar conditions. Considerable conversion was achieved at 70^0C for both systems after 72 h. The reaction progress was monitored using NMR and the products obtained were soluble in common organic solvent.

5.2.1 Monomer synthesis

The synthesis of the monomer involves a multi-step synthetic strategy as shown in Scheme 5.2.

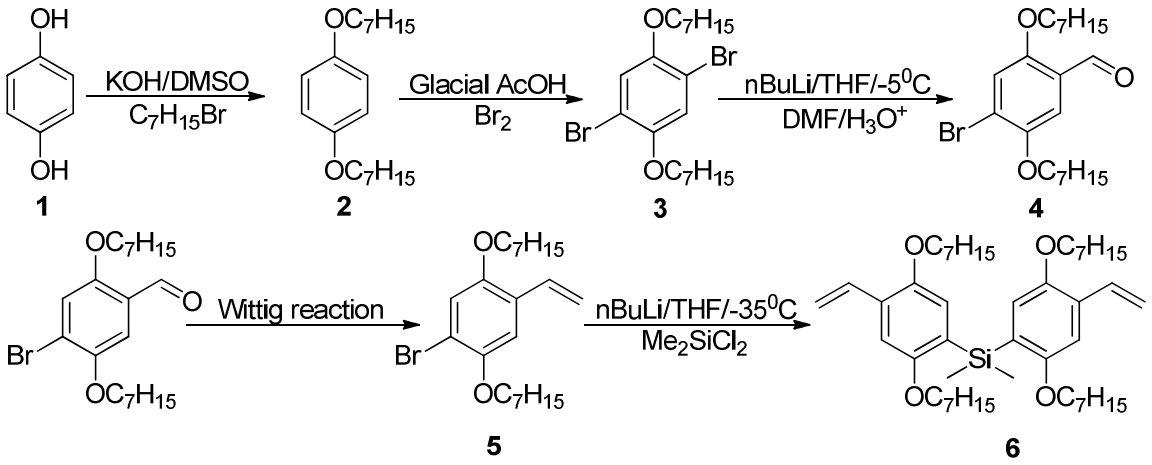

Scheme 5.2 Synthesis of monomer **6**

The synthesis of the monomer involved five steps starting from the conversion of hydroquinone to its di-heptyloxy derivative **2** using bromoheptane and potassium hyhroxide in dimethyl sulfoxide (DMSO). The yield of **2** was ~ 90% after crystallization from cyclohexane. **2** was further treated with bromine in the presence of glacial acetic acid to obtain the dibromo derivative **3**. The yield of **3** after purification was ~ 87%. Next, compound **3** was formylated using butyl lithium and dimethyl formamide to synthesize a bromo-aldehyde **4**. **4** was purified by

column chromatography with a yield ~ 75%. Wittig reaction with the bromo-aldehyde was used to obtain the bromo-vinyl derivative **5** with a yield ~ 70% after purification.

Finally, **5** was lithiated in THF at -35^{0}C for 3 h followed by the addition of dichlorodimethylsilane at -35^{0}C.The reaction was continued over a period of 12 h. The product was isolated by removing the solvent in vacuo. The crude product was then dissolved in hexane, filtered, and further purified by passing through a short silica gel column. The yield of **7** was ~ 30%

5.2.2 ADMET polycondensation

Scheme 5.3 represents the polycondensation of the monomer.

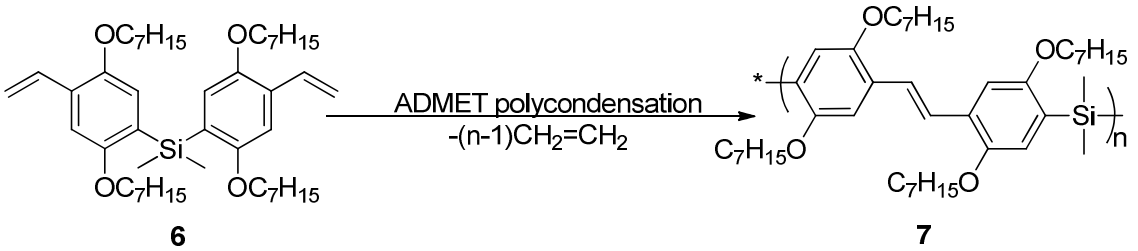

6 **7**

Scheme 5.3 ADMET polycondensation of monomer

The ADMET polycondensation of the monomer was carried out using Grubbs 2nd generation catalyst or Hoveyda-Grubbs 2nd generation catalyst in toluene as a solvent. In both cases, higher temperatures ~ 70^{0}C and longer reaction times (72 h) were necessary to achieve significant molecular weight. Hoveyda – Grubbs 2nd generation catalyst resulted in higher molecular weight product compared to when Grubbs 2nd generation catalyst was used, perhaps an indication of the higher stability of the Hoveyda – Grubbs 2nd generation catalyst, resulting in higher conversion under similar conditions of concentration, time and temperature.

As mentioned in all our earlier systems, reaction temperatures below 50 ^{o}C did not yield any product at all, regardless of catalyst used. Higher ratios of [monomer]/[catalyst] also resulted in

lower conversions. As the chain size increases with conversion, it is expected that the chain growth reaction starts to compete with some ring closing, the result of an expected chain/ring equilibrium, discussed repeatedly above. Thus it is possible that small fractions of the polymeric products consist of cyclic macromolecules. This might explain some of the shoulders on the low molecular weight side of the distributions in the GPC-traces.

5.2.3 Characterization

5.2.3.1 Size analysis

Molecular weights of **7**[a] and **7**[b] were determined by gel permeation chromatography relative to polystyrene as standard. Figure 5.1 represents traces of differential refractive index (dRI) detector responses for **6**, **7**[a] and **7**[b].

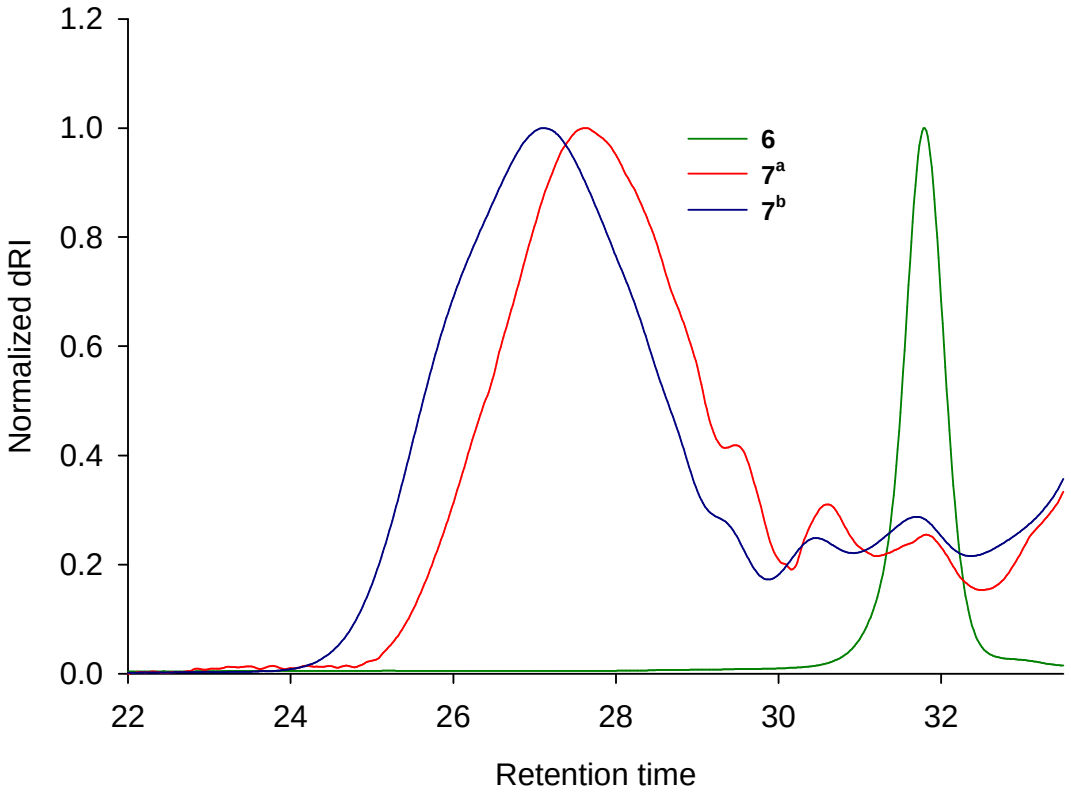

Figure 5.1 GPC traces of **6** and **7**[a, b] ([a]Hoveda – Grubbs 2nd generation catalyst, [b]Grubbs 2nd generation catalyst)

Table 5.1 summarizes the M_n along with the polydispersities of the polymers. The calculated M_n values based on NMR are from end group analysis (integrals of signals from chain end vinyl protons vs. chain internal vinylene protons). The presented results characterize representative polycondensates synthesized in toluene at 70 ^{0}C after 72 h reaction time. The polymers **7**[a] and **7**[b] showed GPC based M_n ~ 6000 and 8500 g/mol (NMR: 3360 and 6228 g/mol), respectively.

Table 5.1 Polycondensation conditions and molecular weights

Entry	Reaction condition		M_n		PDI
	[Monomer]	[Catalyst]	GPC	NMR	
7[a]	61	4.8	5938	3360	1.46
7[b]	51	4.7	8529	6228	1.49

[a] Grubbs 2nd generation catalyst, [b] Hoveyda – Grubbs 2nd generation catalyst T = 70^0C, t = 72h, solvent: toluene.

5.2.3.2 NMR (Microstructure analysis)

The microstructure of both the monomer **6** and the polymers **7** were determined by ^{1}H and ^{13}C NMR spectroscopy as shown in Figures 5.2 – 5.3. $\mathbf{7^a}$ and $\mathbf{7^b}$ represent samples using different catalysts under similar same reaction conditions.

The proton resonances from the terminal vinyl group –CH=C$\mathbf{H_2}$ of the monomer appear as two doublets 5.22 (cis, $\mathbf{H_a}$) and 5.71 (trans, $\mathbf{H_b}$) ppm respectively. The –C$\mathbf{H_c}$=CH_2 proton appear as a double doublet at 7.03 ppm. The resonance signals from the aromatic protons appear at 6.82 ppm and 6.87 ppm as singlets. The signals from the heptyloxy chain lie in the range of 0.86 – 3.81 ppm. The methyl protons resonance signal from the silicon moiety appears as a singlet at 0.52 ppm.

In case of the polymer **7**, a decrease in the intensity of the terminal vinyl group is observed with increase in reaction time. This decrease is more markedly using Hoveyda – Grubbs 2nd Generation catalyst (see above). A new resonance signal at 7.46 ppm arises from the internal vinylene protons (-C$\mathbf{H_b}$,=C**H**-) which once again are in '*all – trans*' configuration. The aromatic protons appear as broader resonances at 7.03 and 6.87 ppm. The proton resonances from the heptyloxy substitution lie in the range of 0.84 – 3.86 ppm.

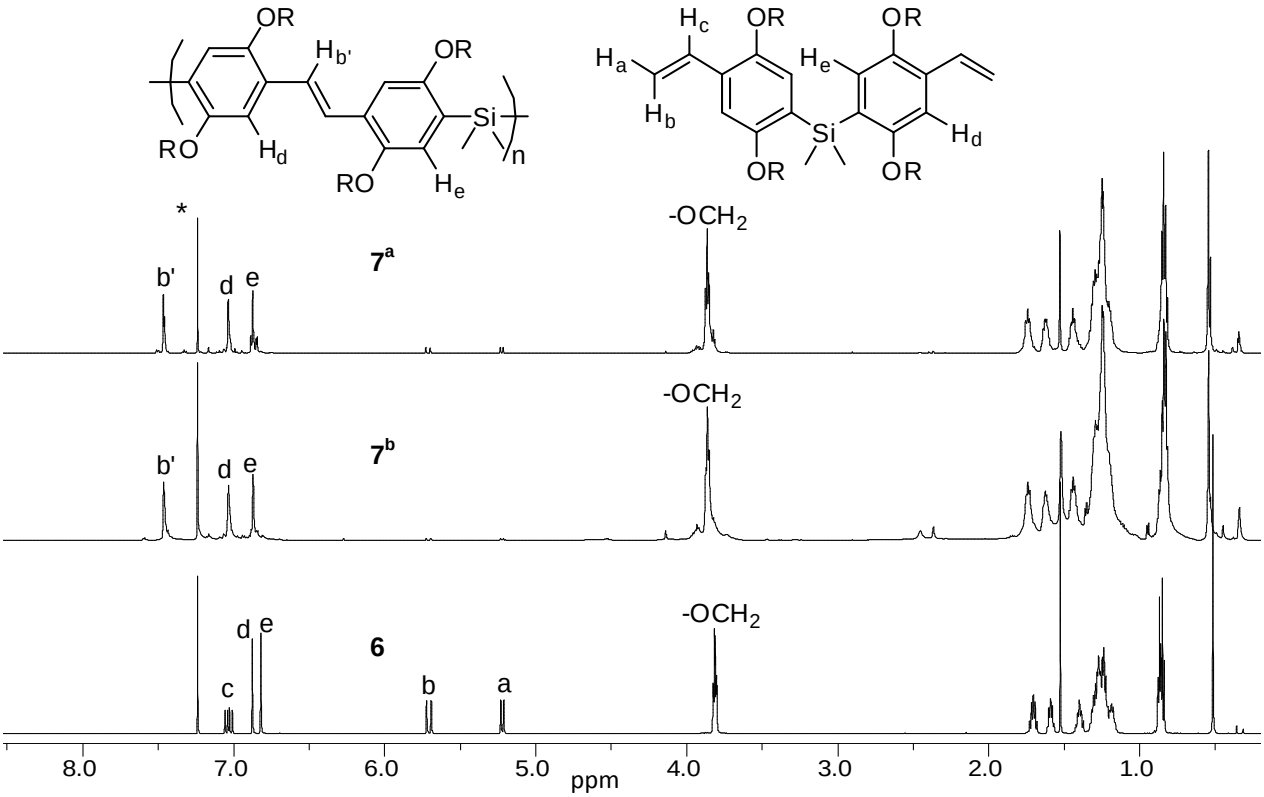

Figure 5.2 ^{1}H NMR (600MHz, $CDCl_3^*$) spectral overlay of **6**, **7^{a}** and **7^{b}**

The carbon resonances associated with the terminal vinyl group $\mathbf{C_1}$ and $\mathbf{C_2}$ are observed at 114.07 and 132.22 ppm. The aromatic carbon resonances are observed at 158.04 ppm, 150.02 ppm, 128.61 ppm, 127.45 ppm, 121.15 ppm, 107.58 ppm. After metathesis, the carbon resonances of the terminal vinyl group disappeared and a new peak around 123.83 ppm appeared corresponding to the internal vinylene carbons $\mathbf{C_{2'}}$.The resonance signals of the aromatic carbons are observed at 158.24 ppm, 150.41 ppm, 129.19 ppm, 127.08 ppm, 121.54 ppm, 107.39 ppm. The complete ^{1}H NMR and ^{13}C NMR assignments of the monomer **6** and polymer **7** are shown in Table 5.2 and Table 5.3 respectively.

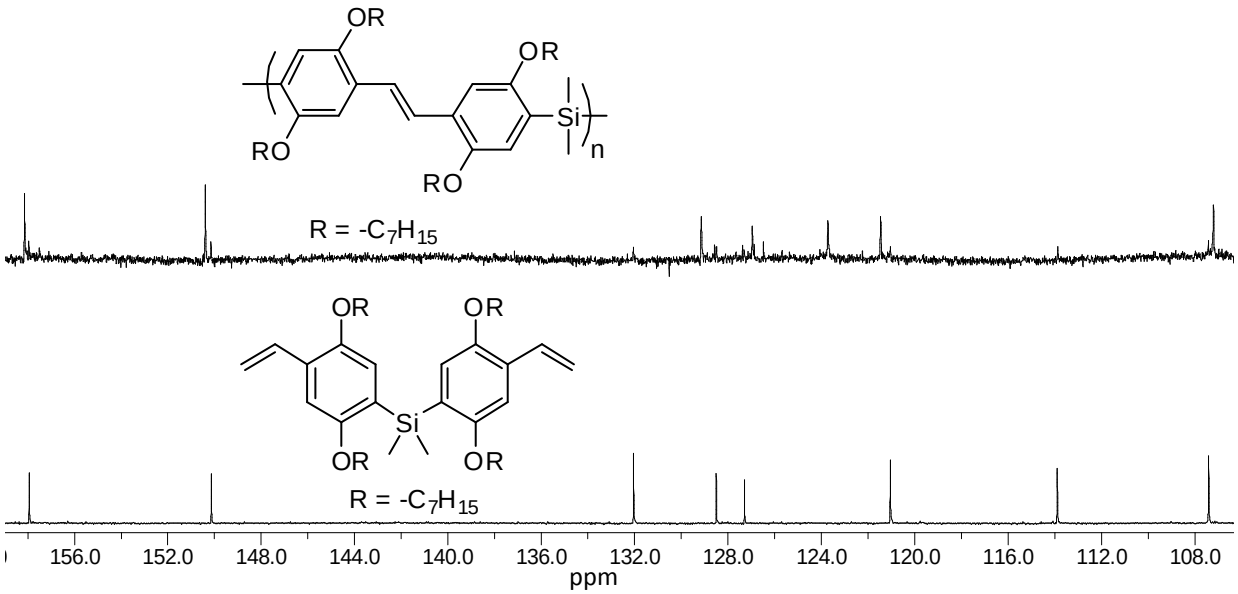

Figure 5.3 ^{13}C NMR (125MHz, $CDCl_3$, selected region) spectral overlays of **6** and **7**

Table 5.2 ^{1}H NMR assignments of **6** and **7**

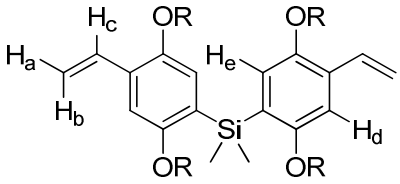

6

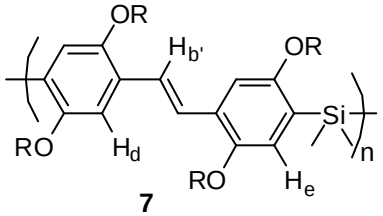

7

	ppm							
Entry	a	b/b'	c	d	e	-OC**H**$_2$	R	-CH_3 (on Si)
6	5.22	5.71	6.82	7.03	6.87	3.81	1.25-1.75	0.52
7	-	7.46	-	7.03	6.87	.3.86	1.30-1.77	0.53

Table 5.3 ^{13}C NMR assignments of **6** and **7**

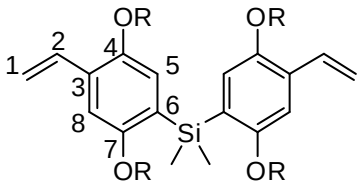

R = $-C_7H_{15}$

6

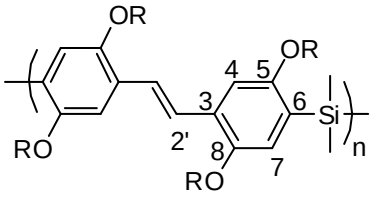

R = $-C_7H_{15}$

7

ppm

Entry	1	2/2'	3	4	5	6	7	8
6	114.07	132.22	127.45	150.02	121.15	128.61	158.04	107.58
7	-	123.83	127.48	150.41	121.54	129.19	158.24	107.39

5.2.3.3 Optical properties (UV/Vis and Fluorescent spectroscopy)

The photophysical properties of the monomer and the polymer are summarized in Figure 5.4. The measurements were performed in hexane solution. The absorption spectrum of monomer **6** showed three different transitions at 225 nm, 258 nm and 332 nm which corresponded to $\pi - \pi^*$ transitions. The absorption maxima of **7** was red shifted compared to the monomer **6** by 40 nm. This is due to π – delocalization in the stilbene segment. Two important transitions were seen in the absorption of the polymer at 297 nm and 371 nm which corresponded to the $\pi - \pi^*$ transitions. The emission spectrum of the polymer **7** was again red shifted by 36 nm compared to the monomer **6**. The emission spectrum of the polymer was characterized by a maximum at 412 nm, a shoulder at 435 nm and a low energy tailing which suggests the presence of aggregation in the excited state. The quantum yield of polymer **7** was found to 0.52 in hexane with trans-stilbene as the reference. The higher quantum yield compared to trans - stilbene may be a result of the reduced vibrational degrees of freedom in the excited state induced by the alkyloxy substituents present on the main chain.

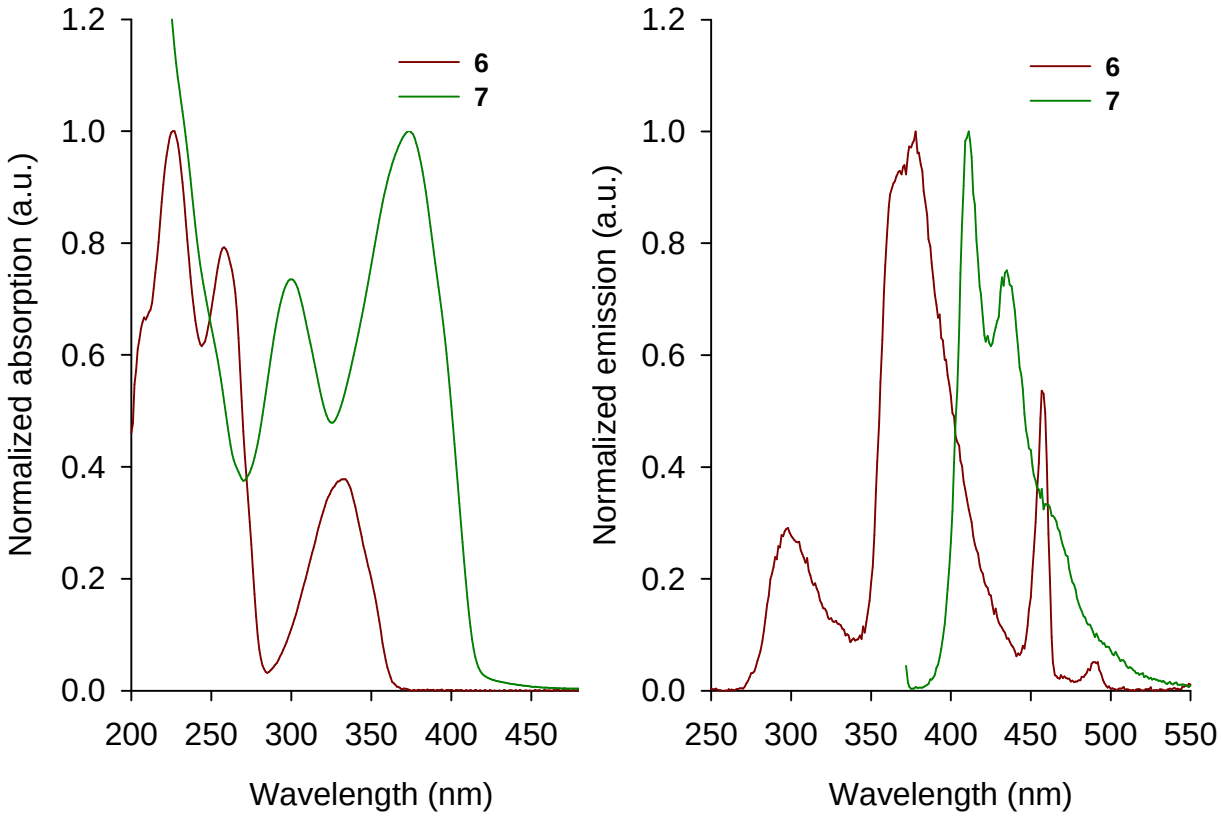

Figure 5.4 Absorption and emission spectral overlay of **6** and **7**

The absorption and the emission spectrum of **7**was compared with that of SiPPV and thiophene based systems, which is shown in Figures 5.5 and Figure 5.6. A strong red shift of the absorption maxima was recorded for **7** compared to the SiPPV systems. The presence of the electron donating heptyloxy group may lower the LUMO resulting in reduction of the band gap compared to that of the unsubstituted SiPPV.

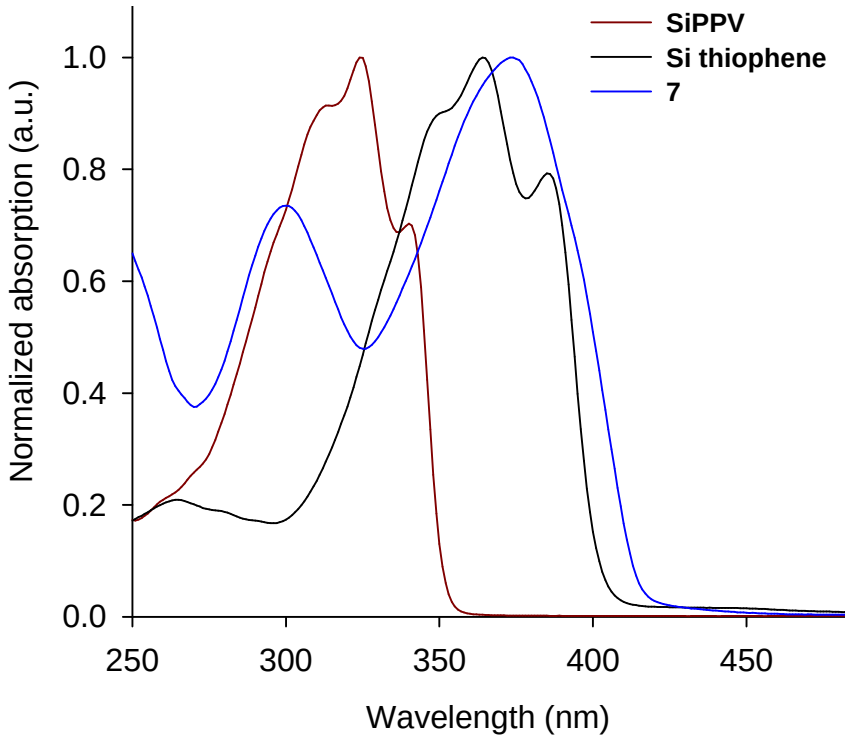

Figure 5.5 Absorption spectral overlay of **7,** SiPPV and Si thiophene (in hexane)

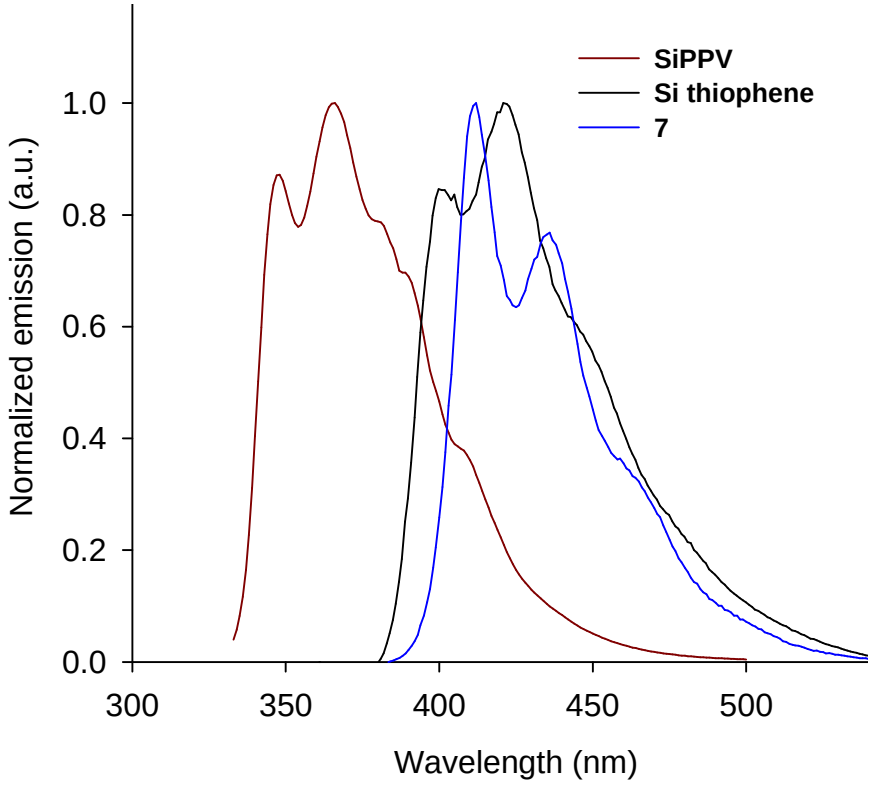

Figure 5.6 Emission spectral overlay **7**, SiPPV and Si thiophene (in hexane)

The recorded UV/Vis and emission data of **7**, SiPPV and Si thiophene are summarized in Table 5.4.

Table 5.4 Experimental absorption and emission values of **7**, SiPPV and Si thiophene

Entry	$\lambda_{max\ (abs)}$ **(nm)**	$\lambda_{max\ (em)}$ **(nm)**	ϕ_{eff}
7	371, 297	412, 435	0.52
SiPPV	327	367	0.25
Si thiophene	363	420	-

5.3 Conclusion

In summary, we have presented the synthesis of a novel SiPPV system where the aromats have heptyloxy substitution. The resulting polymer showed strong bathochromic shift compared to unsubstituted SiPPV due to the electron donating nature of the heptyloxy group. The synthetic approach presented potentially allows access to a variety of structural homologues with different substituted aromatic segments in direct electronic conjugation to Si or other heteroatoms like Ge and Sn. This will enable detailed structure/property investigations into electronically intriguing systems with significant practical importance by tuning the photophysical properties as per application.

5.4 Experimental

General Information

All of the experiments using air/moisture sensitive materials were carried out in a nitrogen filled Labconco protector glove box and/or by the use of dry argon filled dual manifold (inert gas/ vacuum) using standard Schlenk line techniques. All glassware was cleaned and dried for at least 16 h in an oven at 120 ^{0}C prior to use.

Chemicals

Hydroquinone, Grubbs (2nd Generation) and Grubbs-Hoveyda (2nd Generation) catalyst were obtained from Aldrich. Dichloro dimethyl silane was obtained from Sigma Aldrich. Silica gel (230-400 MESH) was purchased from Fisher Sientific. Solvents e.g. tetrahydrofuran (THF), toluene, hexane came from Fisher Scientific. All solvents were dried and degassed by a "Pure Solv" solvent purification system (using activated alumina, copper catalyst, molecular sieves column when appropriate) by Innovative Technology Inc. before use. All other chemicals were used as received.

Instrumentation

^{1}H NMR (600 MHz) and ^{13}C NMR spectra were recorded in $CDCl_3$ on Varian Unity NMR instruments. $CDCl_3$ was used as an internal deuterium lock for the spectra. All of the signals in the NMR spectra are reported in ppm, multiplicity (s = singlet, d = doublet, t = triplet, q = quadruplet, m = multiplet, dd = doublet of doublet).

UV-Visible absorption spectra were recorded using a Perkin Elmer Model 650 UV Spectrophotometer with 1-cm path length cells. The samples were prepared with HPLC grade hexane ("Spectrasolv") in a sample cell.

Photoluminescence spectra were recorded using a Horiba Jobin Yvon Fluoromax-3 spectrofluorometer with 1-cm path length cells. The samples were prepared with HPLC grade hexane ("Spectrasolv") in a sample cell.

GPC analysis was carried out on an Alliance GPCV 2000 (Waters) instrument equipped with four Waters Styragel HR columns, i.e. HR-1, HR-3, HR-4, and HR-5E. HPLC grade THF was used as eluent, at a flow rate of 1.0 mL/min at 40 ^{0}C. Measurements are relative to a calibration with polystyrene standards and third order relative calibration curve was used to measure the molecular weight of unknown samples.

Synthesis of 2, 3, 4, 5

The synthetic strategy for **2**, **3**, **4**, **5** was followed from the dissertation submitted by Dr. Chivin Sun.[116]

Synthesis of monomer 6

Compound **5** (809mg, 1.97mmol) was dissolved in 5ml of THF. The temperature of the resulting solution was reduced to –35^{0}C. At –35^{0}C, nBuLi (2.5M, 1.93mmol) was added dropwise and the reaction mixture was stirred for 3h. Dichloro dimethyl silane (124.5mg, 0.965 mmol) was added to the lithiated solution at –35^{0}C and the reaction mixture was stirred overnight. Solvent was removed from the mixture under reduced pressure and the crude product was dissolved in hexane and filtered. The crude product obtained after purification was further purified by passing through silica gel with hexane and toluene as the eluent in the ration of 5:1. Yield: 25%. ^{1}H NMR (600MHz, $CDCl_3$, ppm) δ = 7.03 (dd, 2H), 6.87 (s, 2H), 6.82 (s, 2H), 5.71 (d, 2H), 5.22 (d, 2H), 3.81 (m, 8H), 1.25 – 1.75 (m, 40H), 0.86 (t, 12H), 0.52 (s, 6H).

^{29}Si NMR (120MHz, $CDCl_3$, ppm): δ = -9.21.

Synthesis of polymer 7[a]

Monomer 6 (110mg, 0.153 mmol) was dissolved in 2.5 ml toluene. To the resulting solution Grubbs 2nd generation catalyst (10mg, 0.012 mmol) was added. The reaction mixture was stirred for 72h at 70^0C. Completion of reaction was indicated by ^{1}H-NMR (dissappearance of resonance from vinyl-protons versus appearance of resonances from vinylene-protons). The crude product was purified by passing it through a short silica gel column with hexane and toluene as the eluent. Yield 70%. ^{1}H NMR (600MHz, $CDCl_3$, ppm) δ = 7.46 (s, br, 2H), 7.03 (s, br, 2H), 6.87 (s, br, 2H), 3.86 (m, 8H), 1.30 – 1.77 (m, 40H), 0.84 (m, 12H), 0.53 (s, br, 6H).

^{29}Si (120MHz, $CDCl_3$, ppm) δ = -9.25.

Synthesis of polymer 7[b]

Monomer 6 (55mg, 0.076 mmol) was dissolved in 1.5 ml toluene. To the resulting solution Hoveyda-Grubbs 2nd generation catalyst (4.6mg, 0.0071 mmol) was added. The reaction mixture was stirred for 72h at 70^0C. Completion of reaction was indicated by ^{1}H-NMR (dissappearance of resonance from vinyl-protons versus appearance of resonances from vinylene-protons). The crude product was purified by passing it through a short silica gel column with hexane and toluene as the eluent. Yield 68%. ^{1}H NMR (600MHz, $CDCl_3$, ppm) δ = 7.46 (s, br, 2H), 7.03 (s, br, 2H), 6.87 (s, br, 2H), 3.86 (m, 8H), 1.30 – 1.77 (m, 40H), 0.84 (m, 12H), 0.53 (s, br, 6H)

^{29}Si (120MHz, $CDCl_3$, ppm) δ = -9.25.

6. References

1. Shirakawa, H.; Louis, E. J.; MacDiarmid, A. G.; Chiang, C. K.; Heeger, A. J. *J. Chem. Soc, Chem. Commun*, **1977**, *578*.

2. Chiang, C. K.; Park, Y. W.; Heeger, A. J.; Shirakawa, H.; Louis, E. J.; MacDiarmid, A. G. *Phys. Rev. Lett.*, **1977**, *39*, 1098.

3. (a) Burroughes, J. H.; Bradley, D. D. C.; Brown, A. R.; Marks, R. N.; Mackay, K.; Friend, R. H.; Burns, P. L.; Holmes, A. B. *Nature (London)* **1990**, *347*, 539 and references therein. (b) Ohmori, Y.; Uchida, M.; Muro, K.; Yoshino, K. *Jpn. J. Appl. Phys.* **1991**, *30*, L1941. (c) Gustafasson, G.; Cao, Y.; Treacy, G. M.; Klavetter, F.; Colaneri, N.; Heeger, A. J. *Nature (London)* **1992**, *357*, 477. (d) Grem, G.; Leditzky, G.; Ullrich, B.; Leising, G. *Adv. Mater.* **1992**, *4*, 36. (e) Akcelrud, L. *Prog. Polym. Sci.* **2003**, *28*, 875 and references therein.

4. D-a ll'O- lio. A.; Dascola. Y.; Varacco. V.: Bocchi. C. R. C. *R. Seances AcadrSci., Ser. C* **1968,** *267*, 433**.**

5. Wudl, F. et al. Chem. Rev. **1988**, *88*, 183-200.

6. (a) Sakurai, H.; Sugiyama, H.; Kira, M. *J. Phys. Chem.* **1990**, *94*,1837. (b) Chen, R.-M.; Chien, K.-M.; Wong, K.-T.; Jin, B.-Y.; Luh, T.-Y.; Hsu, J.-H.; Fann, W. *J. Am. Chem. Soc.* **1997**, *119*, 11321. (c) Chen, Z.-K.; Lai, Y.-H.; Chan, H. S-O.; Ng, S.-C.; Huang, W. *Chem. Lett.* **1999**, *6*, 477. (d) Sumiya, K.-I.; Kwak, G.; Sanda, F.; Masuda, T. *J. Polym. Sci, Part A: Polym. Chem.* **2004**, *42*, 2774.

7. Li, H.; Powell, D. R.; Firman, T. K.; West, R. *Macromolecules* **1998**, *31* 1093.

8. (a) Garnier, F. *Chem. Phys.* **1998**, *227*, 253. (b) Mercuri, F.; Re, N.; Sgamellotti, A. *THEOCHEM* **1999**, *489*, 35. (c) Garten, F.; Hilberer, A.; Cacialli, F.; Esselink, F. J.; Van Dam, Y.; Schlatmann, A. R.; Friend, R. H.; Klapwijk, T. M.; Hadziioannou, G. *Synth. Met.* **1997**, *85*, 1253. (d) Yamashita, H.; de Leon, M. S.; Channasanon, S.; Suzuki, Y.; Uchimaru, Y.; Takeuchi, K. *Polymer* **2003**, *44*, 7089. (e) Mori, A.; Takahisa, E.; Kajiro, H.; Nishihara, Y.; Hiyama, T. *Macromolecules* **2000**, *33*, 1115.

9. Representative review: (a) Yamaguchi, S.; Tamao, K. Sigma- and piconjugated organosilicon polymers. In *Silicon-Containing Polymers*; Jones, R. G., Ando, W., Chojnowski, J., Eds.; Kluwer Academic: Dordrecht, 2000; pp 461-498. (b) Kunai, A. *Organomet. News* **2007**, *3*, 82, and references therein.

10. Kwak, G.; Takagi, A.; Fujiki, M. *Macromol. Rapid Commun.* **2006**, *27*, 1561.

11. (a) Smith, D. W.; Wagener, K. B. *Macromolecules* **1993**, *26*, 1633. (b) The new "bible": *Handbook of Olefin Metathesis*; Grubbs, R. H., Ed.; Wiley-VCH: Weinheim, 2003; Vols. 1-3.

12. Marciniec, B. *Coord. Chem. ReV.* **2005**, *249*, 2374.

13. Miao, Y. J.; Bazan, G. C. *Macromolecules* **1997**, *30*, 7414.

14. Mukherjee, N.; Peetz, R. M. *Polym. Prepr. (Am. Chem. Soc., DiV. Polym. Mater. Sci. Eng.)* **2006**, *94*, 822.

15. Kumagai, T.; Itsuno, S. *Tetrahedron: Asymmetry* **2001**, *12*, 2509.

16. (a) Sakurai, H.; Sugiyama, H.; Kira, M. *J. Phys. Chem.* **1990**, *94*,1837. (b) Chen, R.-M.; Chien, K.-M.; Wong, K.-T.; Jin, B.-Y.; Luh, T.-Y.; Hsu, J.-H.; Fann, W. *J. Am. Chem. Soc.* **1997**, *119*, 11321. (c) Chen, Z.-K.; Lai, Y.-H.; Chan, H. S-O.; Ng, S.-C.; Huang, W. *Chem. Lett.* **1999**, *6*, 477. (d) Sumiya, K.-I.; Kwak, G.; Sanda, F.; Masuda, T. *J. Polym. Sci, Part A: Polym. Chem.* **2004**, *42*, 2774.

17. Li, H.; Powell, D. R.; Firman, T. K.; West, R. *Macromolecules* **1998**, *31* 1093.

18. (a) Garnier, F. *Chem. Phys.* **1998**, *227*, 253. (b) Mercuri, F.; Re, N.; Sgamellotti, A. *THEOCHEM* **1999**, *489*, 35. (c) Yamashita, H.; de Leon, M. S.; Channasanon, S.; Suzuki, Y.; Uchimaru, Y.; Takeuchi, K. *Polymer* **2003**, *44*, 7089. (d) Mori, A.; Takahisa, E.; Kajiro, H.; Nishihara, Y.; Hiyama, T. *Macromolecules* **2000**, *33*, 1115.

19. Representative review: (a) Yamaguchi, S.; Tamao, K. Sigma- and piconjugated organosilicon polymers. In *Silicon-Containing Polymers*; Jones, R. G., Ando, W., Chojnowski, J., Eds.; Kluwer Academic: Dordrecht, 2000; pp 461-498. (b) Kunai, A. *Organomet. News* **2007**, *3*, 82, and references therein.

20. Luh T.-Y. et al., *Macromolecules* **2005**, 38, 4563.

21. Kim D.-H. et al., *Macromolecules* **2005**, *38*(3), 730 – 735.

22. Garten, F.; Hilberer, A.; Cacialli, F.; Esselink, F. J.; Van Dam, Y.; Schlatmann, A. R.; Friend, R. H.; Klapwijk, T. M.; Hadziioannou, G. *Synth. Met.* **1997**, *85*, 1253.

23. Cheng, Y.-J.; Basu, S.; Lou, S-J.; Luh, T-Y. *Macromolecules* **2005**, *38*, 1442 – 1446.

24. Cheng, Y.-J.; Hwu, T.-Y.; Hsu, J.-H.; Luh, T-Y. *Chem. Commun*. **2002**, 1978.

25. Cheng, Y.-J.; Luh, T-Y. Chem. Eur. J. 2004, 10, 5361.

26. Wang, H.W. et al. *Macromolecules* **2007**, *40*, 2666 – 2671.

27. Cheng, Y.-J.; Liang, H.; Luh, T.-Y. *Macromolecules* **2003**, *36*, 5912.

28. van Walree, C. A.; Roest, M. R. P.; Schuddeboom, W.; Jenneskens, L. W. Verhoeven, J. W.; Warman, J. M.; Kooijman, H.; Spek, A. L. *J. Am. Chem. Soc.* **1996**, *118*, 8395.

29. Corriu, R.J.-P.; Deforth, T.; Douglas, W.E.; Guerrero, G.; Siebert, W.S. *Chem. Commun*. **1998** 963.

30. Matsumi, N.; Kensuke, N.; Chujo, Y. *J. Am. Chem. Soc.* **1998**, *120*, 5112.

31. Matsumi, N.; Miyata, M.; Chujo, Y. *Macromolecules* **1999**, *32*, 4467.

32. Sundararaman, A.; Victor, M.; Varughese, R.; Jäkle, F. *J. Am. Chem. Soc.* **2005** *127* 13748.

33. Wu, Q.; Esteghamatian, M.; Hu, N.-X.; Popovic, Z.; Enright, G.; Tao,Y.; D'Iorio, M.; Wang, S. *Chem. Mater*. **2000**, *12*, 79–83.

34. Cui, Y.; Liu, Q.-D.; Bai, D.-R.; Jia, W.-L.; Tao, Y.; Wang, S. *Inorg.Chem.* **2005**, *44*, 601–609.

35. Cui, Y.; Wang, S. *J. Org. Chem.* **2006**, *71*, 6485–6496.

36. Kappaun, S.; Rentenberger, S.; Pogantsch, A.; Zojer, E.; Mereiter, K.; Trimmel, G.; Saf, R.; Mo¨ller, K. C.; Stelzer, F.; Slugovc, C. *Chem. Mater*. **2006**, *18*, 3539–3547.

37. Wang, X.-Y.; Weck, M. *Macromolecules* **2005**, *38*, 7219-7224.

38. Li, H.; Jäkle, F. *Macromolecules*, **2009**, *42*, 3448-3453.

39. Allcock, H. R.; Kellam III, E. C.; Hoffmann, M. A. *Macromolecules*, **2001**, *34*(15), 5140

40. Gómez, F. J.; Wagener, K. B. *J. Organomet. Chem.* **1999**, *592*, 271-277.

41. (a) Dragutan, V.; Balaban, A. T.; Dimonie, M. *Olefin Metathesis and Ring-Opening Polymerization of Cycloolefins*, Wiley, J. & Sons Ltd.: Chichester/Editura Academiei, Bukarest, **1985.** (b) Ivin, K. J.; Mol, J. C. *Olefin Metathesis and Metathesis Polymerization*, Academic Press: London, **1997.** (c) Fürstner, A. *Alkene Metathesis in Organic Synthesis*; Springer: Berlin, **1998**. (d) Grubbs, R. H.; Chang, S. *Tetrahedron* **1998**, *54*, 4413. (f) Ivin, K. J. *J. Mol. Catal. A* **1998**, *133*, 1. (e) Fu¨rstner, A. *Angew. Chem*. **2000**, *112*, 3140; *Angew.Chem., Int. Ed. Engl*. **2000**, *39*, 3013. (f) Trnka, T. M.; Grubbs, R. H. *Acc. Chem. Res*. **2001**, *34*, 18. (g) Grubbs, R.H. *Handbook of Metathesis*, Wiley-VCH: Germany, **2003**. (h) Grubbs, R.H. *Tetrahedron* **2004,** *60*, 7117.

42. Hérisson, J. L., Chauvin, Y. *Makromol. Chem.* **1971**, *141*, 161.

43. (a) Katz, T. H, McGinnis, J. *J. Am. Chem. Soc.* **1977**, *99* 1903. (b) Grassmann, P. C.; Johnson, T. H. *J. Am. Chem. Soc.* **1976**, *98*, 6055.

44. Calderon, N. *Adv. Chem. Ser*. **1969**, *91*, 399.

45. (a) Schneider, M. F.; Blechert, S. *Angew. Chem. Int. Ed. Engl.* **1996**, *35*, 410. (b) Tallarico, J. A.; Bonitatebus, Jr. P. J.; Snapper, M. L. *J. Am. Chem. Soc.* **1997**, *119*, 7157. (c) Schneider, M. F.; Lucas, N.; Velder, J.; Blechert, S.; *Angew. Chem. Int. Ed. Engl.* **1997**, *36*, 257. (d) Seiders, T. J.; Ward, D. W.; Grubbs, R. H. *Org. Lett.* **2001**, *3*, 3225.

46. (a) Armstrong, S. K.; *J. Chem. Soc., Perkin Trans.* **1998**, *1*, 371. (b) Maier, M. E. *Angew. Chem. Int. Ed. Engl.* **2000**, *39*, 2073.

47. (a) Brumer, O. ; Ruckert, A. ; Blechert, S. *Chem. Eur. J.* **1997**, *3*, 441. (b) Diver, S. T.; Schreiber, S. L. *J. Am. Chem. Soc.* **1997**, *119*, 5106. (c) Schuster, M.; Lucas, N.; Blechert, S. *Chem. Commun.* **1997**, 823.

48. Lindmark-Hamberg, M.; Wagener, K. B. *Macromolecules* **1987**, *20*, 2951.

49. Dall'Asta, G.; Stigliani, G.; Greco, A.; Motta, L. *Chim. Ind. (Milan)* **1973**, *55*, 142.

50. (a) Doyle, J. *Catalysis* **1973**, *30*, 118. (b) Zuech, E. A.; et al. *J. Am. Chem. Soc.* **1970**, *92*, 528

51. Thorn – Csanyi, E., Ruhland, K. *Macromol. Symp*. **2000**, 153

52. (a) Schrock, R. R. *J. Organomet. Chem*. **1986**, *300*, 249. (b) Schrock, R. R.; Murdzek, J. S.; Bazan, G. C.; Robbins, J.; DiMare, M.; O'Regan, M. *J. Am. Chem. Soc.* **1990**, *112*, 3875. (c) Schrock, R. R. *Acc. Chem. Res.* **1990**, *23*, 158. (c) Schrock, R. R. *Tetrahedron* **1999**, *55*, 8141.

53. (a) Schwab, P.; France, M. B.; Ziller, J. W.; Grubbs, R. H. *Angew. Chem. Int. Ed. Engl.* **1995**, *34*, 2039; Angew. *Chem.* **1995**, *107*,2179 and references therein. (d) Schwab, P.; Grubbs, R. H.; Ziller, J. W. *J. Am. Chem. Soc*. **1996**, *118*, 110. (d) Dias, E. L.; Nguyen, S. T.; Grubbs, R. H. *J. Am. Chem. Soc.* **1997**, *119*, 3887.

54. (a) Scholl, M.; Ding, S.; Lee, C. W.; Grubbs, R. H. *Org*. *Lett*. **1999**, *1*, 953. (b) Chatterjee, A. K., Grubbs, R. H. *Org. Lett.* **1999**, *1*, 1751. (c) Romero, P. E.; Piers, W. E.; McDonald, R. *Angew. Chem. Int. Ed. Engl.* **2004**, *41*, 6161 and reference therein.

55. (a) Harrity, J. P. A.; La, D. S.; Cefalo, D. R.; Visser, M. S.; Hoveyda, A. H. *J. Am. Chem. Soc.* **1998,** *120*, 2343. (b) Kingsbury, J. S.; Harrity, J. P. A.; Bonitatebus, Jr., P. J.; Hoveyda, A. H. *J. Am. Chem. Soc.* **1999,** *121*, 791.

56. Garber, S. B.; Kingsbury, J. S.; Gray, B. L.; Hoveyda, A. H**.** *J. Am. Chem. Soc.* **2000,** *122*, 8168 and references therein.

57. Hong, S. H.; Grubbs, R. H. *J. Am. Chem. Soc*. **2006,** *128*, 3508.

58. Recent developement in metathesis catalyst: (a) Zhu, S.; Cefalo, D. R.; La, D. S.; Jamieson, J. Y.; Davis, W. M.; Hoveyda, A. H.; Schrock, R. R. *J. Am. Chem. Soc.* **1999**, *121*, 8251. (b) Jafarpour, L.; Stevens, E. D.; Nolan, S. P. *J. Organomet. Chem.* **2000**, *606*, 49. (c) Ackermann, L.; El Tom, D.; Furstner, A. *Tetrahedron***2000**, *56*, 2195. (d) Aeilts, S. L.; Cefalo, D. R.; Bonitatebus, P. J.; Houser, J. H.; Hoveyda, A. H.; Schrock, R. R. *Angew. Chem. Int. Ed. Engl.* **2001**, *40*, 1452. (e) Van Veldhuizen, J. J.; Garber, S. B.; Kingsbury, J. S. Hoveyda, A. H. *J. Am. Chem. Soc.* **2002**, *124*, 4954.

59. Thorn-Csanyi, E; Herzog, O. *J. Mol. Catal. A: Chemical* **2004**, *213(1)*, 123.

60. Nomura, K.; Miyamoto, Y.; Morimoto, H.; Geerts, Y. *J. Polym. Sci., Part A: Polym. Chem.* **2005**, *43(23)*, 6166.

61. (a) Wagener, K. B.; Smith, D. W. *Macromolecules* **1991**, *24*, 6073. (b) Smith, D. W., Wagener, K. B. *Macromolecules* **1993**, *26*, 1633. (c) Smith, D. W.; K. B. Wagener, *Macromolecules* **1993**, *26*, 3533. (d) Cummings, S.; Smith, D.; Wagener, K.; Miller, R.; Ginsburg, E. *Polym. Prepr. (Polym. Chem.)* **1995**, *36(1)*, 697.

62. (a) Solmaz, K.; Cemil, A.; Buelent, D.; Imamoglu, Y. *J. Mol. Catal. A: Chemical* **2006**, 254*(1-2)*, 186. (b) Karabulut, S.; Aydogdu, C.; Duez, B.; Imamoglu, Y. *J. Inorg. Organomet. Polym.* **2006**, *16(2)*, 115.

63. (a) Wu, Z.; Papandrea, J. P.; Apple, T.; Interrante, L. V. *Macromolecules* **2004,** *37*, 5257 and references therein. (b) Hyun, J. Y.; Oh, K.; Ryu, C. Y.; Interrante, L. V. *Polym. Prepr. (Polym. Chem.)* **2005**, *46(2)*, 1053.

64. Schrock, R. R.; De Pue, R. T.; Feldman, J.; Schverin, C. J.; Dewan, S. C.; Liu, A. H. *J. Am. Chem. Soc.* **1988**, *110*, 1423.

65. Marciniec, B; Lewandowski, M. *J. Inorg. Organomet. Polym.* **1995**, *5(2)*, 115.

66. Miao, Y.-J.; Bazan, G. C. *Macromolecules* **1997**; *30(24);* 7414.

67. (a) Abkowitz, M. A.; Stolka, M. *Synth. Met.* **1996**, *78*, 333. (b) Suzuki, H.; Hoshino, S.; Yuan, C. -H.; Fujiki, M.; Toyoda, S.; Matsumoto, N. *IEEE J. Sel. Top. Quantum Electron.* **1998**, *4*, 129. (c) Chen, Z-K.; Lai, Y.-H.; Chan, H. S-O; Ng, S.-C.; Huang, W. *Chem. Lett.* **1999**, 6, 477.

68. Brouwer, H. J.; Krasnikov, V.; Hil- berer, A.; Hadziioannou,G. *Adv. Mater.* **1996**, *8*, 935.

69. Wolfe, P. S.; Gomez, F. J.; Wagener, K. B. *Macromolecules*, **1997**, *30*, 714-717.

70. Wolfe, P. S.; Wagener, K. B. *Macromolecules*, **1999**, *32*, 7961.

71. Davidson K. A.; Wagener, K. B.; Priddy, D. B. *Macromolecules* **1996**, *29*(2), 786 – 788.

72. Mukherjee, N., Peetz, R. M. *Macromolecules*, **2008**, *41*(18), 6677.

73. Kvara, A., Konaadsson, A. E., Evans. C., Geirsson, J. K. F. *Journal of Molecular Structure*, **2000**, *553*, 79.

74. Kotha, S.; Singh, K. *European Journal of Organic Chemistry*, **2007**, *35*, 5909.

75. Wang, X.; Olmstead, M. M.; Fettinger, J. C.; Phillip, P. P. *J. Am. Chem. Soc*. **2009**, *131*, 14164 - 4165.

76. T. Allen, D.G. Whitten, *Chem. Rev*. **1989**, *89*, 1691.

77. (a) Fabrizia N.; Giorgio O.; Francesco Z., *J. Phys. Chem*. **1989**, *93*, 5124;(b) Importa R.; Santoro F.; Dietl C.; Papstathopoulos E.; Gerber G.; *Chem. Phys.Lett*. **2004**, *387* 509.

78. Becke, A. D. *J. Chem. Phys*. **1993**, *98*, 5648.

79. Lee C.; Yang W.; Parr R.G., *Phys. Rev*. **1988**, *B 37* 785.

80. Ghosh S.G.; Chaitanya K.; Bhanuprakash Md.K.; Nazeeruddin K.; Greatzel M.; Reddy Y P. *Inorg. Chem*. 2006, *45*, 7600.

81. Hu Y.H.; Su M.D.;*Chem. Phys. Lett*. **2003**, *371*, 246

82. Frisch M.J,. Trucks G.W,. Schlegel H.B,. Scuseria G.E,. Robb M.A, Cheeseman J.R., Montgomery J.A.. Vreven Jr., T, Kudin K.N., Burant J.C., Millam J.M., Iyengar S.S., Tomasi J., Barone V., Mennucci B., Cossi M., Scalmani G., Rega N., Petersson G.A., Nakatsuji H., Hada M., Ehara M., Toyota K., Fukuda R., Hasegawa J., Ishida M., Nakajima T., Honda Y., Kitao O., Nakai H., Klene M., Li X., Knox J.E., Hratchian H.P.,. Cross J.B, Bakken V., Adamo C., Jaramillo J., Gomperts R., Stratmann R.E., Yazyev O., Austin A., Cammi J.R., Pomelli C., Ochterski J.W., Ayala P., Morokuma Y.K., Voth G.A., Salvador P., Dannenberg J.J., Zakrzewski V.G., Dapprich S., Daniels A.D., Strain M.C., Farkas O., Malick D.K., Rabuck A.D., Raghavachari K., Foresman J.B., Ortiz J.V., Cui Q., Baboul A.G., Clifford Cioslowski S.J., Stefanov B.B., Liu G., Liashenko A., Piskorz P., Komaromi I., Martin R.L., Fox D.J., Keith T., Al-Laham M.A., Peng C.Y., Nanayakkara A.M., Challacombe, Gill P.M.W., Johnson B., Chen W., Wong M.W., Gonzalez C., Pople J.A., Gaussian 03, Revision C.02, Gaussian,Inc., Wallingford, CT, **2004**.

83. Hu Y.H.; Su M.D.; *Chem. Phys. Lett*. **2003**, *378*, 289.

84. Tyrell, J.; Yuoakim, A. *J. Phys. Chem*. **1981**, *85*, 3614.

85. Dufresne, E.; Gaultois, M.; Skene, W.G. *Acta Cryst*. **2007**, *E63*, m2714.

86. (a) Sumiya, K-I.; Kwak, G.; Sanda, F.; Masuda, T. *Journal of Polymer Science Part A: Polymer Chemistry* **2004** *42*(11), 2776. (b) Matsumoto, F.; Matsumi, N.; Chujo, Y.; *Polymer Bulletin* **2001**, *46*, 257 – 262.

87. Rathore, J. S.; Interrante, L. V. *Macromolecules* **2009**, *42*(13), 4614.

88. Gomez, F. J.; Wagener, K. B. *Journal of Organomet. Chem*. **1999**, *592*, 271 – 277.

89. Wolfe, P. S.; Wagener, K. B. *Macromolecules* **1999**, *32*, 7961.

90. Dissertation submitted by Dr. Ami Doshi (Rutgers University).

91. Li, H.; Jäkle, F. *Angew. Chem. Int. Ed.* **2009**, *48*, 2313-2316.

92. Dieter, N., *Macromol. Rapid. Commun*, **2001**, *22*, 1365 – 1385.

93. Yang, J. S.; Swager, T. M. *J. Am. Chem. Soc.* **1998**, *120*, 5321-5322.

94. Yang, J. S.; Swager, T. M. *J. Am. Chem. Soc.* **1998**, *120*, 11864-11873.

95. Kim, Y.; Zhu, Z.; Swager, T. M. *J. Am. Chem. Soc.* **2004**, *126*, 452-453.

96. H. Li and F. Jaekle *Macromolecules* **2009**, *42*, 3448-3453.

97. Pangkuan, C.; Roger, L. A.; Jaekle, F. *Journal of American Chemical Society* **2011**, 133, 8802 – 8805.

98. Cui, Y.; Wang, S. *J. Org. Chem.* **2006**, *71*, 6485–6496.

99. Jäkle, F. *Chem. Rev*. **2010**, *110*, 3985 – 4022.

100. Natalie, M. S.; Thomas, S.; Oleg, T.; Rhett, K. *Eur. J. Inorg. Chem.* **2004**, 3297-3304.

101. Neumann, R.; Weber, E.; Moeckel, A.; Subklew, G. *J. Prakt. Chemie/Chemiker-Zeitung* **1998**, *340*, 613-622.

102. I.F.Perepichka, D.F.Perepichka, H.Meng, F.Wudl Adv Mater. **2005**, 17, 2281 – 2305.

103. Sudha Devi L.; Al-Suti M K.; Zhang N.; Teat S J.; Hazel M L.; Sparkes A.; Raithby P R.; Khan M S.; Ko¨hler Anna**,** *Macromolecules* **2009**, *42*, 1131-1141.

104. McCullough, R. D. *Adv. Mater*. **1998**, *10*, 93.

105. Fahlman, M.; Birgesson, J.; Kaeriyama, K.; Salaneck, W. R. *Synth. Met*. **1995** *75*, 223.

106. Leclerc, M.; Beaupre, S. *Macromolecules* **2003**, *36*, 8986.

107. Roncali, J. *Acc. Chem.Res*. **2000**, *33*, 147.

108. Drolet, N.; Tao, Y.; Leclerc, M. *Chem Mater*. **2004**, *16*, 4619.

109. Herrema J. K.; Hutten P. F. V.; Gill R. E.; Wildeman J.; Wieringa R. H.; Hadziioannou G. *Macromolecules* **1995**, *28*, 8102.

110. Yoshino, K.; Hirohata, M.; Sohoda, T.; Hidayat, R.; Fujii, A.; Naka, A.; Ishiwaka, M. *Synth. Met*. **1999**, *102*, 1158

111. Miao, Y-J.; Bazan, G. *Macromolecules* **1997**, *30*, 7414 – 7418.

112. Melucci M.; Barbarella G.; Zambianchi M.; Benzi M.; Biscarini F.; Cavallini M.; Bongini A.; Fabbroni S.; Mazzeo M.; Anni M.; Gigli G. *Macromolecules*, **2004**, *37*, 5692 – 5702.

113. Edited by Perepichka, I. F.; Perepichka, D. F. Handbook of Thiophene – based materials. Application in Organic Electronics and Photonics, *Wiley*, **2009.**

114. Cotton F. A.; Wilkinson, G.; Murillo, C. A.; Bochmann, A. *Wiley-Interscience*, 6th edition, New York **1999.**

115. Chu, Q.; Pang, Y. *Macromolecules* **2003**, *36*, 4614-4618.

116. Dissertation submitted by Dr. Chivin Sun.